NOTICE

The quality of this microfiche is heavily dependent upon the quality of the original thesis submitted for microfilming. Every effort has been made to ensure the highest quality of reproduction possible.

If pages are missing, contact the university which granted the degree.

Some pages may have indistinct print especially if the original pages were typed with a poor typewriter ribbon or if the university sent us a poor photocopy.

Previously copyrighted materials (journal articles, published tests, etc.) are not filmed.

Reproduction in full or in part of this film is governed by the Canadian Copyright Act, R.S.C. 1970, c. C-30. Please read the authorization forms which accompany this thesis.

THIS DISSERTATION
HAS BEEN MICROFILMED
EXACTLY AS RECEIVED

AVIS

La qualité de cette microfiche dépend grandement de la qualité de la thèse soumise au microfilmage. Nous avons tout fait pour assurer une qualité supérieure de reproduction.

S'il manque des pages, veuillez communiquer avec l'université qui a conféré le grade.

La qualité d'impression de certaines pages peut laisser à désirer, surtout si les pages originales ont été dactylographiées à l'aide d'un ruban usé ou si l'université nous a fait parvenir une photocopie de mauvaise qualité.

Les documents qui font déjà l'objet d'un droit d'auteur (articles de revue, examens publiés, etc.) ne sont pas microfilmés.

La reproduction, même partielle, de ce microfilm est soumise à la Loi canadienne sur le droit d'auteur, SRC 1970, c. C-30. Veuillez prendre connaissance des formules d'autorisation qui accompagnent cette thèse.

LA THÈSE A ÉTÉ
MICROFILMÉE TELLE QUE
NOUS L'AVONS REÇUE

THE ANALYSIS OF FIN LINES USING TRANSMISSION LINE MATRIX AND TRANSVERSE RESONANCE METHODS

by

Yi-Chi Shih

A Thesis
presented to the University of Ottawa
in partial fulfillment of the
requirements for the degree of
Master of Applied Science
in
Department of Electrical Engineering

Ottawa, Ontario, 1980

ABSTRACT

The cutoff frequencies and the dispersion characteristics in unilateral, bilateral and insulated fin lines are evaluated using the TLM method and the transverse resonance method.

The errors affecting the TLM solutions are analyzed and corrected, and the cutoff frequencies in fin lines are obtained with an accuracy better than one percent.

Simple but accurate expressions based on the transverse resonance method are developed for the design of fin lines. The effect of the dielectric substrate on the susceptance of the fin is taken into account by introducing correction factors which are obtained from the TLM solutions at cutoff. A dispersion characteristic obtained in this fashion agrees with published measurements, numerical solutions and the three-dimensional TLM solutions within one percent.

ACKNOWLEDGEMENTS

The author wishes to express his sincere gratitude to his supervisor, Dr. W.J.R. Hoefer, for his encouragement and guidance throughout this work.

Thanks are also due to all the members of the Department of Electrical Engineering, specially Mr. R. LeHénaff and Miss E. Dagenais, for their assistance.

The author also likes to express his appreciation to Y.C. Chen, Greg. Gajda, Art. Thansandote and A.K. Sharma for their revision of the text and fruitful discussion.

LIST OF ACRONYMS

EM	ElectroMagnetic
FE	Finite Element
MIC	Microwave Integrated Circuit
TLM	Transmission-Line Matrix
TR	Transverse Resonance

SUMMARY

This thesis deals with the analysis of integrated fin lines. In chapter I, the introduction describes the basic features of fin lines and the advantages over microstrips in the mm-wave range. The purpose of this study and the methods to be used are also described.

In chapter II, the transverse resonance method is briefly reviewed by analyzing a finned waveguide (a special case of fin lines with no dielectric substrate). The cutoff frequency, guide wavelength and characteristic impedance are obtained.

Chapter III lays the foundation for the two-dimensional TLM analysis of fin lines. The TLM method is reviewed and applied to analyze the finned waveguide discussed in chapter II. The normalized cutoff frequency is obtained from the impulse response of the simulating network via Fourier transformation. The errors associated with it are extensively investigated and a linear extrapolation technique is developed to eliminate the errors. After the error correction, the cutoff frequencies of the finned waveguide are obtained with an accuracy better than one percent.

In chapter IV, the three-dimensional TLM method is briefly described and applied to evaluate finned waveguides. A finned rectangular cavity is analyzed and the resonant frequency is obtained from the impulse response of the TLM network via Fourier transformation. Two components of the coarseness error affecting the TLM solutions are defined and analyzed. They are the transverse and longitudinal coarseness errors. Error characteristics are proposed for the error correction of the TLM solutions of finned waveguides and for the error approximation of the TLM analysis of fin lines.

In chapter V, three fin line configurations, namely unilateral, bilateral and insulated fin lines, are analyzed using the two-dimensional TLM method. The normalized cutoff frequencies of the fundamental and second order modes are obtained. The associated coarseness error is analyzed and the linear extrapolation technique is found to be appropriate for extrapolating the fundamental cutoff frequencies. To eliminate the errors in the second order mode cutoff , a logarithmic curve fitting technique is used. After correcting the errors, the cutoff frequencies obtained are of high accuracy (better than one percent). In addition, the transverse E field lines in fin lines are plotted since the information on the field intensity is available on all the nodes in the TLM network.

Chapter VI discusses the three-dimensional TLM simulation of fin lines. Cavities containing unilateral, bilateral and insulated fin lines are analyzed and the resonant frequencies are obtained. In addition to the errors discussed in chapter IV, an error due to the simulation of the dielectric boundary is analyzed. Asymptotic values of the normalized propagation constant λ/λ_g are obtained graphically. The results are about one to two percent higher than the published transverse resonance solutions.

In chapter VII, simple but accurate expressions are developed for the design of fin lines. The transcendental equations which represent the transverse resonance conditions in fin lines are reviewed. The effect of the dielectric substrate on the susceptance of the fin is taken into account by introducing correction factors. These correction factors are obtained from the two-dimensional TLM solutions at cutoff. The normalized propagation constant calculated in this way agrees with published measurements, numerical solutions and the three-dimensional TLM solutions (agreement better than one percent).

Finally, chapter VIII describes future research on the problem of fin line discontinuities and contains the conclusion for this study.

TABLE OF CONTENTS

LIST OF FIGURES

LIST OF TABLES

Chapter I

INTRODUCTION

At microwave frequencies, MIC technology is widely used to realize low-cost, compact modules. In recent years, active and passive solid-state devices have conquered the millimeter-wave range. At present, new circuit technology must be developed to accomodate these devices.

Microstrip technology is very successful in applications up to about 18GHz, but microstrip circuitry becomes increasingly lossy and difficult to fabricate at higher frequencies. In particular, radiation losses are severe at millimeter wavelengths. Extensive research is now being undertaken on the development of alternate transmission media for the millimeter-wave range. Among the most successful candidates for integrated mm-wave circuit realizations is the fin line which was first proposed by Meier[1].

1.1 FIN LINE

The cross sections of some typical fin lines are shown in Fig.1.1. Depicted are unilateral, insulated, bilateral and antipodal fin lines. In fin-line structures, thin metal

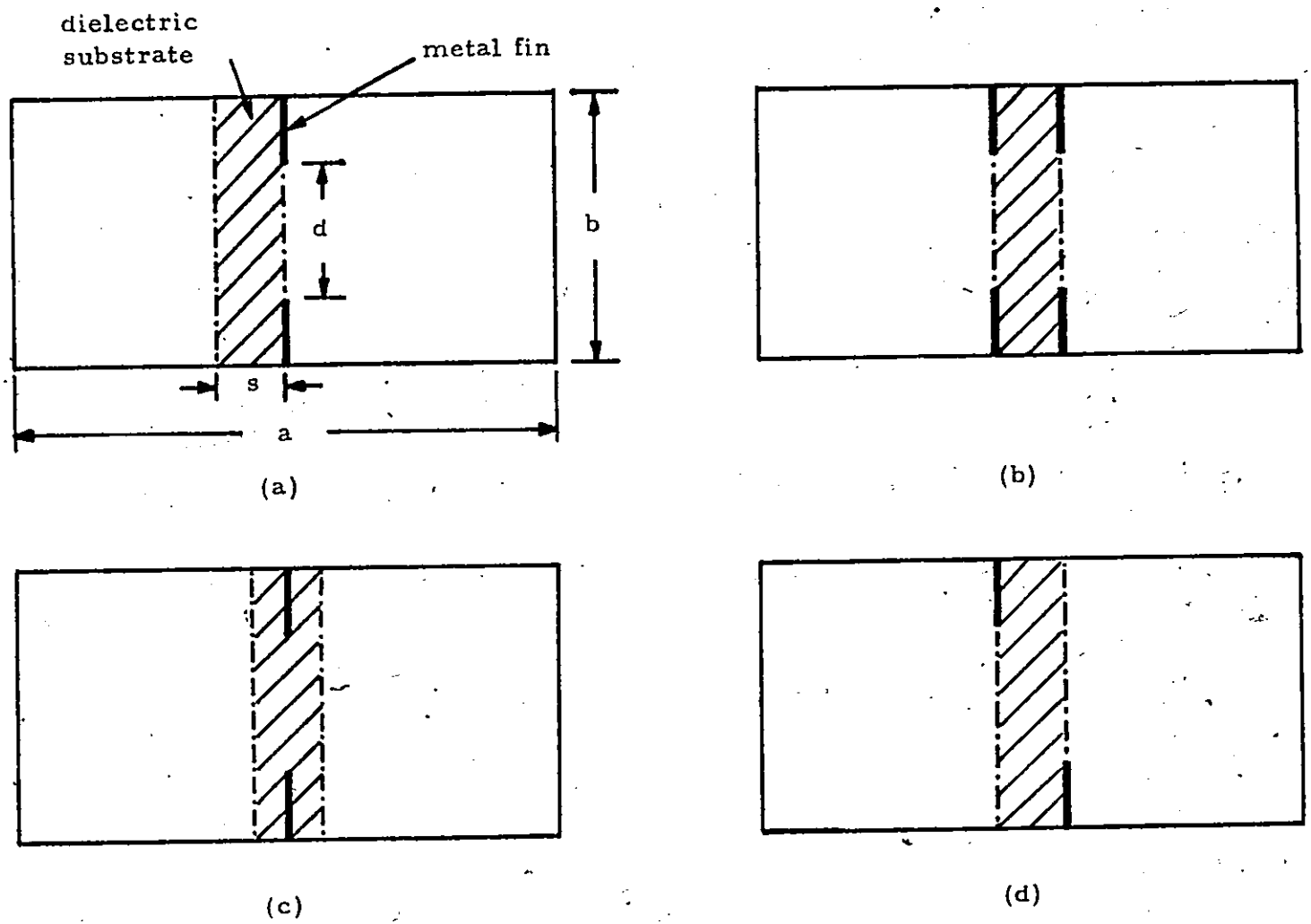

Figure 1.1: Cross section of (a) unilateral, (b) bilateral, (c) insulated, (d) antipodal fin lines.

fins are printed on a dielectric substrate which bridges the broad side of a rectangular waveguide. The structure may be viewed as a slot line with a shield, a ridged waveguide partially filled with dielectrics, or as a slab loaded waveguide with thin fins deposited on the slab. Solid-state devices can be mounted on the substrate and connected to the fins either in parallel or in series. In order to accomodate active devices, the fins must be insulated from the waveguide walls so that a dc bias can be applied.

In practice, when a fin line is constructed, the dielectric substrate may either be inserted into a slit in a rectangular waveguide mount[12] (as shown in Fig. 1.2a) or passed through the broad wall of the shield (see Fig. 1.2b) and fixed between the two halves of the housing with nylon screws[1]. In the latter case, to electrically close the wall opening in the dielectric region, the wall thickness is made equal to one quarter of the wavelength in the dielectric, thereby causing an RF short circuit to appear between the fin and the inner wall of the shield.

Fin line is superior to microstrip in several respects at millimeter-wave frequencies. It is characterized by:

1. higher unloaded Q factor,

2. broader single mode bandwidth,

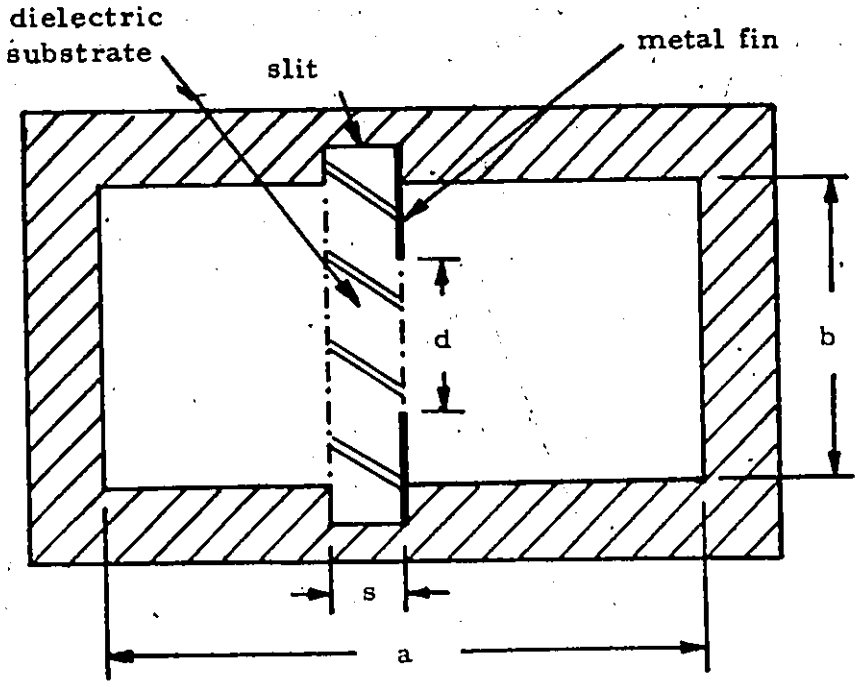

(a)

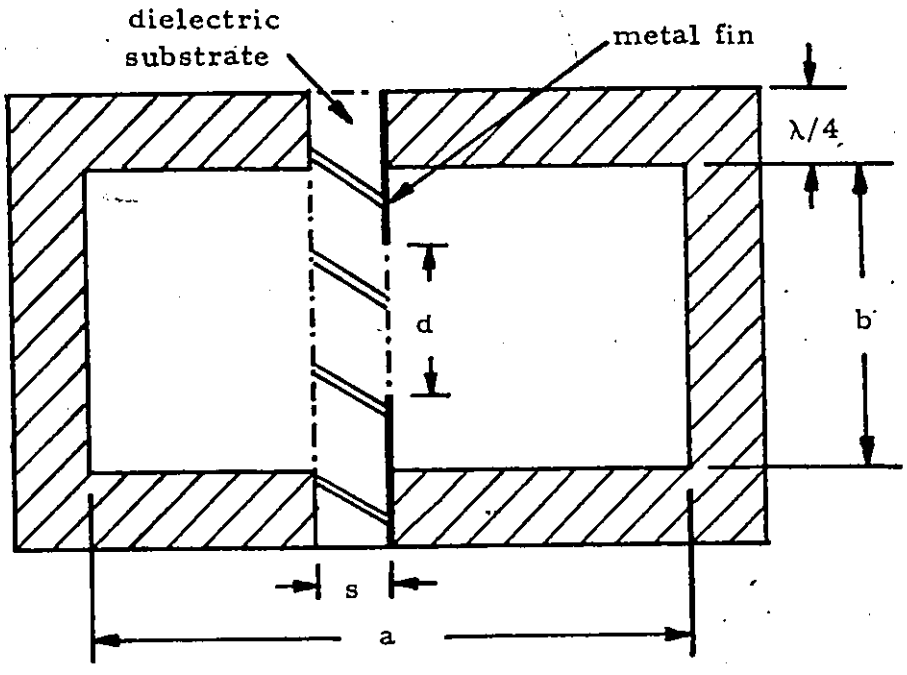

(b)

Figure 1.2: Practical fin-line construction,

Dielectric substrate is (a) inserted into the slit.

(b) passed through broad walls.

3. freedom from radiation,

4. better compatibility with hybrid devices,

5. simpler interfaces with rectangular waveguide.

Many applications of fin lines have been reported in the literature. Fin lines have been used in the design of PIN-attenuators, filters, broadband dectectors, balanced mixers, power dividers and oscillators [1,2,3,5,6,4].

Methods for the evaluation of the guided wavelength (or alternatively the effective dielectric constant) and characteristic impedance in fin lines have been presented by Meier[1], Hofmann[2], Saad and Begemann[7], Chang and Itoh[8], and Hoefer[23]. Most of these methods are very complex, requiring either extensive computer programming or precision measurement (as in Meier's case). Since there is some disagreement between their results, it was considered appropriate to verify them either by precision measurements or by a computer simulation inspiring the same confidence.

1.2 PURPOSE OF STUDY

The purpose of the present study is twofold:

1. to present results which are sufficiently accurate to serve as a reference for other methods of fin-line analysis,

2. to develop simpler but nevertheless accurate expressions for the design of fin lines of arbitrary geometry.

To obtain accurate results, the Transmission-Line Matrix (TLM) [9] method is used. This is not a numerical method for solving Maxwell's equations, but rather a computer simulation of field propagation in guiding structures. In order to obtain the required accuracy, an extensive analysis and correction of errors affecting the method must be carried out.

Even though the TLM method yields results of high accuracy (typically better than 1%), it is too involved to be applied in the design of fin lines. Much simpler expressions for the guided wavelength and characteristic impedance can be obtained using the Transverse Resonance (TR) method which has been applied by Hoefer[23] to the analysis of fin lines. The transcendental equations to be solved are relatively simple and contain a correction factor which accounts for the effect of the dielectric substrate on the transverse susceptance of the fins. The results obtained with this method are quite accurate once the

correction factor has been obtained accurately. Hoefer[23] has calculated the correction factor by modifying Cohn's formula[13] for the transverse susceptance of slot lines. In the present study, correction factors are calculated via two-dimensional TLM analysis which is more accurate than the modified Cohn's formula.

Chapter II

ANALYSIS OF FINNED WAVEGUIDES USING THE TRANSVERSE RESONANCE METHOD

2.1 INTRODUCTION

Finned waveguide (a waveguide with a central ridge of zero thickness) is a special case of fin line without a dielectric substrate. Considerable design information for this structure is available in the literature [14,15,16,17]. In the present chapter, the TR analysis of this special case of fin line is briefly reviewed in order to better demonstrate its application to the analysis of the general case. The determination of three parameters, namely cutoff frequency, guided wavelength and characteristic impedance is discussed.

2.2 TRANSVERSE RESONANCE CONDITION AT CUTOFF

The cross section of a finned waveguide is shown in Fig.2.1. The electromagnetic fields at the cutoff frequency represent a wave traveling in the transverse direction without any longitudinal propagation. Such a structure may be treated by assuming that it is an infinitely wide, parallel-plate transmission line of height b, short-circuited at x=0 and x=a, and containing two infinitely long fins at x=a/2. For

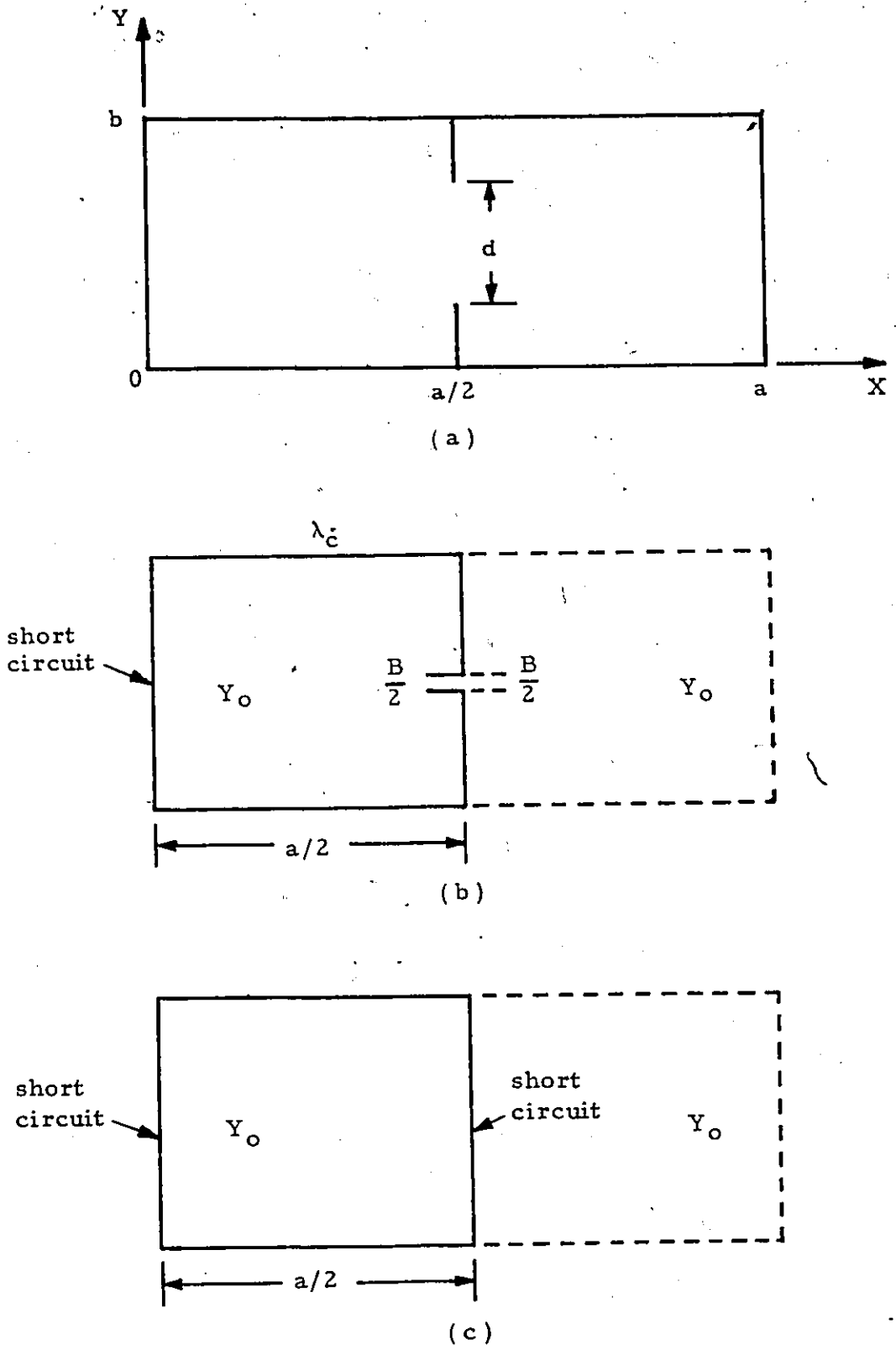

Figure 2.1: Finned waveguide. (a) Cross section, and transverse equivalent network for (b) odd-order resonance, (c) even-order resonance.

b<a (which is satisfied in all applications), cutoff of the dominant fin-line mode (a distorted TE_{10} mode in rectangular waveguide) occurs at the frequency at which this plate transmission line has its lowest order resonance. The cutoff of the higher order modes of this type (TE_{mo}) occurs at the corresponding m-order resonance frequencies. For m odd, the total transverse suseptance is zero at the center of the cross section. For m even, this susceptance must be infinite. A resonant condition may therefore be defined by setting the transverse input susceptance of half the cross section equal to zero or infinity (Fig.2.1). The discontinuity susceptance of the fin must be included in the calculation.

For the odd distorted TE_{mo} mode, the transverse resonance condition (or the cutoff condition) is:

$$\frac{1}{2}\frac{B}{Y_o} - \cot\frac{\pi a}{\lambda_c} = 0 \qquad (2.1)$$

where λ_c is the cutoff wavelength. The normalized susceptance B/Yo is given by Marcuvitz [17] as

$$\frac{B}{Y_o} = \frac{4b}{\lambda_c}\left[\ln\left(\csc\frac{\pi d}{2b}\right) + \frac{Q\cos^4\frac{\pi d}{2b}}{1+Q\sin^4\frac{\pi d}{2b}} + \frac{1}{16}\left(\frac{b}{\lambda_c}\right)^2\left(1-3\sin^2\frac{\pi d}{2b}\right)^2\cos^4\frac{\pi d}{2b}\right] \qquad (2.2)$$

$$\text{with } Q = \left[1-\left(\frac{b}{\lambda_c}\right)^2\right]^{-\frac{1}{2}} - 1 \qquad (2.3)$$

For the even modes, the equivalent circuit is shown in Fig. 2.1(c). In this case, the cutoff condition becomes

$$\cot \frac{\pi a}{\lambda_c} = 0 \qquad (2.4)$$

This is exactly the condition defining the even TE_{mo} modes in empty rectangular waveguides. This is physically evident since for these modes, the electric field is zero at the location of the fins.

2.3 CUTOFF FREQUENCY AND GUIDED WAVELENGTH

Equation (2.1) is correct only if the effect of the side walls on the fin susceptance is fully taken into account. However, in all cases where b/a = 1/2, this proximity effect is negligible and Marcuvitz's formula for B/Yo is sufficiently accurate.

The cutoff wavelength is obtained by finding values for λ_c which satisfy the transcendental equations (2.1) or (2.4). This is done by using a root-finding algorithm. The guided wavelength can then be obtained using the simple formula:

$$\lambda_g = \lambda \left[1-(\lambda/\lambda_c)^2\right]^{-1/2} \qquad (2.5)$$

where λ is the free space wavelength.

2.4 CHARACTERISTIC IMPEDANCE

The wave impedance of any TE wave in a uniform waveguide of arbitrary cross section is given by

$$Z_{TE} = \sqrt{\mu/\varepsilon} \cdot \lambda_g/\lambda \qquad (2.6)$$

In waveguide problems, however, the definition of the characteristic impedance (Z_o) depends on the application. In the majority of cases, Z_o is defined as a voltage-to-current ratio or is defined in terms of the power transmitted for a given voltage or a given current. Similar to the wave impedance, Zo is expressed as

$$Z_o = Z_\infty \cdot \lambda_g/\lambda \qquad (2.7)$$

where Z_∞ is the characteristic impedance at infinite frequency.

2.4.1 Voltage-Current Definition

The voltage-to-current-ratio impedance is defined as

$$Z_o(V,I) = V_o/I \qquad (2.8)$$

where V_o is the line integral over the electric field taken along the center of the waveguide cross section, and I is

the total longitudinal current flowing in the top or bottom of the guide. In the formulation of this ratio for a finned waveguide, the current is separated into two components: (a) a longitudinal component in the top plane of the waveguide, which excites the principal field, and (b) a longitudinal component on the fin which produces the local field. The first component is derived from the field distribution in the waveguide cross section [14], and the second component may be determined by considering the field distribution in the vicinity of the discontinuity. The characteristic impedance, $Z_{\infty}(V,I)$, of the finned waveguide thus obtained is given by [16]

$$Z_{\infty}(V,I) = \left[120\pi^2 b/\lambda_c\right] / \left[\frac{1}{2}\frac{B}{Y_o} + \tan(\pi a/2\lambda_c)\right] \qquad (2.9)$$

where B/Yo is given in eqn.(2.2).

2.4.2 Power-Voltage Definition

The power-voltage definition of the characteristic impedance is defined as

$$Z_o = V_o^2/2P \qquad (2.10)$$

where P is the average power carried by the guide and V_o is the peak value of the voltage as defined in eqn.(2.8). In his

paper on ridged waveguides, Hopfer[15] has given an expression for P. By using this expression, the impedance is derived as

$$Z_{\infty}(P,V) = \left[120\pi^2 b/\lambda_c\right] \Big/ \left[\frac{2b}{\lambda_c}\ln\left(\csc\frac{\pi d}{2b}\right) + \left(\frac{\pi a}{2\lambda_c} - \frac{1}{4}\sin\frac{2\pi a}{\lambda_c}\right)\csc^2\frac{\pi a}{\lambda_c}\right] \qquad (2.11)$$

The characteristic impedances as defined by eqns.(2.9) and (2.11) can be obtained once the transverse resonance condition eqn.(2.1) has been solved. Fig.2.2 presents the characteristic impedance of a finned waveguide at infinite frequency as a function of normalized gap width d/b for an aspect ratio of b/a = 1/2. The value of $Z_{\infty}(P,V)$ is shown to be larger than that of $Z_{\infty}(V,I)$, similar to the impedances defined for an empty waveguide. (Note that a finned waveguide with d/b = 1 is an empty guide.) This is caused by the way the impedances are defined and by the value of V_o selected.

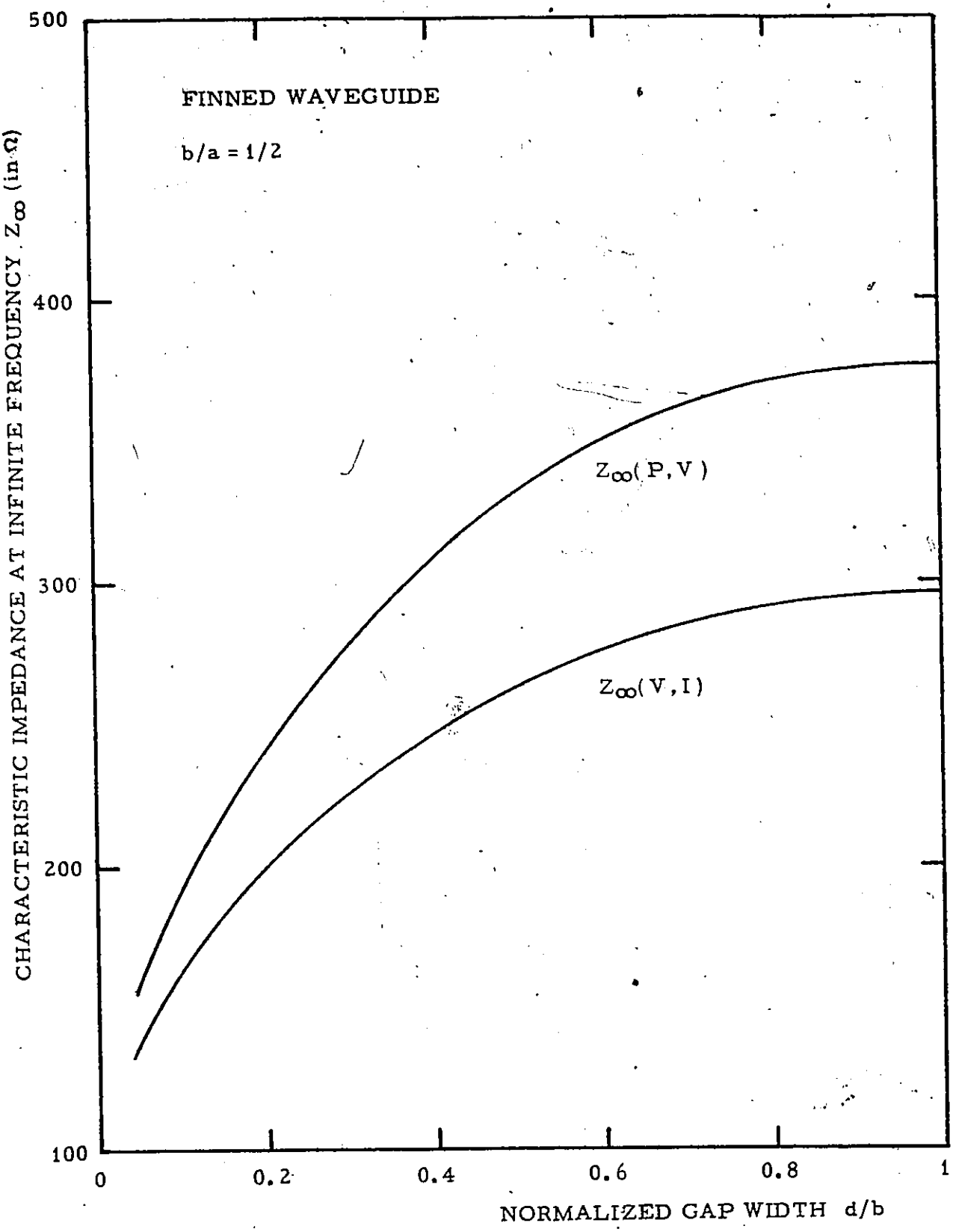

Figure2.2 Characteristic impedance of finned waveguide at infinite frequency.

2.5 DISCUSSION

Finned waveguide has been analyzed using the transverse resonance method. Transverse resonance conditions are expressed by transcendental equations from which the cutoff frequencies and guide wavelengths are obtained. The expressions for characteristic impedance based on voltage-current definition and power-voltage definition are also presented. Since a finned waveguide is a special case of a fin line, this information is helpful in the understanding of the analysis of fin lines.

Chapter III

ANALYSIS OF FINNED WAVEGUIDE USING THE TWO-DIMENSIONAL TLM METHOD

3.1 INTRODUCTION

The two-dimensional Transmission-Line Matrix (TLM) method was first proposed in 1971 by Johns and Beurle [18] and has been successfully applied to waveguide bifurcation problems [18] and to a ridged waveguide problem [20].

It is a powerful tool for solving the homogeneous wave equation in complex structures and can therefore be used to verify the accuracy of approximate solutions, provided that the errors affecting the TLM solution are known and can be compensated. The aforementioned authors have specified three types of errors affecting the results obtained with this method, namely truncation error, velocity error, and "coarseness" error. While the first two types of errors can be readily defined and predicted, the "coarseness" error which reflects the spacial resolution of the transmission line matrix, is more difficult to evaluate and to analyze.

This chapter investigates these three errors as they occur in the TLM analysis of finned waveguide. The finned

waveguide was chosen for the following reasons: (i). This structure was used successfully by Konishi et al. [21,22] in the realization of converters and filters. It is thus of practical interest. (ii). It can be analyzed very accurately using the transverse resonance method. Results can thus be verified for accuracy. (iii). This structure is a special case of the fin line which is of particular interest.

3.2 SHORT DESCRIPTION OF THE TWO-DIMENSIONAL TLM METHOD

In the TLM model, propagation in a two-dimensional medium is represented by the voltages and currents on a Cartesian mesh of transmission lines. Analysis of the mesh is accomplished by considering an impulsive excitation and following the progress of impulses as they propagate throughout the matrix. The mesh is represented at each node by a submatrix of four numbers describing the magnitude of the incident voltages along the four coordinate directions. The matrix as a whole consists of a number of submatrices corresponding to the number of nodes in the matrix.

At any instant, the impulsive voltages incident onto a node are scattered and yield reflected pulses. The reflected pulses from each node then become the incident pulses of neighboring nodes and the process is repeated on an iteration basis. Each iteration corresponds to a unit of

time which is the time required for pulses to travel from one node to its neighbor.

Fig.3.1 shows a typical shunt-node two-dimensional TLM network. Note that here each single line represents a pair of parallel wires forming a transmission line. These transmission lines are shunt connected at the so-called "nodes". If ${}_kV_n(x,y)$ is the unit voltage impulse reflected from the node at (x,y) into the direction n at time $k\frac{\Delta\ell}{c}$, the iteration process at the node (x,y) is summarized by

$$ {}_{k+1}\begin{bmatrix} V_1(x,y) \\ V_2(x,y) \\ V_3(x,y) \\ V_4(x,y) \end{bmatrix} = S \cdot {}_{k}\begin{bmatrix} V_3(x,y-1) \\ V_4(x-1,y) \\ V_1(x,y+1) \\ V_2(x+1,y) \end{bmatrix} \tag{3.1} $$

where the scattering matrix S is given by

$$ S = \frac{1}{2}\begin{bmatrix} 1 & 1 & 1 & 1 \\ 1 & 1 & 1 & 1 \\ 1 & 1 & 1 & 1 \\ 1 & 1 & 1 & 1 \end{bmatrix} - I \tag{3.2} $$

I is the unit matrix, Δl is the distance between neighboring nodes and c is the velocity of light. The coordinate directions n= 1, 2, 3 and 4 correspond to -y, -x, +y and +x, respectively (see Fig.3.1).

In order to simulate the boundaries of a complex structure, appropriate reflection and transmission coefficients must be introduced in the simulating network. These boundaries may be electric walls, magnetic walls, impedance walls or dielectric boundaries. If , for instance, the electric field in space is represented by a voltage in the simulating network (as shown in Fig.3.2a), boundaries in the TLM network are the same as those in the real structure. However, if the magnetic field is represented by a voltage (as shown in Fig.3.2b), boundaries in the network are dual to those in the real structure, i.e., a short-circuited wall in space is represented by an open-circuited wall in TLM network and vice versa.

The TLM technique calculates the impulse response of the simulating network. The output impulse function can be taken at any node in the matrix. It consists of a stream of pulses which arrive at the output node. The impulse function for a closed structure contains not only information on the dominant mode but also on all higher order modes which are excited by the impulsive source. The

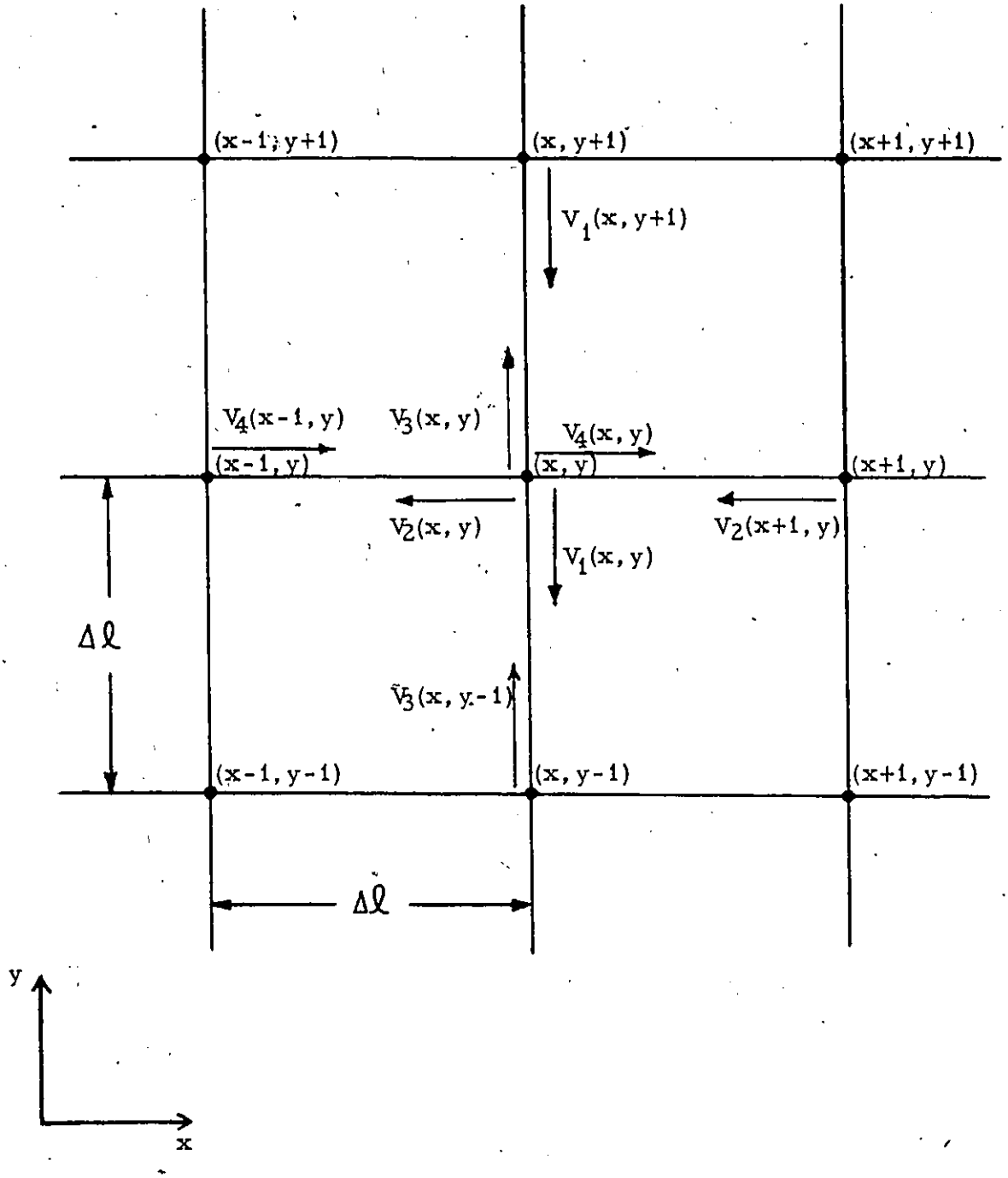

Figure 3.1: Shunt -connected two-dimensional TLM network.

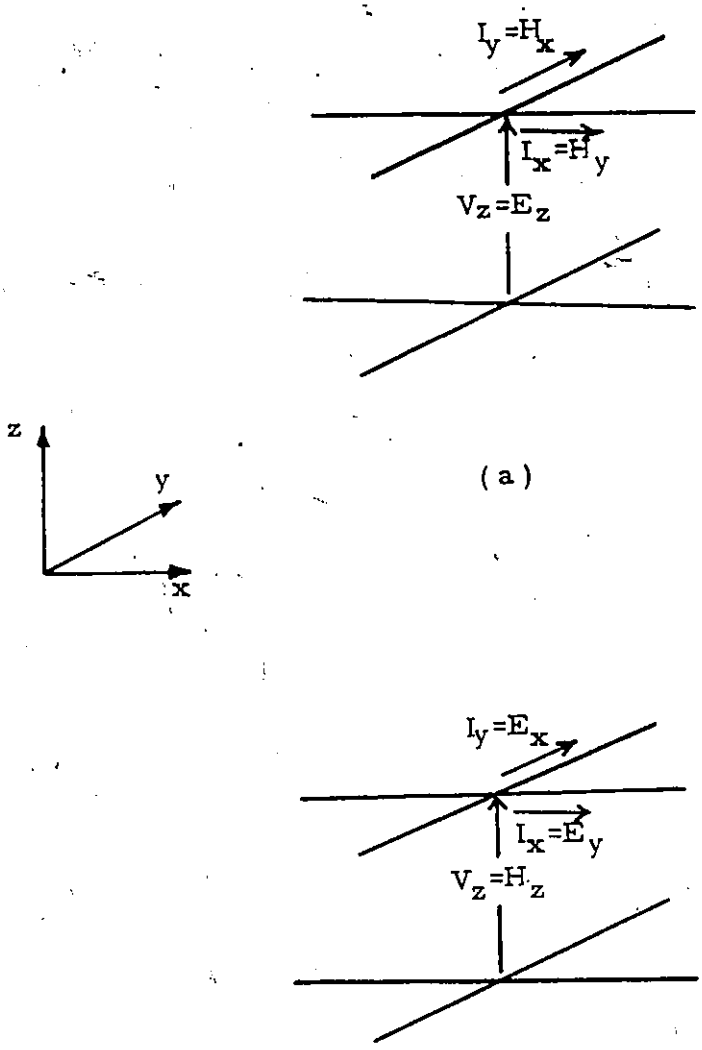

Figure 3.2: Field representation of TLM shunt node.
Voltage representing (a) E field, (b) H field.

required information is extracted from the output impulse function by computing its Fourier transformation.

The TLM network can also be made up of the series-connected node [19] as shown in Fig.3.3. The basic iteration process and programming procedure for this network are similar to those for the shunt-connected network. However, the voltage scattering matrix for the series-nodes becomes[19]

$$S = \frac{1}{2}\begin{bmatrix} -1 & 1 & 1 & -1 \\ 1 & -1 & -1 & 1 \\ 1 & -1 & -1 & 1 \\ -1 & 1 & 1 & -1 \end{bmatrix} + I \qquad (3.3)$$

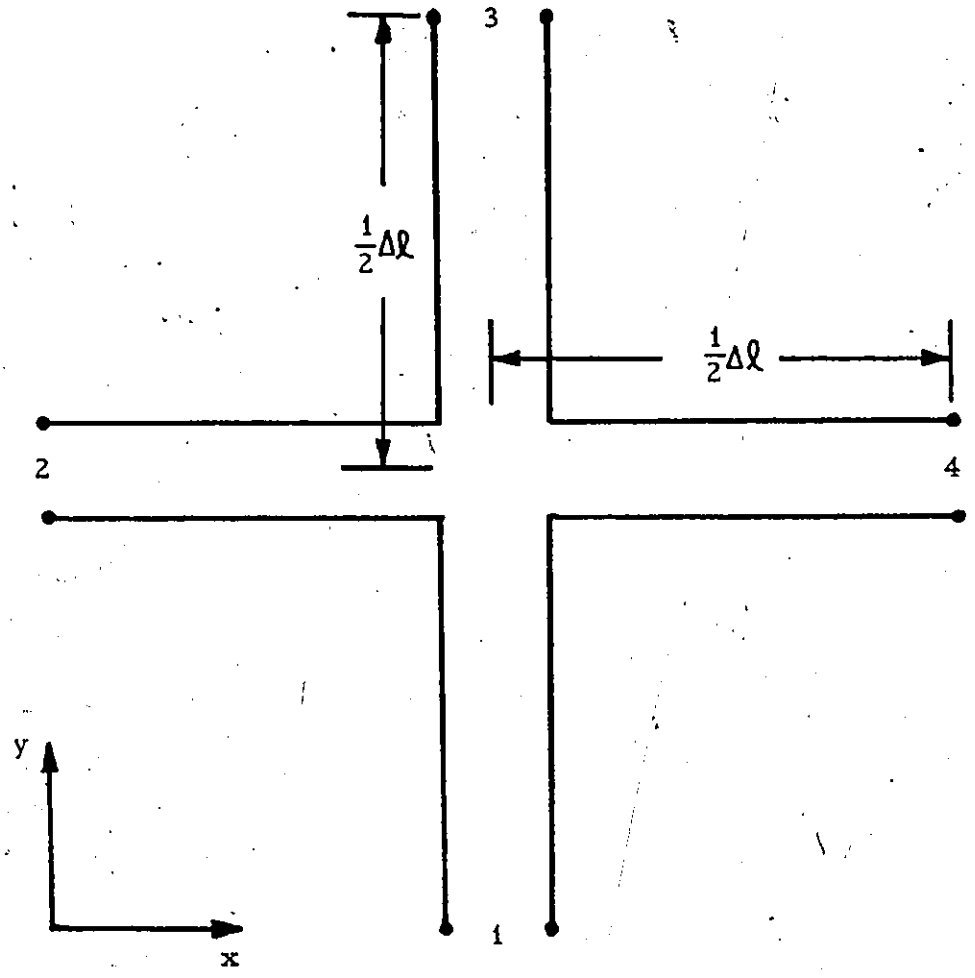

Figure3.3: Series-connected TLM node.

3.3 THE TLM SIMULATION AND THE COMPUTER PROGRAM

Fig.3.4 shows the cross section of a finned rectangular waveguide as well as its simulating TLM network consisting of shunt-connected transmission lines. Through the introduction of appropriate symmetry conditions, only one quarter of the cross section is required for the analysis of the TE_{10} mode. Note that in the TLM network, boundaries are dual to those in the real structure since the magnetic field is represented by the transmission line voltage in this case.

Based on the voltage scattering matrix in eqn.(3.1), a TLM program was written in FORTRAN IV and requires 4 locations to represent one node. The storage array required for a 16 x 8 matrix (see Fig.3.4) is thus 4 x 16 x 8 locations. An additional number of locations (usually 600) is required for temporary storage and final results. The reserved arrays and the program itself require a total core memory of about 10 K bytes. An IBM 360/65 System executes 800 iterations in about 8 seconds of CPU time.

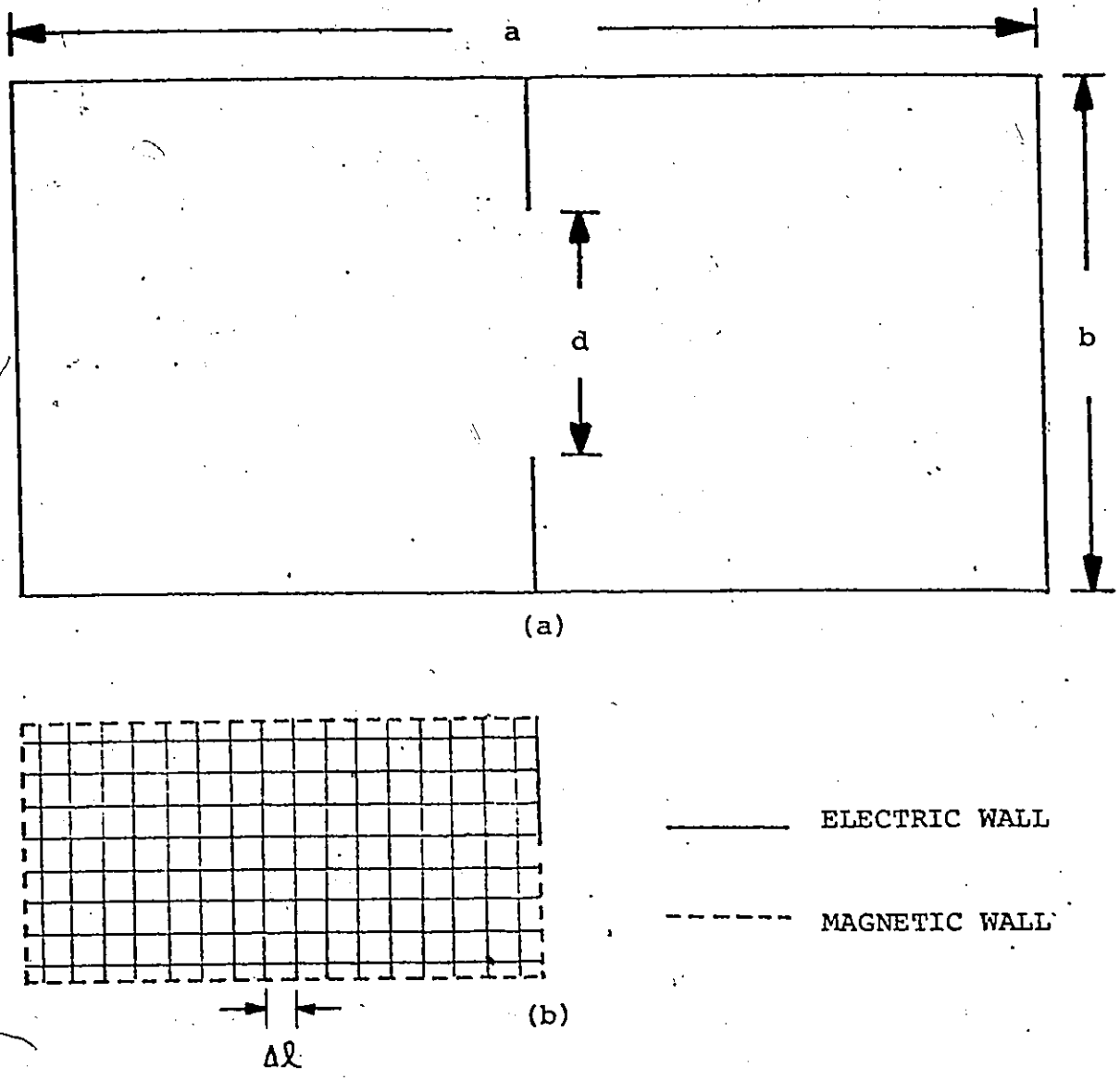

Figure3.4: (a). Cross section of finned waveguide.

(b). Equivalent two-dimensional shunt-node TLM network.

Through introduction of appropriate symmetry conditions, only one quarter of the cross-section is required for the analysis of the TE_{10}-mode. Note that in the TLM-network, boundaries are dual to those in the real structure.

3.4 ERROR ANALYSIS AND CORRECTION

3.4.1 Truncation Error

When the resonant frequency of a structure is evaluated with the TLM method, the impulse response of a transmission line network simulating this structure is computed, as described in the preceding section. In a practical calculation this impulse response must be limited in time. The error introduced by this limitation is the truncation error E_T. Its maximum value is determined [19] by:

$$E_T = \frac{\Delta S}{\Delta \ell / \lambda_C} = \pm \frac{3\lambda_C}{SN^2\pi^2\Delta\ell} \qquad (3.4)$$

where S is the frequency separation (expressed in terms of $\Delta\ell/\lambda$) between two neighboring peaks in the frequency response obtained from the impulse response via Fourier transformation. N is the number of iterations processed, $\Delta\ell$ is the mesh parameter of the transmission line lattice, and λ is the free space wavelength. The expression for E_T shows that the truncation error decreases when the separation S increases. It is therefore desirable to suppress all unwanted modes close to the mode of interest. This can be achieved by choosing appropriate input and output points in the TLM network and by introducing symmetry conditions.

Normally the truncation error is smaller than the maximum value obtained with the above formula, and decreases rapidly with an increasing number of iterations.

3.4.2 Velocity Error

Due to the slow wave characteristic of the transmission line lattice, the velocity of a wave traveling through this network depends on the angle between the propagation direction and the mesh axes. By assuming, however, as Johns and Beurle [21] suggested, that the propagation velocity is independent of the direction of propagation and equal to $c/\sqrt{2}$, a velocity error E is introduced.

If the wave propagates along one of the axes of the mesh, its propagation velocity is defined by the following equation

$$\sin\left(\frac{\beta_n \Delta \ell}{2}\right) = \sqrt{2}\,\sin\left(\frac{\omega \Delta \ell}{2c}\right) \tag{3.5}$$

$\beta_n = 2\pi/\lambda_n$, where λ_n is the wavelength of propagation along this axis. Thus, if a rectangular waveguide is treated with the TLM method, the velocity error can be eliminated in the case of the TE_{10} mode by determining the wave velocity in the direction of the broad wall directly from equation (3.5).

To demonstrate the effectiveness of the correction of the velocity error, Table 3.1 lists the values for the cutoff frequency of the TE_{10} mode in a rectangular waveguide of aspect ratio $b/a = 1/2$, obtained with the TLM method using different mesh sizes. In all calculations, the number of iterations was sufficiently high to keep the truncation error below 0.2 percent. It is found that, by assuming a velocity of $c/\sqrt{2}$, the coarsest mesh yields a cutoff frequency which is too low by 5.7 percent. If, however, eqn.(3.5) is applied to correct the velocity error, the remaining inaccuracy is negligible and may be attributed to truncation (< 0.2%).

In finned rectangular waveguides, the velocity error in the TE_{10} cutoff frequency may be practically eliminated by applying eqn.(3.5) in spite of the fact that in the immediate vicinity of the fins, the wave propagation does not exactly coincide with a mesh axis. Even if the residual velocity error is not negligible, it will be automatically eliminated when correcting the so-called coarseness errors described below.

3.4.3 Coarseness Error

It has been shown in the previous section that the TLM evaluation of the fundamental cutoff frequency in rectangular waveguides is quite accurate, even if a very

Number of nodes along side b $b/\Delta\ell$	Assumption: $v = c/\sqrt{2}$ as proposed in [1]		Assumption: V as defined by eq.(3.5)		Accurate value
	Normalized TE_{10} cutoff frequency b/λ_c	Velocity plus truncation errors $E_V + E_T$(%)	Normalized TE_{10} cutoff frequency b/λ_c	Velocity plus truncation errors $E_V + E_T$(%)	b/λ_c
1	0.23570	-5.7	0.25003	0.01	
2	0.24667	-1.3	0.24996	-0.02	
4	0.24924	-0.3	0.25005	0.02	0.25
8	0.24974	-0.1	0.24994	-0.02	
16	0.24981	-0.08	0.24986	-0.06	

TABLE 3.1: Comparison of the TLM solutions of b/λ_c in rectangular waveguides using different mesh sizes.

coarse mesh is used, provided that the velocity error is corrected. However, if transverse discontinuities (e.g. ridges or fins) are present in the guides, the TLM mesh must be fine enough to resolve the fields in the regions where the gradient of the electric potential is highest. The question is, in other words, how many nodes should be chosen in the immediate vicinity of the discontinuity in order to keep the error due to mesh coarseness within desired limits?

Unfortunately, there are no general rules or equations to evaluate this error. In order to study its behavior in the case of finned waveguides, the normalized TE_{10} cutoff frequency, b/λ_c, of the guide shown in Fig3.4 was calculated using several mesh sizes. An aspect ratio of $b/a = 1/2$ was chosen, and several values of $b/\Delta\ell$ were selected for the mesh parameter. The corresponding TE_{10} cutoff frequencies are presented in Fig.3.5. Note that in all cases, the error due to truncation is smaller than 0.2 percent, and the velocity error is negligible after corrections according to eqn.(3.5) . Circles represent the results obtained for a normalized gap width of $d/b = 1/2$, and triangles correspond to $d/b = 1/4$.

It appears that the normalized cutoff frequency of the fundamental mode increases practically linearly as $\Delta\ell/b$

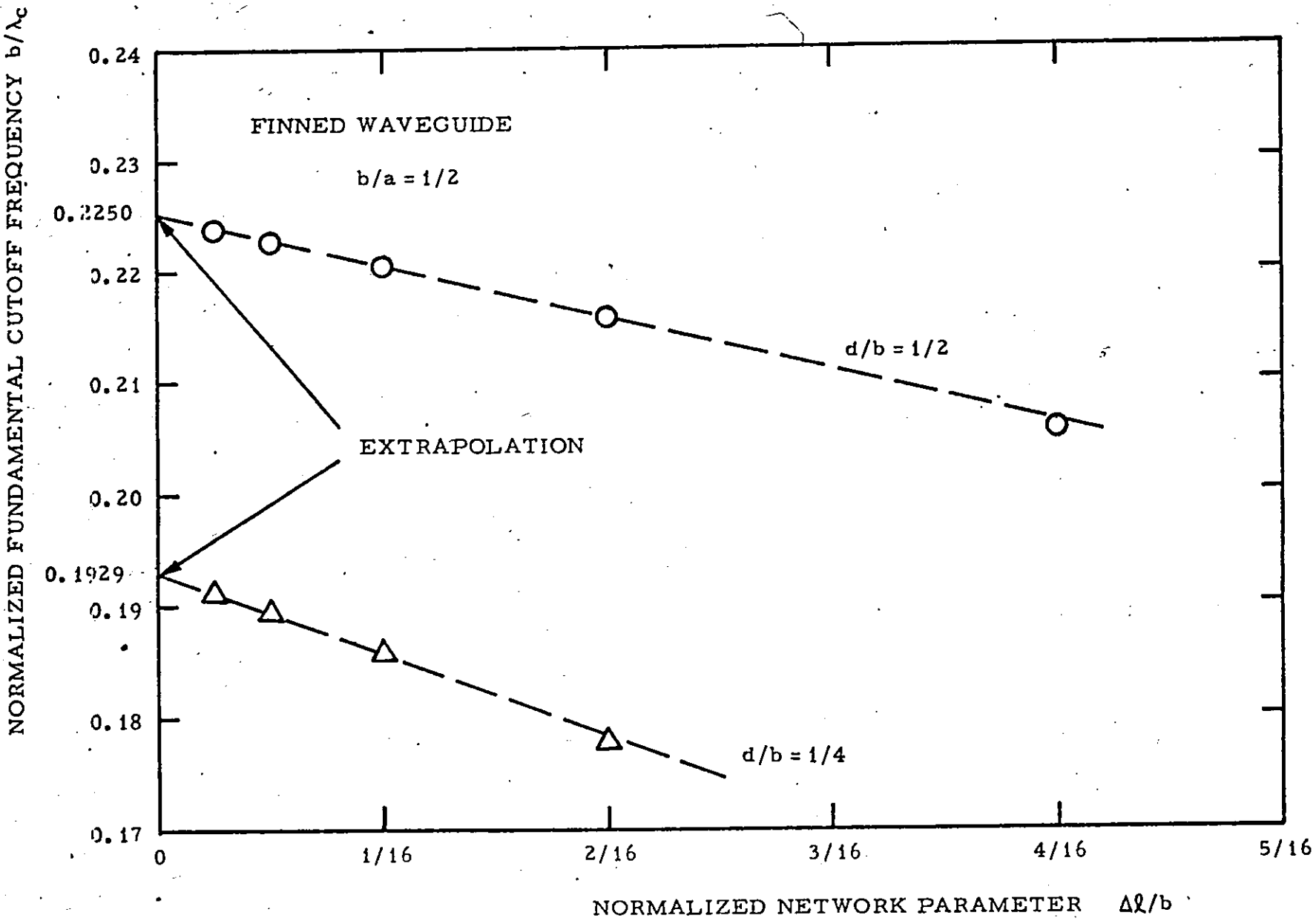

Figure 3.5 Linear extrapolation minimizing the errors affecting TLM solutions of b/λ_c in finned waveguide.

decreases. The coarseness error can thus be dramatically reduced by linear extrapolation toward $\Delta\ell/b=0$. Using this procedure, the cutoff frequency is determined by extrapolation using a straight line fitted through the points corresponding to different values of the mesh parameter $\Delta\ell/b$, as illustrated in Fig.3.5.

Furthermore, the dependence of the coarseness error on the number of nodes situated within the gap separating the fins has been investigated. (The error was always evaluated with respect to the extrapolated value of the cutoff frequency.) Fig.3.6 shows this error in percent as a function of the normalized gap width d/b. The waveguide aspect ratio was kept constant at b/a = 1/2, and calculations have been made with two, four and eight nodes situated between the fins. It appears that whatever the coarseness of the TLM mesh, the error is always maximum in the vicinity of d/b = 1/2, which is henceforth considered to be the "worst case".

Assuming this worst case to prevail, the coarseness error was then evaluated for various values of $\Delta\ell/a$ and presented in Fig.3.7. Since d/b is constant (equal to 1/2), the circles represent the maximum coarseness error for finned guides of various aspect ratio b/a, all featuring two nodes between the fins. Triangles correspond to four nodes

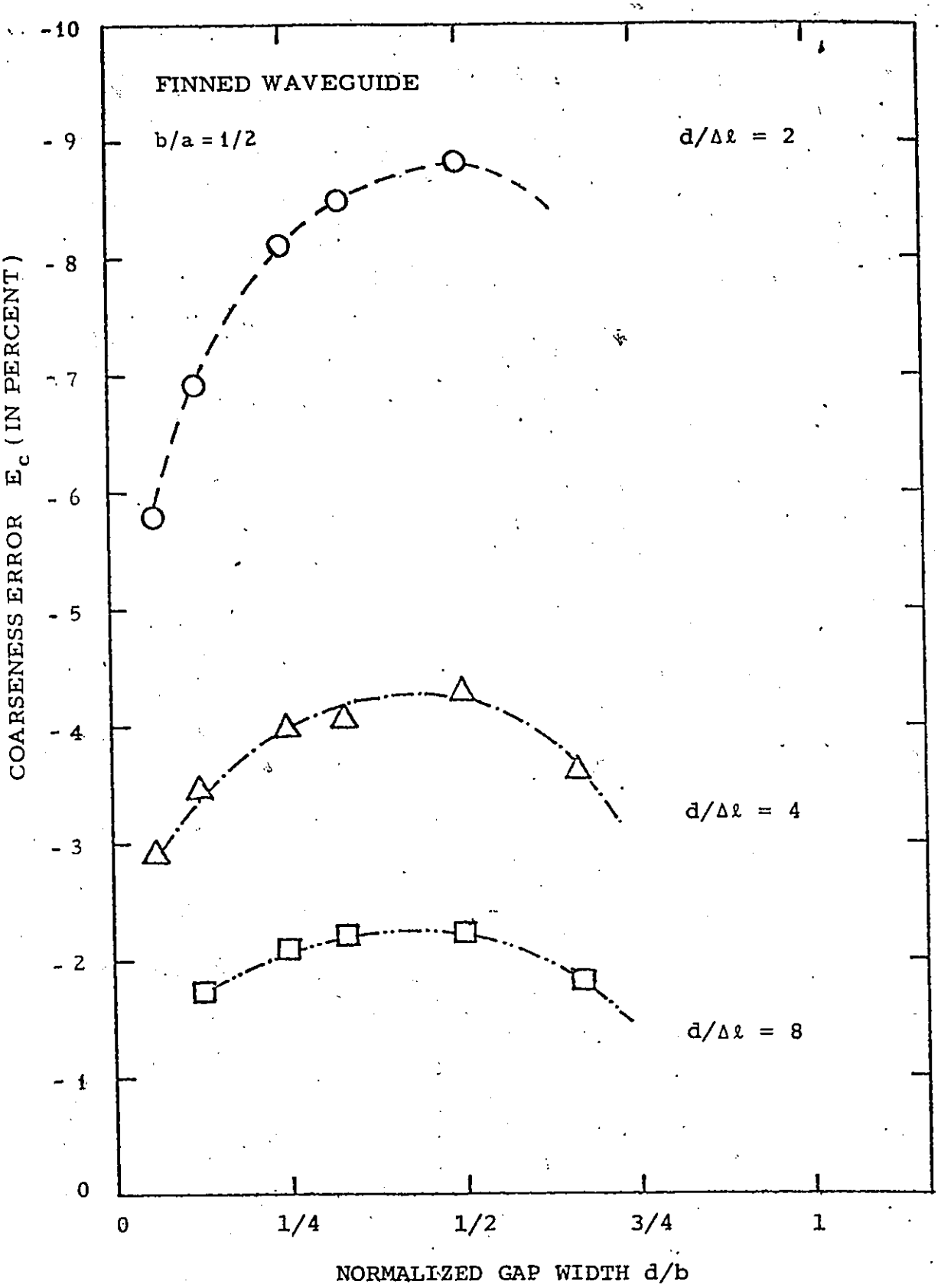

Figure3.6: Coarseness error affecting the TLM solutions of b/λ_c for the TE_{10} mode in finned waveguide.

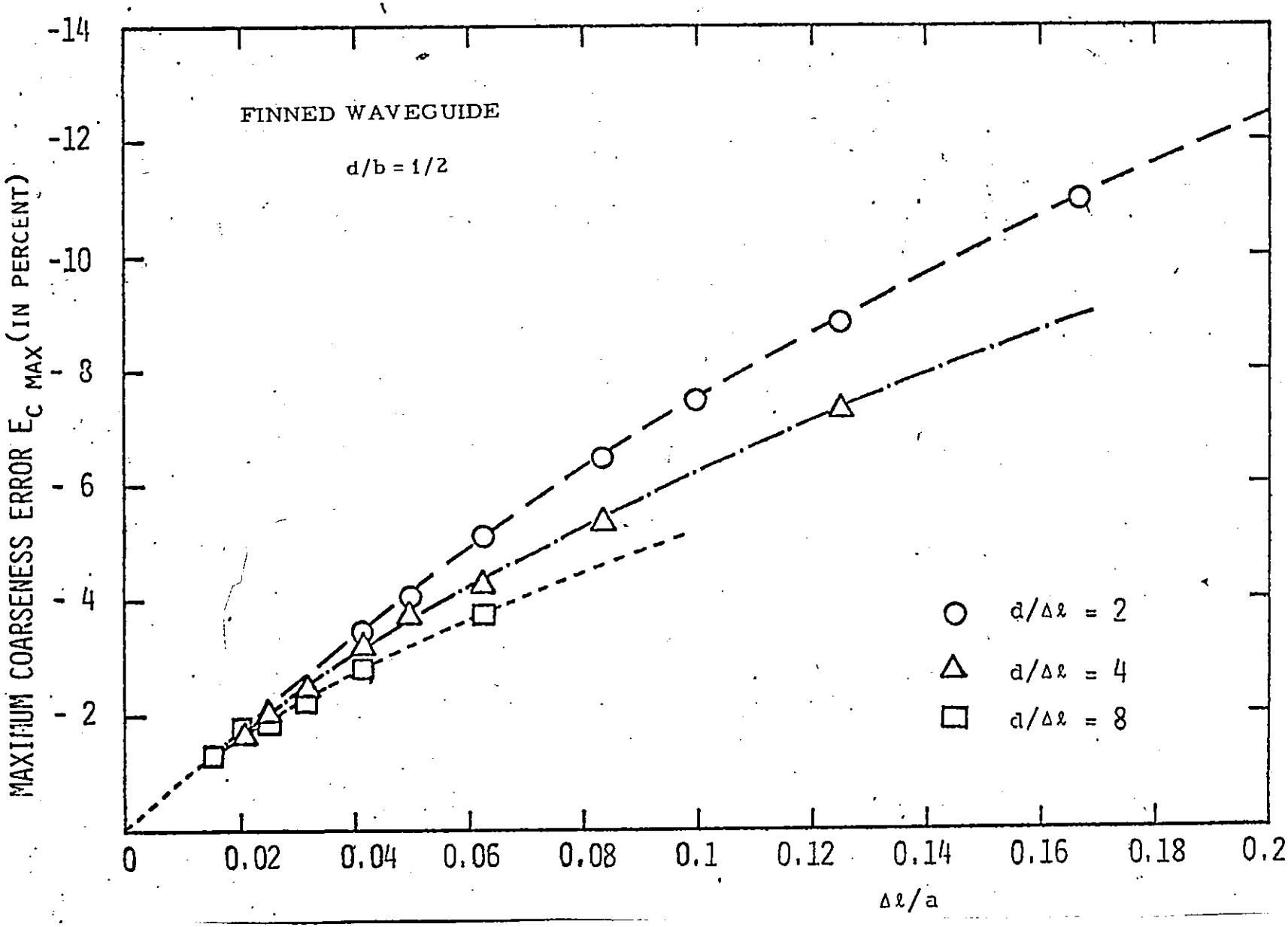

Figure 3.7: Maximum coarseness error affecting the TLM solutions of b/λ_c for the TE_{10} mode in finned waveguides.

between fins, and squares to eight nodes. Hence, it is possible to deduce the maximum coarseness error when calculating the cutoff frequency of the lowest mode of propagation in a finned rectangular waveguide with the TLM method from Fig.3.7.

3.5 RESULTS

Table3.2 shows the extrapolated values of b/λ_c in finned waveguides for various gap widths d/b. For comparison, the cutoff frequencies calculated with a special finite element program[1] and with the transverse resonance method [23] are also shown. Excellent agreement exists between these methods.

---

[1]to be published.

Normalized Gap Width d/b	Normalized TE_{10} cutoff frequency (b/λ_c)				Standard Deviation in %
	FE method	TLM method	TR method	Average value	
1	0.25000	--	0.25000	0.25000	0
2/3	--	0.2391	0.2389		
1/2	0.22577	0.2253	0.22492	0.22533	0.2
1/3	--	0.2054	0.2052		
1/4	0.19414	0.1932	0.19277	0.19337	0.4
1/8	0.17099	0.1697	0.16905	0.16991	0.6
1/16	--	0.1522	0.15183		

TABLE3.2: Comparison of the values of b/λ_c for the TE_{10} mode in finned waveguides obtained using the TLM, FE and TR methods.

3.6 DISCUSSION

When the cutoff frequency of the TE_{10} mode in finned waveguides is calculated with the TLM method, truncation, velocity and coarseness errors occur.

The truncation error can be evaluated easily using eqn.(3.4). The velocity error can be corrected by applying eqn.(3.5). The coarseness error, which is the dominant error in the structure discussed here, was found to be maximum for a normalized gap width of $d/b = 1/2$, regardless of the aspect ratio b/a and the coarseness of the TLM mesh. Its value can be predicted with the aid of Fig.3.11 for a wide range of guide dimensions and mesh sizes. More important, the coarseness error can be eliminated by linearly extrapolating results obtained with lattices of different mesh parameters. For reasons of geometrical similarity, this study is relevant to the TLM analysis of fin lines, since the latter differ from finned waveguides only by the presence of a thin dielectric sheet of low permittivity adjacent to the fins.

Chapter IV

ANALYSIS OF FINNED WAVEGUIDES USING A THREE-DIMENSIONAL TLM METHOD

4.1 SHORT DESCRIPTION OF THE THREE-DIMENSIONAL TLM METHOD

The three-dimensional TLM method has been fully developed by Akhtarzad and Johns [24,25,26] to evaluate structures such as inhomogeneous waveguide cavities [25] and microstrip resonators [26].

In order to represent a three-dimensional space, a new TLM model was developed[25,26] by interlacing the two-dimensional shunt-connected and series-connected networks. Each three-dimensional TLM node consists of three shunt nodes and three series nodes as shown in Fig.4.1. There is a shunt node in each of the co-ordinate planes, the voltage across which represents E_x E_y and E_z and a series node in each of the planes, with currents representing H_x H_y and H_z. To accommodate discontinuities such as slabs of dielectric or magnetic materials, open-circuited and shunt-circuited stubs of variable normalized characteristic constants Y_o and Z_o are added to shunt and series nodes, respectively[19,24]. Note here that the spacing between the individual two-dimensional nodes and the length of stubs are

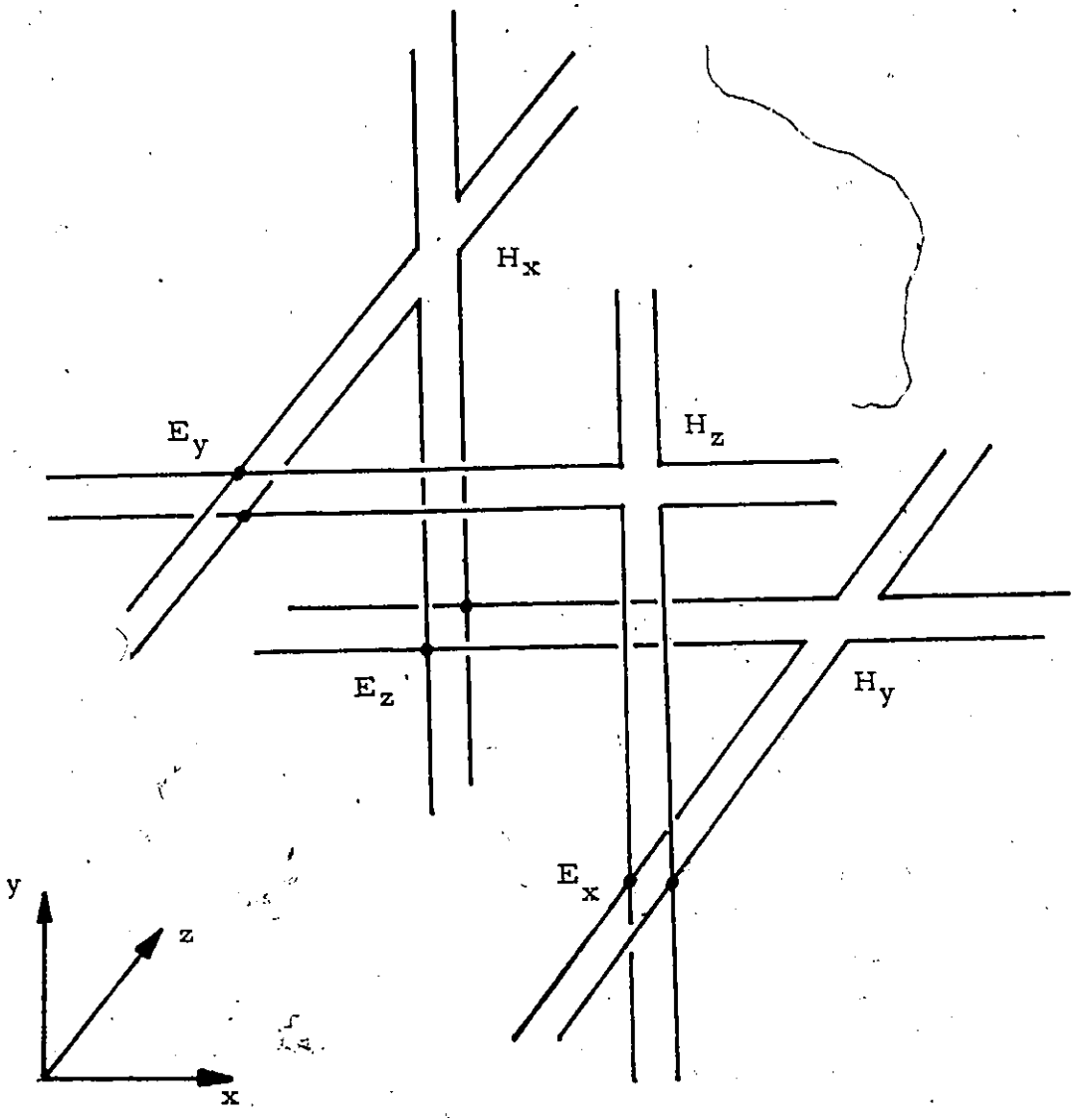

Figure 4.1: A three-dimensional TLM node.

$\Delta\ell/2$. The three-dimensional geometry of a problem is set up by connecting many such three-dimensional nodes together.

Conducting boundaries are simulated in the model by short-circuiting the the individual shunt nodes in the plane of the boundary. Open-circuited planes may be utilized to make use of the onefold, twofold, or threefold symmetries of a particular structure, thus considerably reducing both the memory size and the execution time requirement of a program. An open circuit plane may be simulated by open-circuiting the individual series nodes lying in that plane.

The impulse response of the network representing a medium is then evaluated by a numerical routine based on the voltage impulse scattering matrix of the individual two-dimensional nodes forming the three-dimensional node as expressed in eqns. (3.2) and (3.3). For the purpose of analysis, any of the six EM field components is excited by introducing impulses at various points in the network. These impulses travel along the ideal transmission lines, are scattered on the individual two-dimensional nodes, and spread out filling the whole model. In this way, the time domain propagation of all six EM field compononts is obtained simultaneously. A solution for any (or all) of the field components is available anywhere within the geometry of the problem. The output consists of a stream of impulses

whose amplitudes correspond to the output impulse function for the particular field component under consideration. Finally, the Fourier transformation of this function is taken to yield the frequency response of the structure.

A FORTRAN program based on the preceding analysis has been written [24]. This program is actually an extension of the two-dimensional program. All the information relating to a three-dimensional structure, such as conducting boundaries, strip patterns, permeability and permittivity at different points, is simply fed into the computer.

4.2 ERROR ANALYSIS

4.2.1 Truncation Error and Velocity Error

To obtain the resonant frequency of a closed structure using the three-dimensional TLM method, the impulse response of the simulating network must be truncated in time. This gives rise to a truncation error whose maximum value can be predicted by eqn. (3.4).

Because of the directional dependence of the wave propagation velocity in the TLM network, a velocity error results from the assumption of constant speed in all directions. Only when the network parameter $\Delta\ell$ is small compared with the wavelength, is this error negligible. Besides, the velocity error is also practically eliminated by the extrapolation technique for error correction [9].

4.2.2 Coarseness Error

In chapter III, the coarseness error associated with the two-dimensional TLM solution has been defined and analyzed. This error occurs because the TLM simulation can not perfectly resolve the nonuniform field distribution in the structure due to the finite mesh size of the matrix.

The dispersion characteristic of a finned waveguide is expressed by the formula

$$(b/\lambda_g)^2 = (b/\lambda)^2 - (b/\lambda_c)^2 \qquad (4.1)$$

where λ, λ_c, and λ_g are the free-space, cutoff, and guided wavelengths, respectively. Since the two-dimensional TLM program yields, after error correction, the cutoff in finned waveguides with high accuracy, eqn.(4.1) represents a very accurate relation between b/λ and b/λ_g. Based on this, the errors associated with the three-dimensional TLM solutions will be analyzed.

In order to directly calculate the dispersion in finned guides, a cavity of variable length is formed by placing two short-circuited walls on two cross sections at a distance ℓ from each other as shown in Fig.4.2. The resonant frequencies are then calculated using the three-dimensional TLM program. At the resonant frequency corresponding to the TE_{10} mode, ℓ is equal to 1/2 of the guide wavelength λ_g.

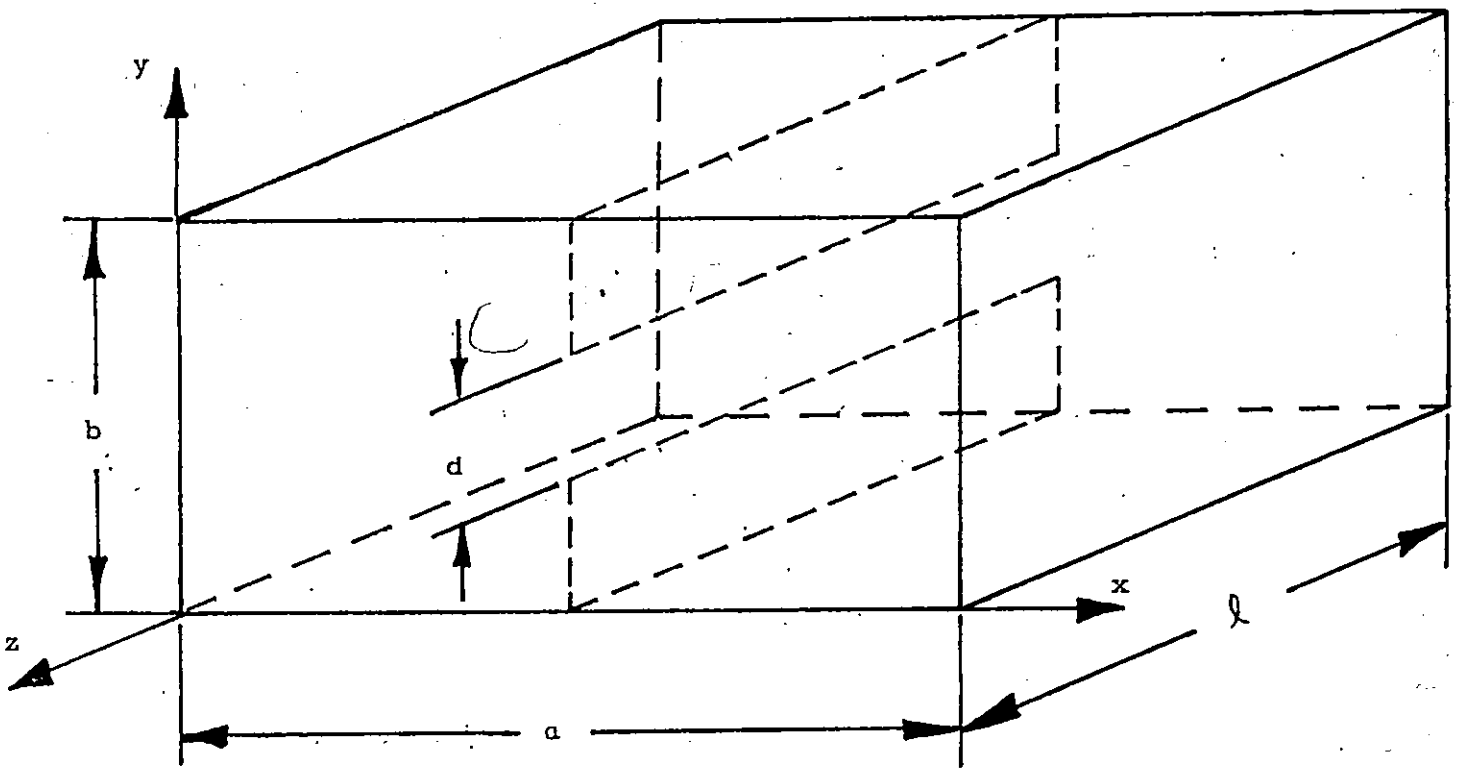

Figure 4.2: Finned waveguide cavity.

The percentage error in the normalized resonant frequency (b/λ) thus obtained is shown in Fig.4.3 as a function of $\Delta\ell/\ell$. The waveguide aspect ratio b/a was kept constant at 1/2 and various gap widths and mesh sizes were used. Systematically, the errors drop quickly at first, pass through a minimum and rise again as $\Delta\ell/\ell$ increases.

To gain further insight into the nature of the coarseness error, the dielectric slab loaded waveguide shown in Fig.4.4 was studied. The total error in b/λ is plotted as a function of $\Delta\ell/\ell$ in Fig.4.5 for various thicknesses of the dielectric slab and several mesh sizes of the TLM network. The error increases as $\Delta\ell/\ell$ increases and is not affected too much by a change in the slab thickness and in the mesh size.

A comparison of Fig.4.3 and 4.5 shows that in both cases, the error increases with $\Delta\ell/\ell$ except for the region close to cutoff ($\Delta\ell/\ell = 0$), where the finned waveguide solution again shows a considerable increase in coarseness error. It is very probable that this discrepancy resides in the "transverse coarseness error" reflecting insufficient resolution of transverse fields as discussed in chapter III. While in finned waveguides, this error is quite important, no significant coarseness error has been found in the two-dimensional analysis of the slab-loaded waveguide since

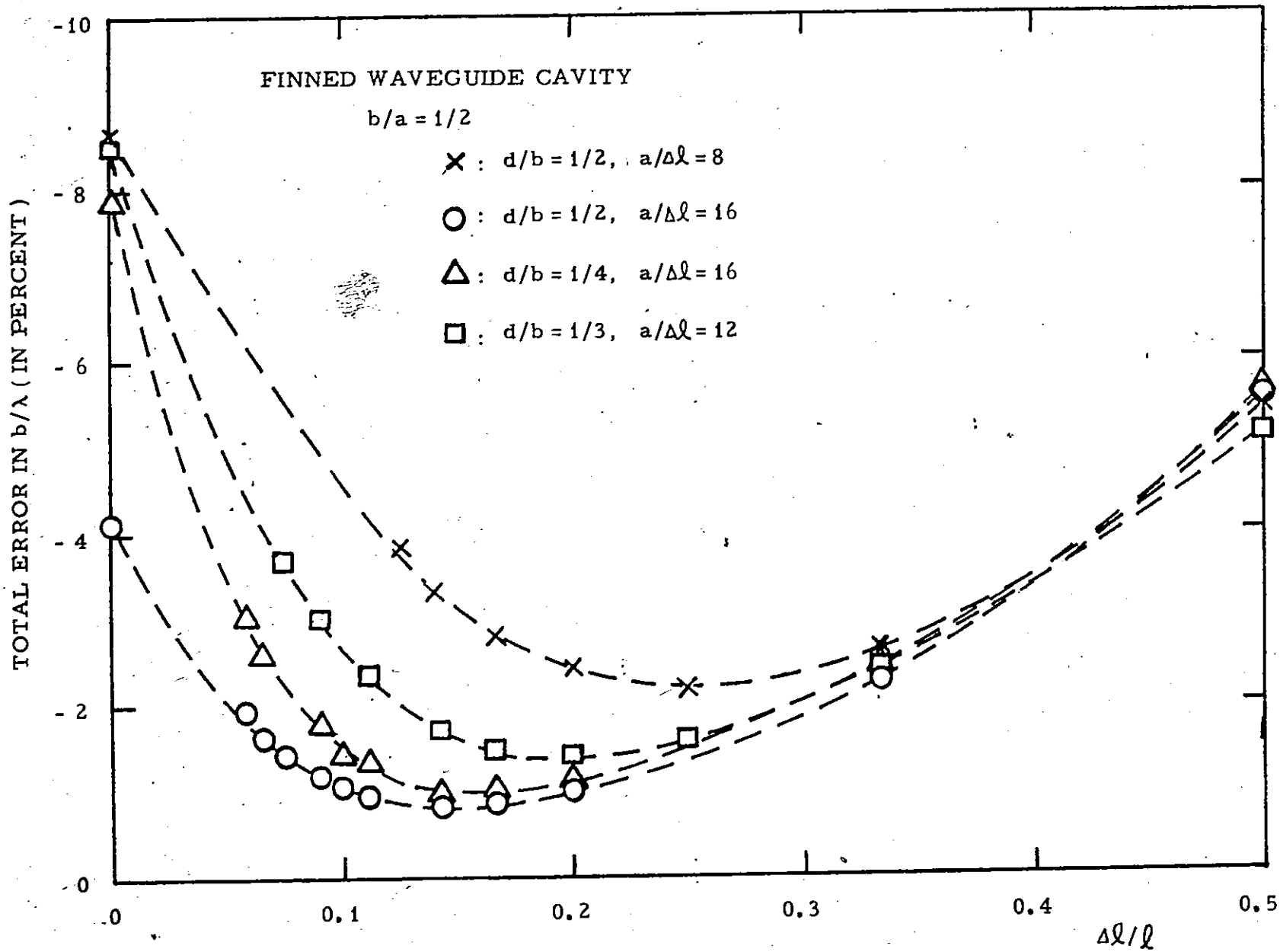

Figure4.3: The coarseness error affecting the three-dimensional TLM solutions of b/λ in finned waveguides.

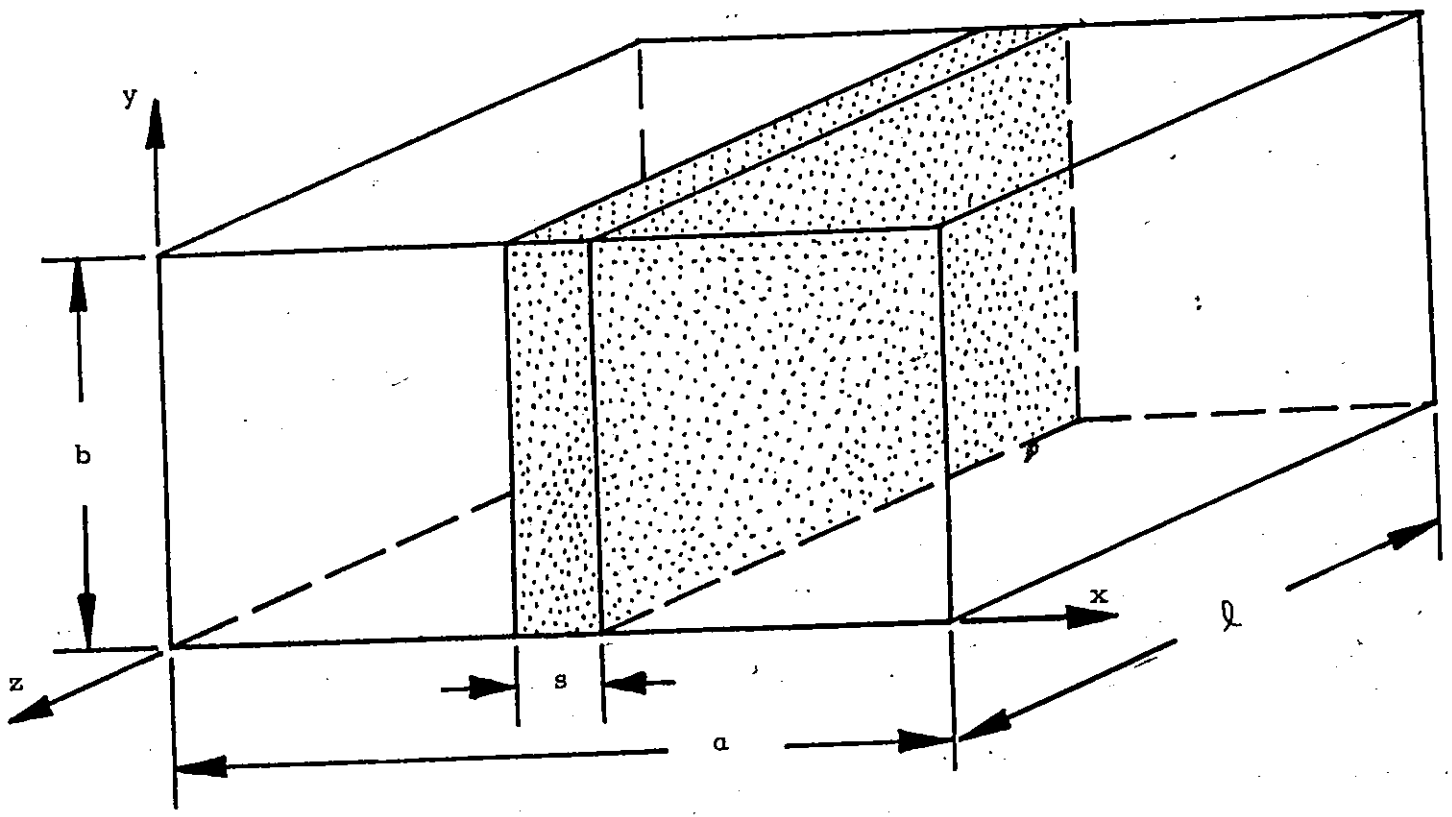

Figure 4.4: Slab-loaded waveguide cavity.

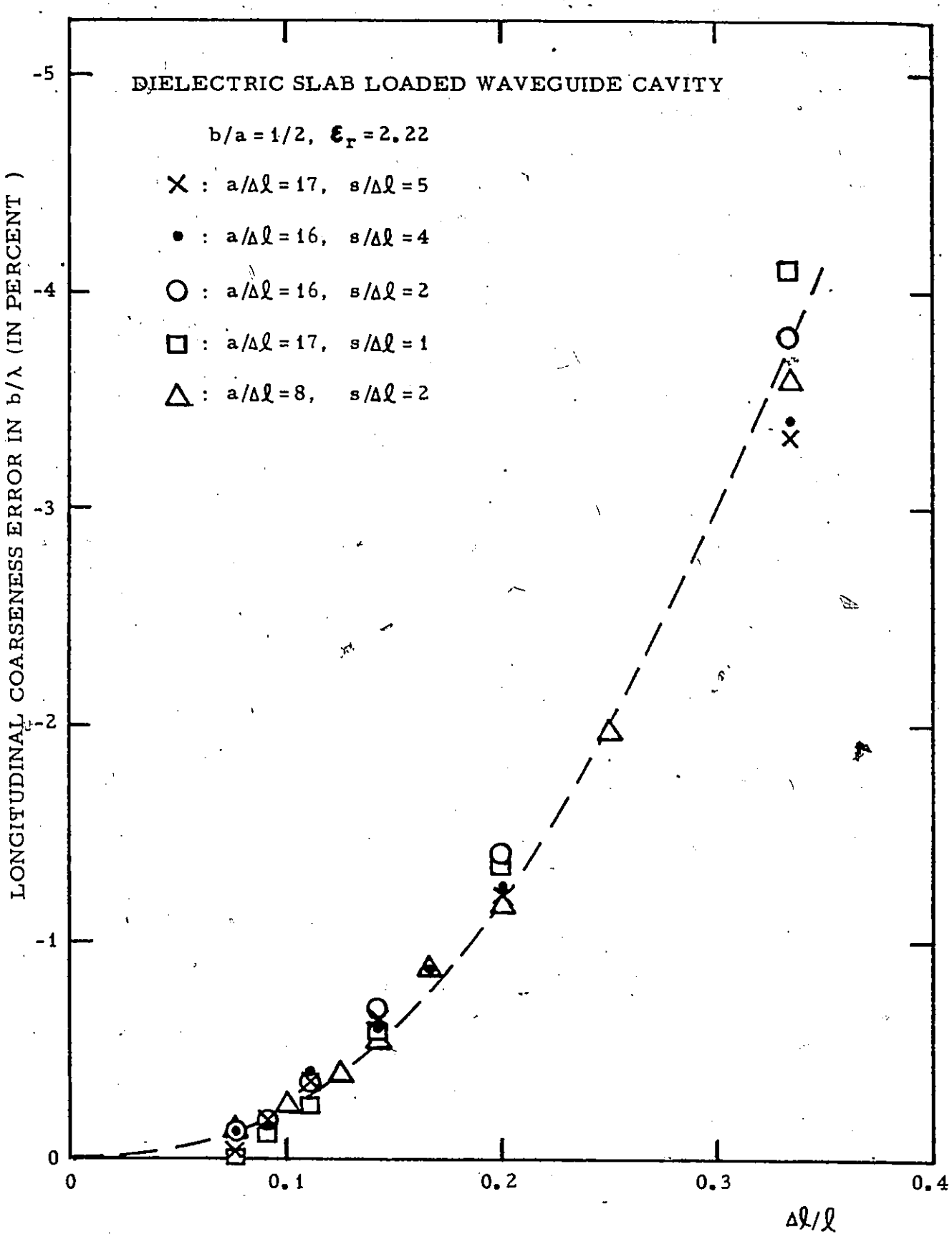

Figure 4.5: The coarseness error affecting the three-dimensional TLM solutions in slab-loaded waveguide.

the slab does not create any higher order modes resulting in high non-uniformity of the transverse fields[2].

Assume that the coarseness error at cutoff contributes an error component to the total coarseness error in b/λ according to equation (4.1). This error component is thus given by

$$E_{(b/\lambda)} = E_{(b/\lambda)} \cdot (b/\lambda_c)^2 / (b/\lambda)^2 \qquad (4.2)$$

where $E_{(b/\lambda_c)}$ is the "transverse coarseness error" in the two-dimensional TLM solution.

When the transverse coarseness error component is eliminated from Fig.4.3, the characteristic shown in Fig.4.6 results. This "longitudinal coarseness error" behaves like the error shown in Fig.4.5. It depends mainly on the number of nodes along the longitudinal direction (i.e. $\ell/\Delta\ell$) and is suspected to occur due to the loss of information on the series nodes situated on the short-circuiting end walls.

---

[2]See appendix B.

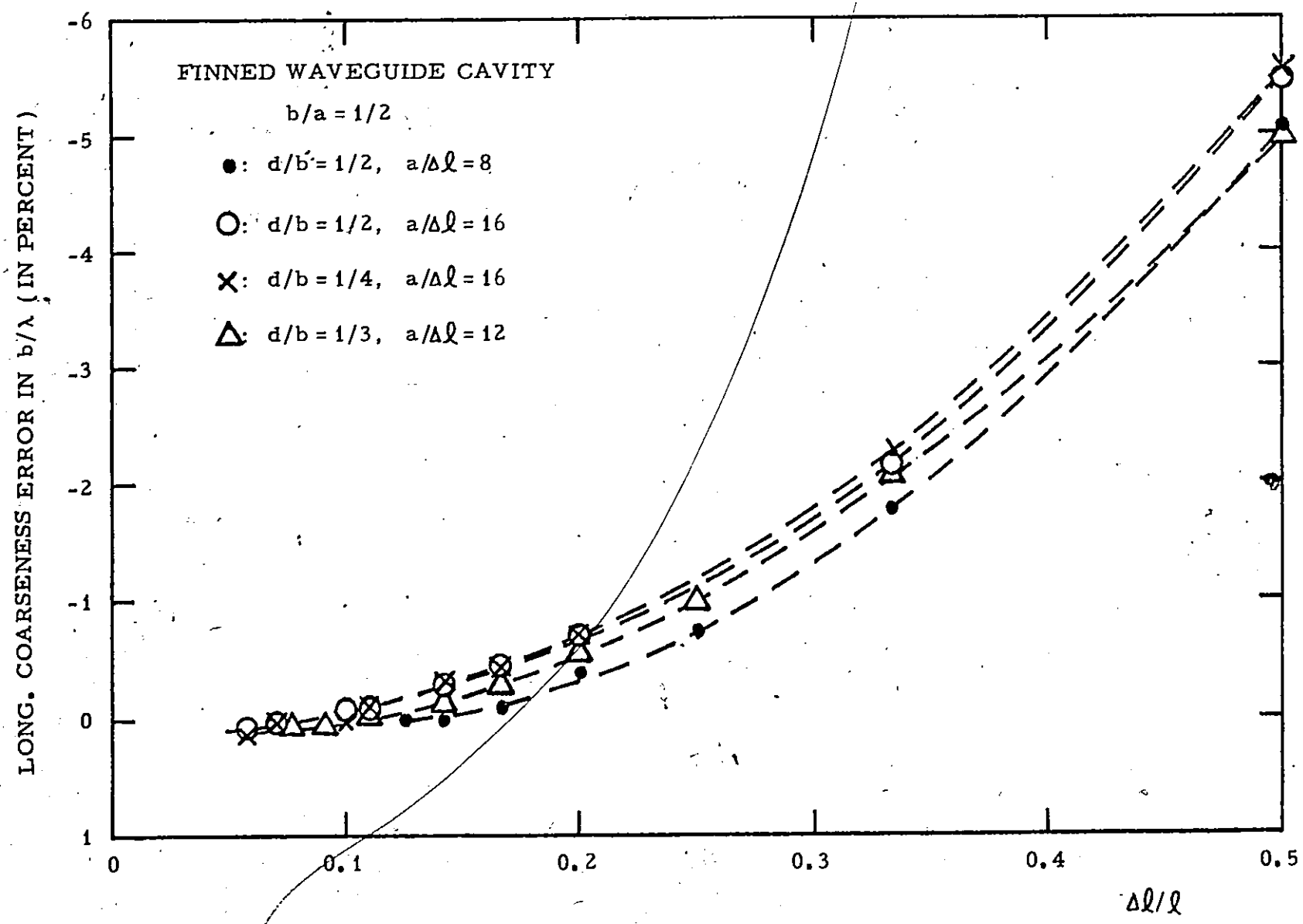

Figure 4.6: The longitudinal coarseness error component in the three-dimensional TLM solutions of finned waveguides.

4.3 DISCUSSION

The errors affecting the three-dimensional TLM solution have been classified as the truncation error, the velocity error and the coarseness error. Among them, the coarseness error is usually the most significant.

The curves in Fig.4.3 and 4.5 may be used for the error rectification of the three-dimensional analysis of finned waveguides and dielectric slab loaded waveguides, respectively. Also, they may be considered as a guide to the error evaluation of the three-dimensional TLM analysis of fin lines.

Chapter V

ANALYSIS OF FIN LINES USING TWO-DIMENSIONAL TLM METHOD

5.1 INTRODUCTION

Various methods for evaluating the electrical parameters of fin lines have been presented by Meier[1], Hofmann[2], Saad and Begemann[7], Chang and Itoh[8], Hoefer[23] and Hoefer and Ros[11]. The purpose of this chapter is to present results for the general fin line case which are sufficiently accurate to serve as a reference for other methods of fin line analysis. The two-dimensional Transmission-Line Matrix (TLM) program described before was used in this study.

Since the two-dimensional program yields only the cutoff frequencies of the fundamental and higher order modes of the structure, it does not directly yield the dispersion characteristic because of the inhomogeneous nature of the dielectric constant in the fin line cross section. However, by using the method of transverse resonance and by evaluating the equivalent susceptance of the fin via the TLM solution at cutoff,[3] the dispersion can be predicted

---

[3]To be discussed in chapter VII.

accurately enough for all practical purposes. Therefore, an accurate knowledge of the cutoff wavelength is useful beyond the scope of determining the frequencies at which each mode begins to propagate.

In the following, the cutoff frequencies of the fundamental and first higher order mode are determined in unilateral, bilateral and insulated fin lines. These modes become the TE_{10} and TE_{20} waveguide modes in the limit $d/b \rightarrow 1$. Errors associated with the TLM method are carefully corrected to ensure that results are accurate within 1 percent. Results obtained with a finite element program agree with the TLM solutions within that error margin.

In addition, the field distributions in fin lines are available at the same time from the TLM program. Plots for electric field lines in unilateral and insulated fin lines are also presented.

5.2 THE TLM SIMULATION

In order to reduce computational efforts to a minimum, electric and/or magnetic walls are introduced in the cross section to take advantage of symmetry. This arrangement also suppresses some unwanted higher order modes which could increase the truncation error. The cutoff frequencies of the desired modes can thus be determined more accurately[20].

Fig.5.1 shows the cross sections of three types of fin lines and their simulating TLM networks for the determination of the fundamental mode cutoff. The dielectric substrate is simulated by loading the corresponding nodes with open-stubs[19].

Since a shunt-connected transmission line matrix[20] is used to simulate transverse wave propagation in the fin line structure, the longitudinal magnetic field H_z is represented by a voltage in the TLM network. Therefore, boundary conditions in the TLM model are dual to those in the real structure, i.e., magnetic walls in the model correspond to electric walls in the fin line and vice versa. The impulse response of the network yields, after Fourier transforming, the spectrum of eigenmodes in the structure.

A typical program for a unilateral fin line simulated by a 34 x 10 TLM matrix requires a core memory of 17 K bytes. Programs of this size can easily be implemented on a PDP-11/34 computer. When 1200 iterations are executed on an IBM 360/65, the required CPU time is about 80 seconds. For bilateral and insulated fin lines, half the CPU time and half the TLM matrix storage are required. To evaluate the cutoff for the second order mode, an electric wall must be inserted in the center of the bilateral and insulated fin lines. This amounts to introducing a magnetic wall at

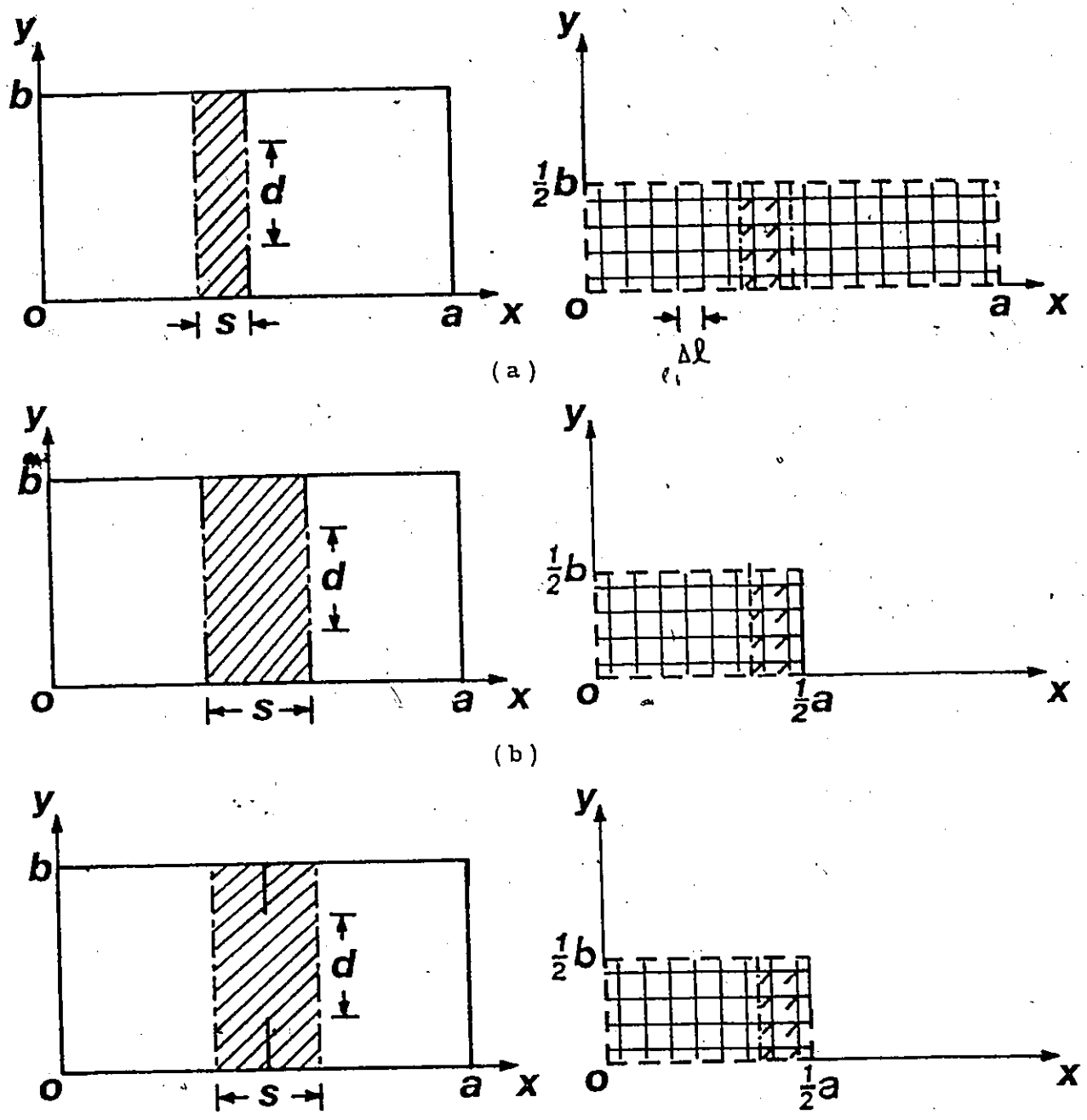

Figure 5.1: Cross sections and equivalent TLM networks of (a) unilateral, (b) bilateral and (c) insulated fin lines.

$x = a/2$ in the TLM networks. The second order mode then corresponds to the first resonance in this modified TLM model. For the unilateral fin line, the TLM model is the same for both the fundamental and second order modes which correspond to the first and second resonant frequencies respectively.

5.3 ERROR SOURCES AND CORRECTION

The three principal errors affecting the TLM solution are the truncation, velocity and coarseness errors.

5.3.1 Truncation Error and Velocity error

Truncation error stems from the necessity to limit the impulse response of the TLM network in time. The maximum truncation error can be predicted by equation (3.4). For the calculations in this chapter, the number of iterations was always kept sufficiently large so that the truncation error was negligible (< 0.1%).

If the wavelength in the TLM network is large compared with the network parameter $\Delta\ell$ ($\lambda_n > 10\Delta\ell$), it can be assumed that the fields propagate with the same velocity $v_n = v_m/\sqrt{2}$ in all directions. (v_m is the propagation velocity in the medium filling the real structure). However, if the network parameter $\Delta\ell$ is commensurate with

the wavelength λ_n, the velocity of propagation depends on the direction. In this case, the assumption of constant velocity in the network leads to a velocity error[20].

In practice, the substrate thickness in fin lines is small compared with the waveguide dimensions. In order to accurately represent the field distribution in the substrate, at least two TLM nodes must be situated in the dielectric. It follows that $\Delta\ell \leq s/2$ where s is the substrate thickness. Thus, the velocity error is negligible as long as $s/a << 0.2$. Even in cases where the velocity error is not negligible, it will be automatically eliminated when the coarseness error is corrected, as discussed later. It is therefore not necessary to correct the velocity error separately.

5.3.2 Coarseness Error

For all three fin-line structures, the TLM solutions of the fundamental frequency increases practically linearly as $\Delta\ell/b$ decreases (see Fig.5.2). It can thus be dramatically reduced by linear extrapolation toward $\Delta\ell/b = 0$ exactly as in the case of the finned waveguide in chapter III. To this end, the cutoff frequency is extrapolated by fitting a line through three frequency values corresponding to three different mesh parameters $\Delta\ell$, as demonstrated in Fig.5.2.

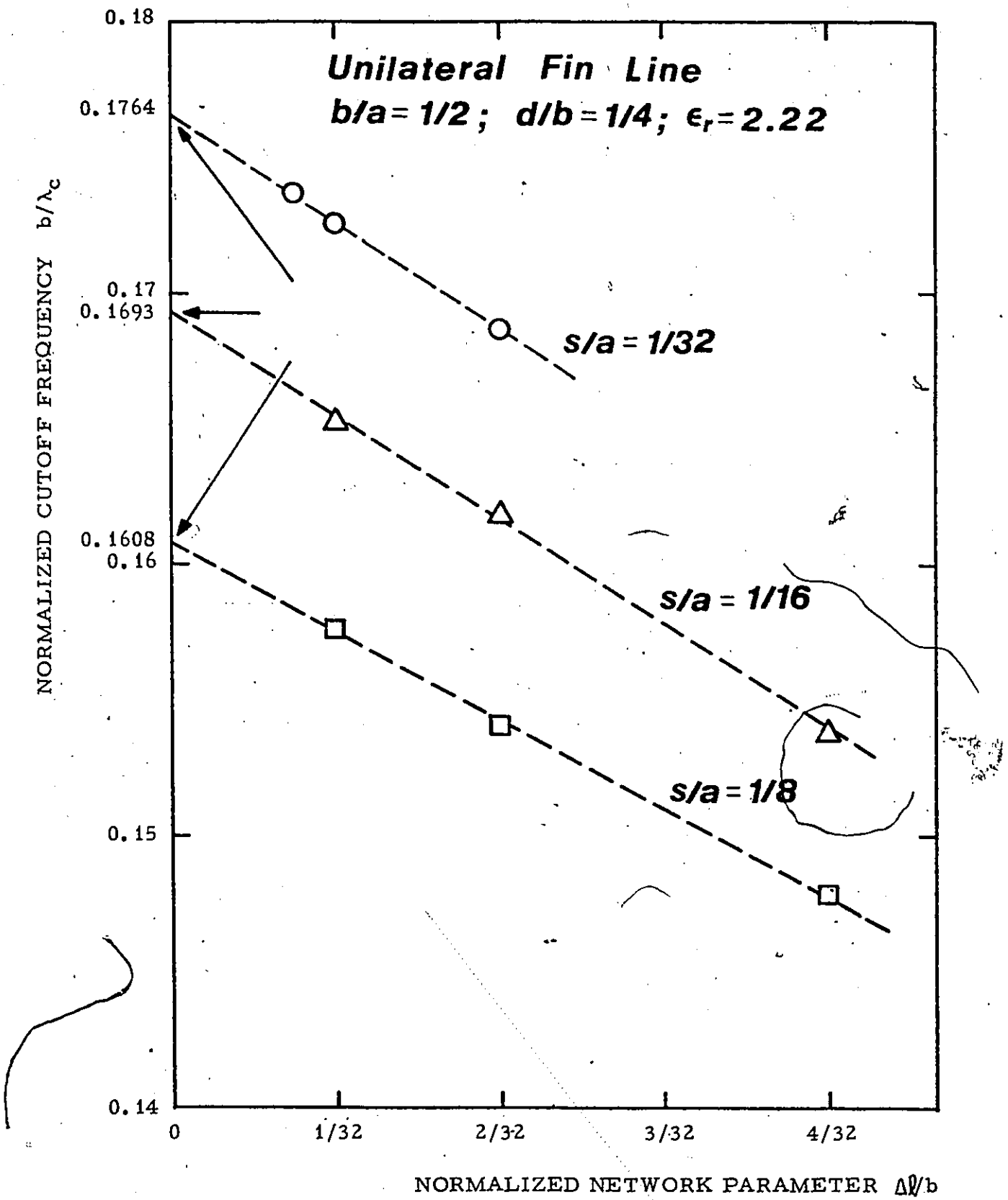

Figure 5.2: Extrapolation technique minimizing errors in the fundamental cutoff frequency b/λ_c.

In the calculation of the second order mode cutoff, the relationship between the cutoff frequency and the network parameter $\Delta\ell$ is no longer linear because velocity error becomes significant (see Fig.5.3). Nevertheless, fairly accurate extrapolation can be achieved by fitting a logarithmic function through the calculated points and determining its value for $\Delta\ell = 0$.

5.3.3 Overall Error

In chapter III we have evaluated the cutoff frequencies of finned waveguides (identical to fin lines with dielectric constant $\varepsilon_r = 1$) using three completely different methods, namely the transverse resonance method, the finite element method and the TLM method. For gap widths ranging from $d/b = 1/16$ to $1/2$, all three methods yield frequency values which agree within 0.5 percent. Since

1. there is no indication that all three methods are affected by a systematic error of identical sign and magnitude,

2. the introduction of a dielectric with $\varepsilon_r > 1$ represents no new source of error in the TLM calculation,

3. the coarseness error (which is the major source of error) can be eliminated by the same

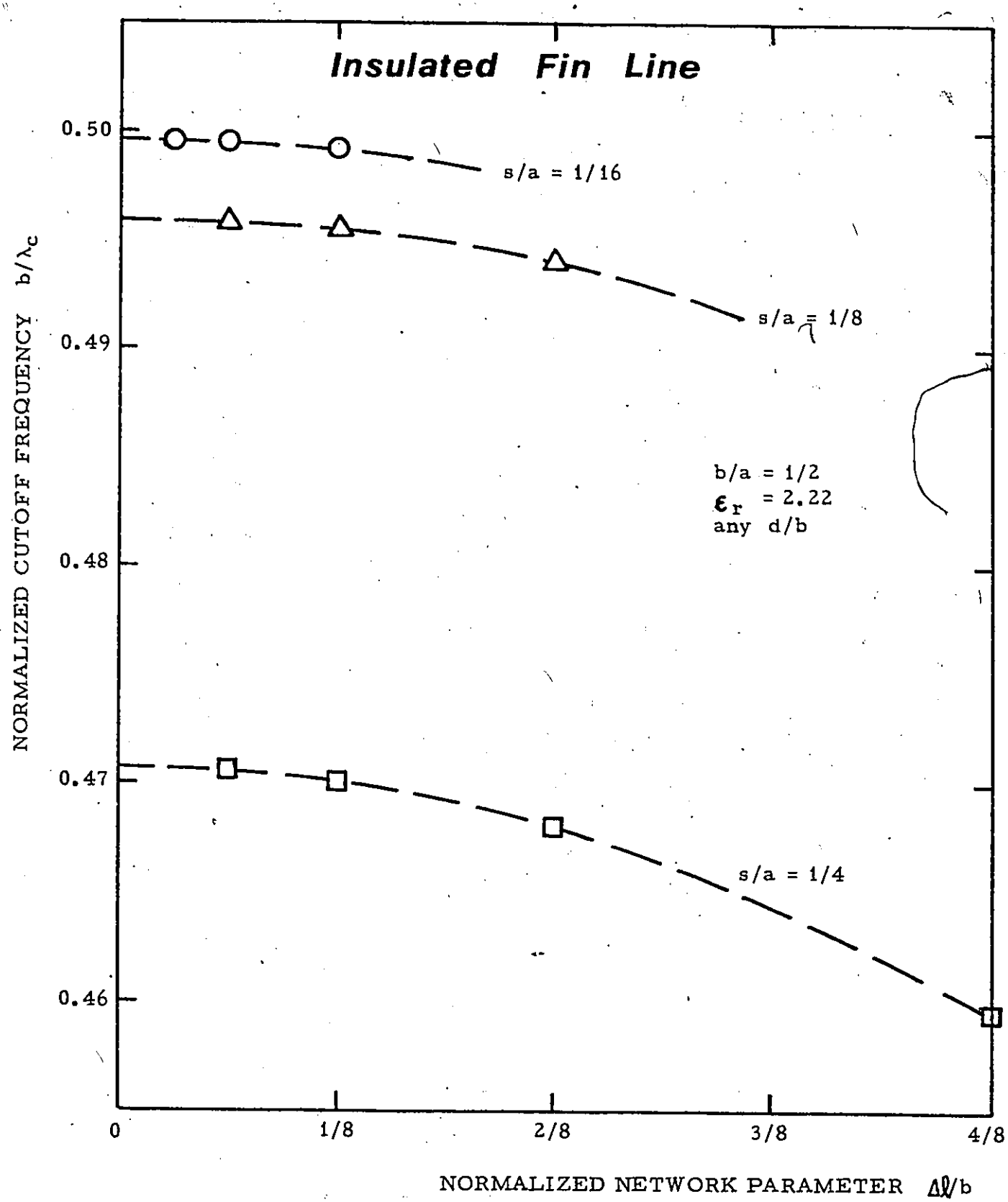

Figure 5.3: Extrapolation technique minimizing errors in the cutoff frequency of the second order mode.

extrapolation procedure as the one used for finned waveguide,

it is assumed that the TLM method, when applied to fin line analysis, yields cutoff frequencies which are accurate within at least 1 percent, for all gap widths of practical interest.

5.4 RESULTS

Figures 5.4, 5.5 and 5.6 show the normalized fundamental cutoff frequencies (b/λ_c) in unilateral, bilateral and insulated fin lines. Results obtained with the Transverse Resonance Method[23] are compared with the TLM solution. Cutoff frequencies of the second order mode in unilateral and insulated fin lines are shown in Fig.5.7, while Fig.5.8 shows the same frequencies for bilateral fin line. In all cases, the waveguide aspect ratio b/a is equal to 1/2, and the substrate permittivity is $\varepsilon_r = 2.22$.

Finally, some results obtained with a special finite element program for inhomogeneously filled waveguides (to be published) are compared with TLM results in Table 5.1. Results agree within 1 percent.

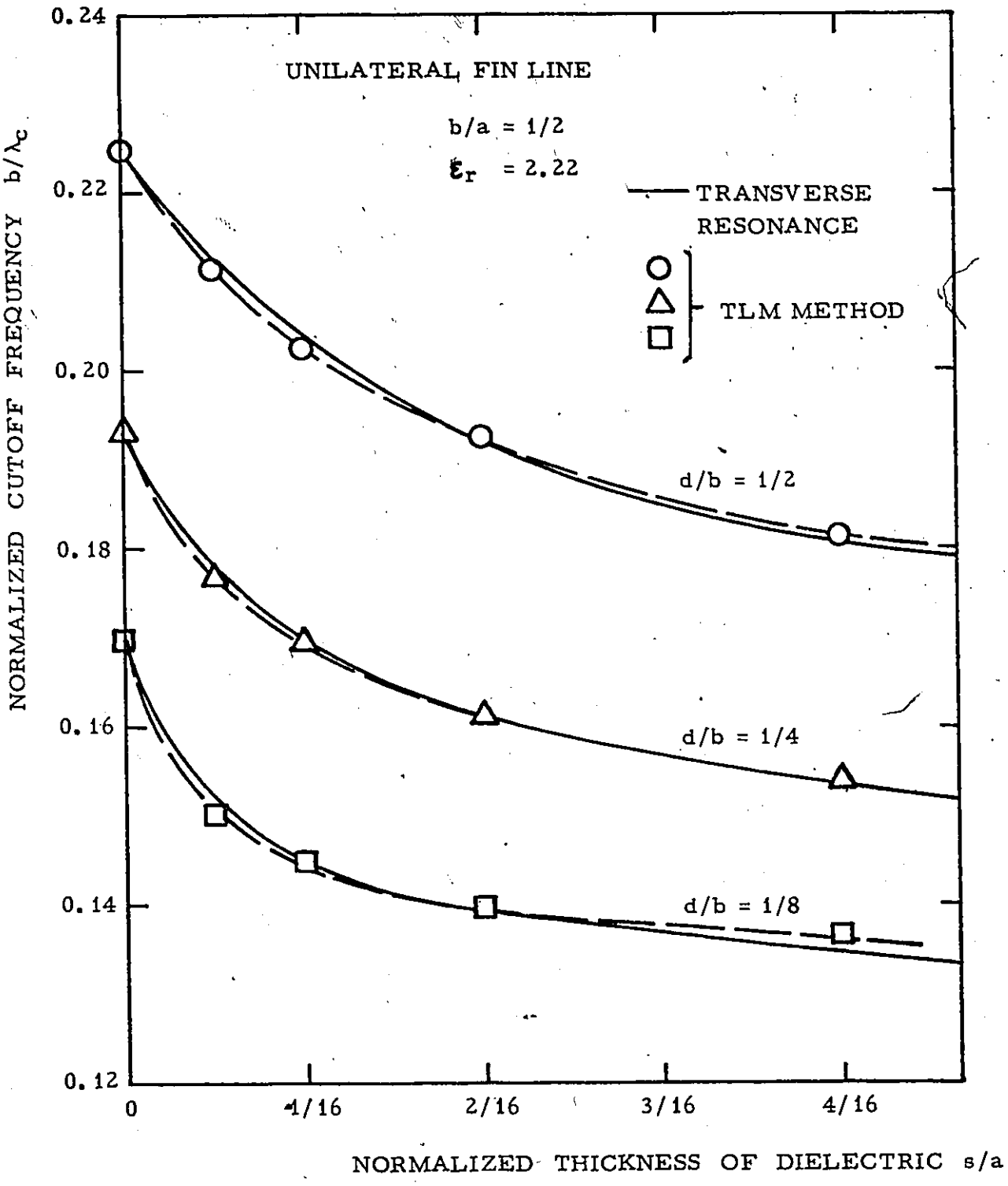

Figure 5.4: Normalized fundamental cutoff frequency in unilateral fin lines.

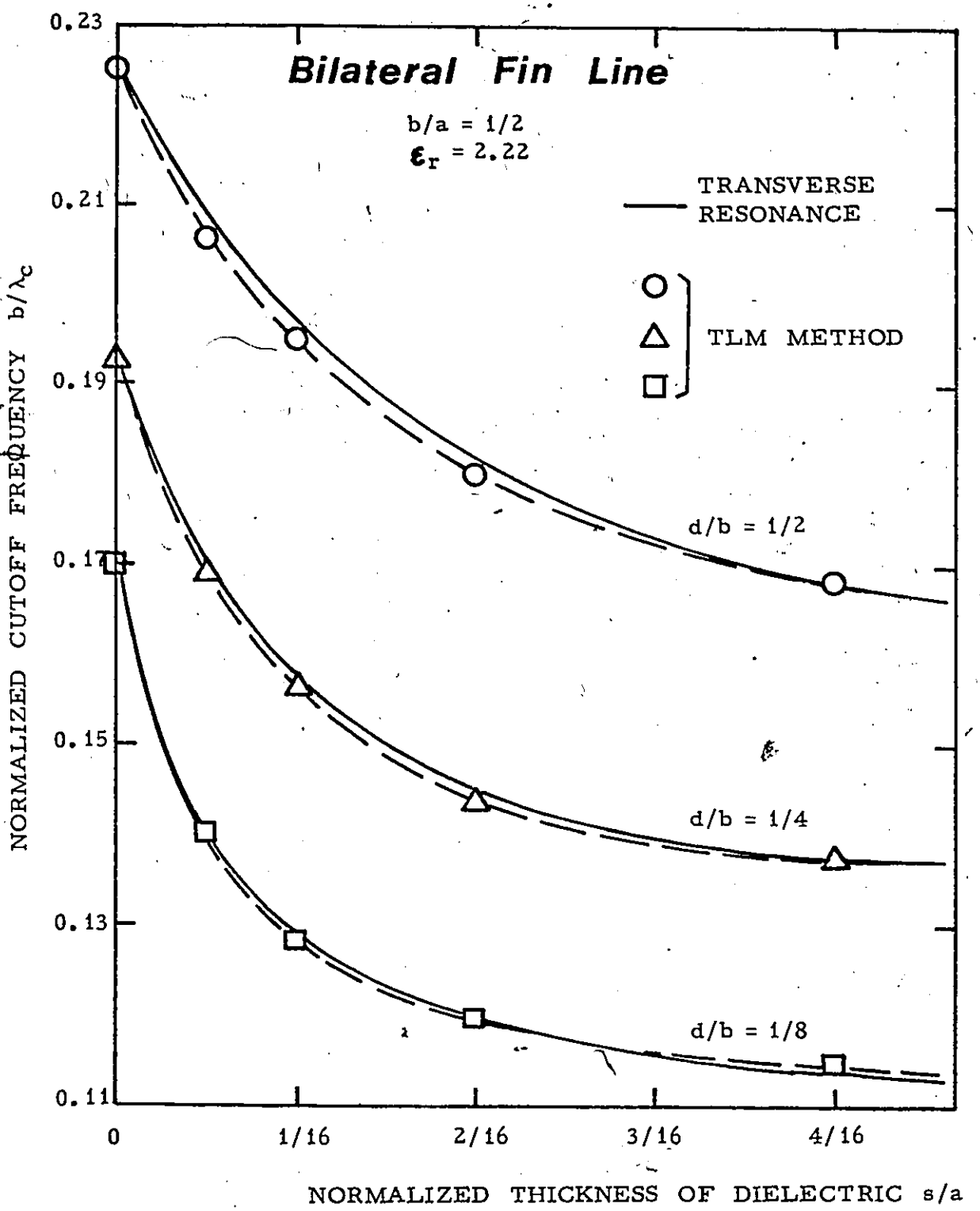

Figure 5.5: Normalized fundamental cutoff frequency in bilateral fin lines.

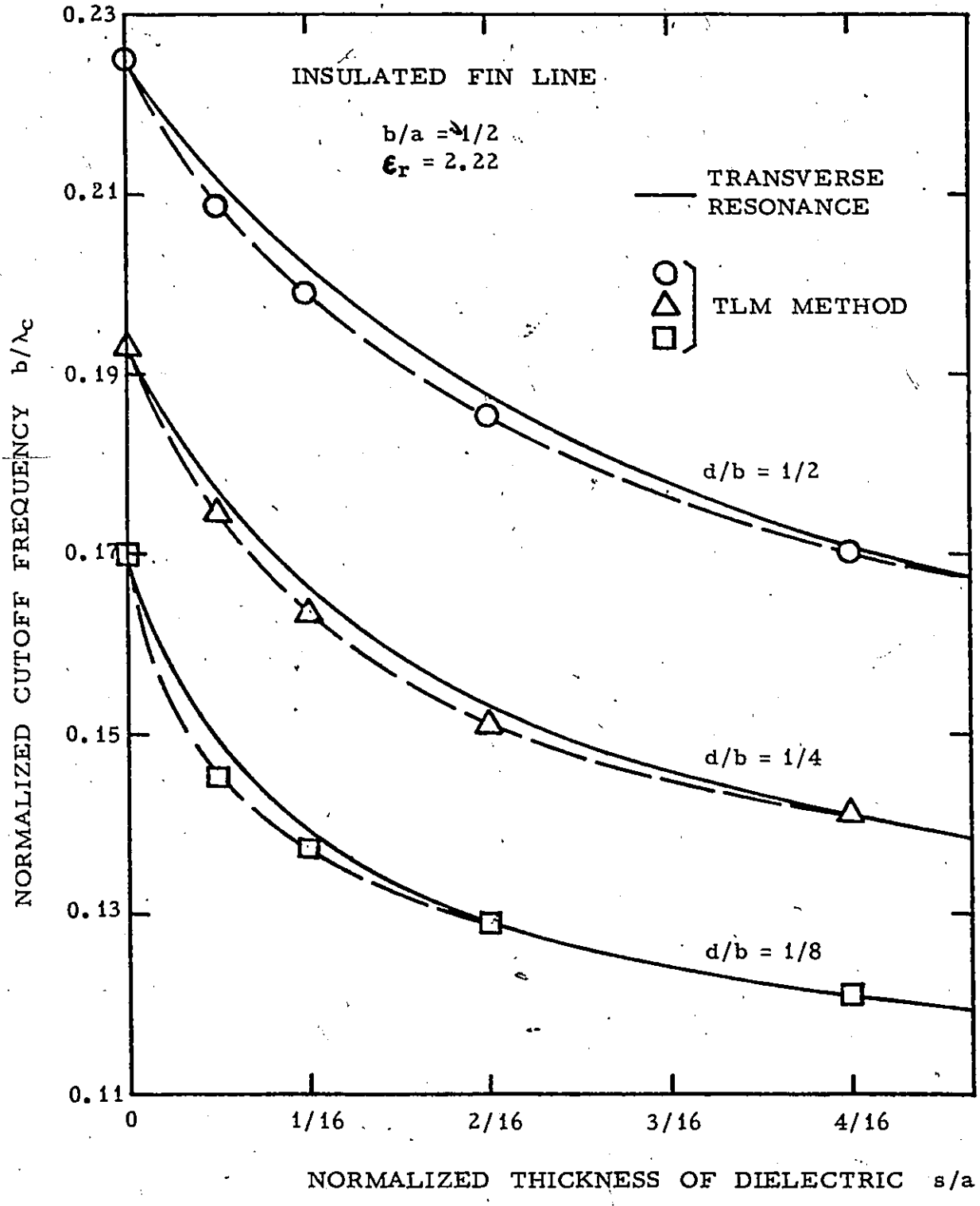

Figure 5.6: Normalized fundamental cutoff frequency in insulated fin lines.

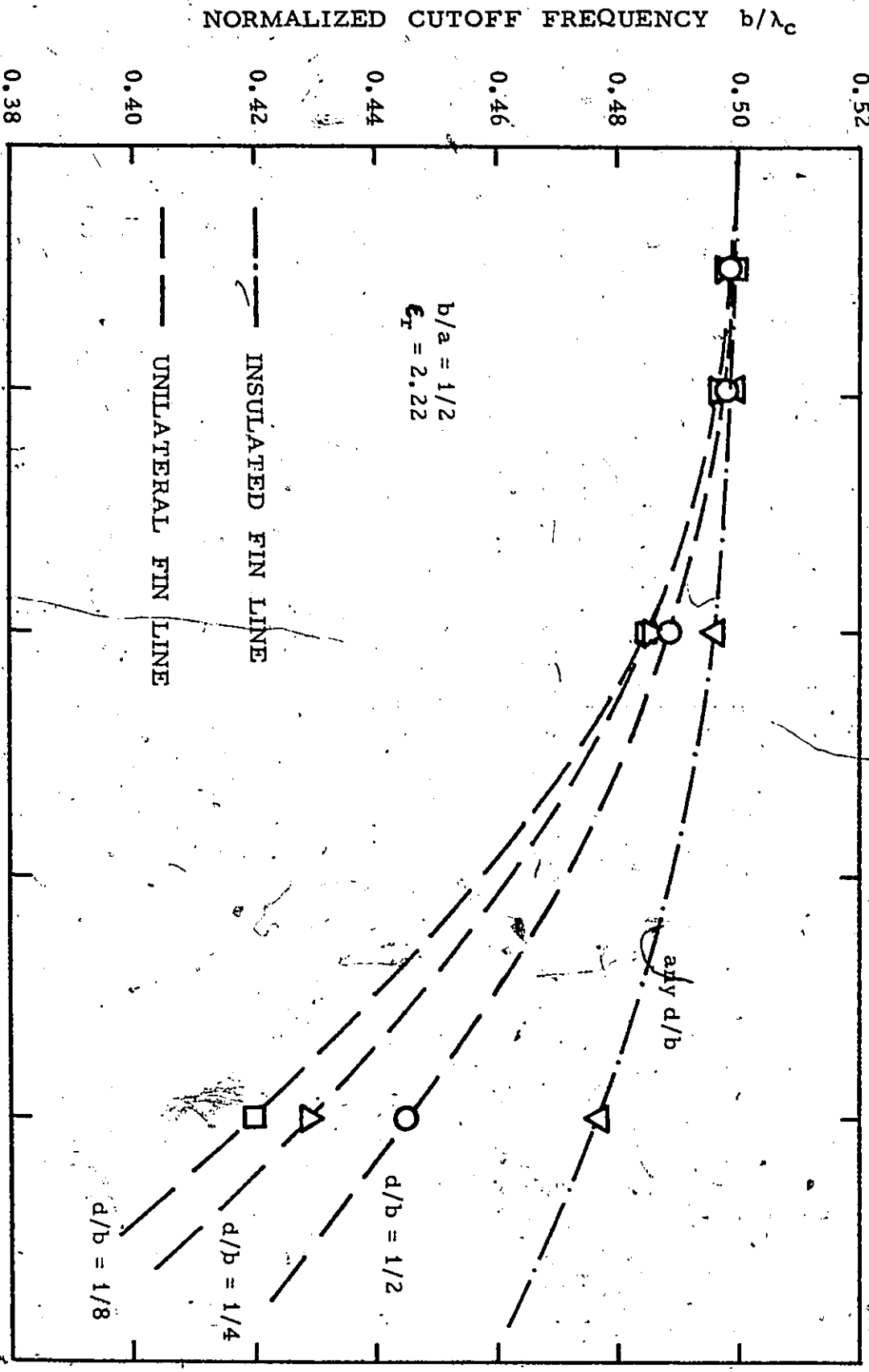

Figure 5.7: Normalized second order cutoff frequency in unilateral and insulated fin lines.

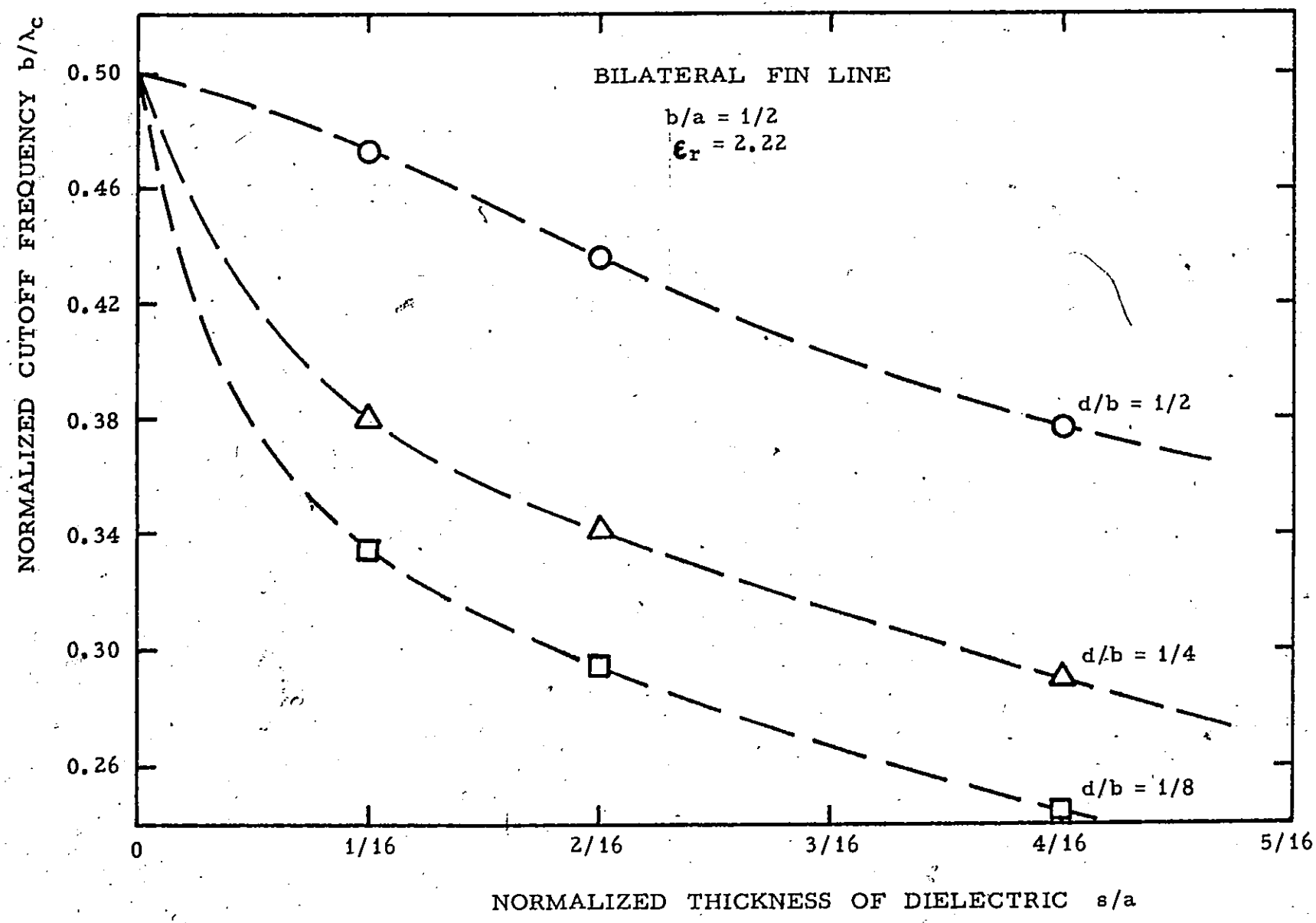

Figure 5.8: Normalized second order cutoff frequency in bilateral fin lines.

		Cutoff Freq. of Dom. Mode		Cutoff Freq. of 2^d Order Mode	
	d/b	b/λ_{c_1} TLM Method	b/λ_{c_1} F E Method	b/λ_{c_2} TLM Method	b/λ_{c_2} Accurate value (TR)
s/a = 1/8	1/8	0.1285	0.1299		
	1/4	0.1512	0.1529	0.4961	0.49601
	1/2	0.1853	0.1868		
	3/4	0.2090	0.2098		
s/a = 1/16	1/8	0.1373	0.1394		
	1/4	0.1630	0.1647		
	1/2	0.1989	0.2003	0.4996	0.49951
	3/4	0.2229	0.2235		
	1	0.2325	0.2325		

TABLE 5.1: Comparison of the normalized cutoff frequencies b/λ_c in insulated fin lines obtained with three different methods.

5.5 FIELD CONFIGURATIONS

Since the TLM simulation describes the propagation of electric and magnetic field components in the form of traveling voltage and current pulses in a transmission line mesh, the field information is available at all mesh nodes.

Figures 5.9, 5.10 and 5.11 show transverse field lines which correspond to lines of constant magnetic field in the longitudinal direction. The latter can be shown by the following argument: According to the second Maxwell's equation:

$$\text{curl } \vec{H}_z = j\omega\varepsilon\vec{E}_t \qquad (5.1)$$

where $\vec{H}_z$ is the longitudinal magnetic field, and $\vec{E}_t$ the transverse electric field, if curl $\vec{H}_z$ is taken in a plane of constant H_z it will obviously be equal to zero. Thus, the transverse electric field must always be parallel to the planes of constant H_z

In the field plots presented, the electric field lines have been found as contours of constant magnetic field, evaluated in unit steps from zero to ten.

The contours have been drawn using cubic spline interpolation between grid points. These figures are, to

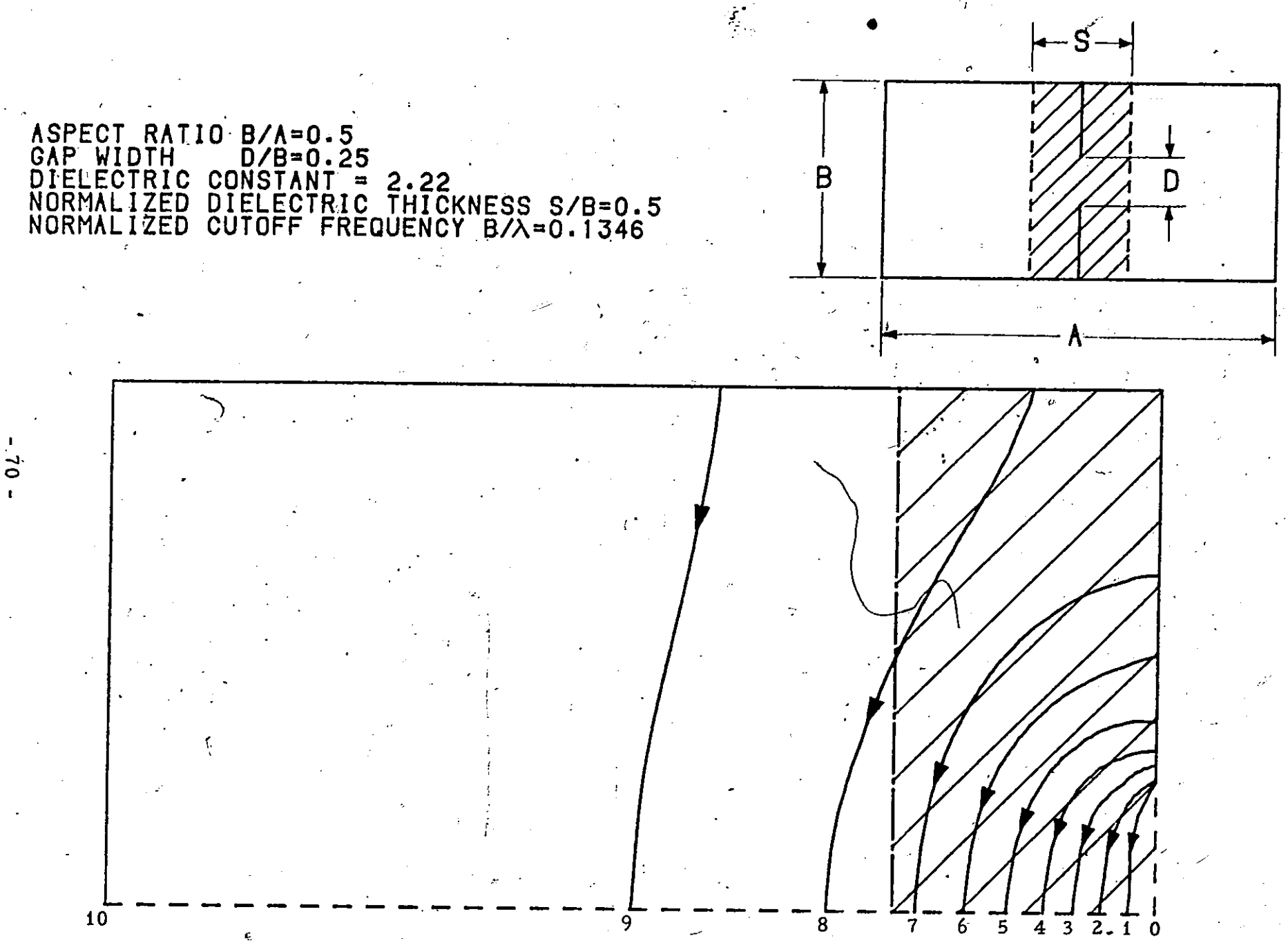

Figure 5.9: The transverse E field lines of the fundamental mode in an insulated fin line.

Aspect Ratio $b/a = 0.5$
Normalized Gap Width $d/b = 0.5$
Normalized Substrate Thickness $s/b = 0.25$
Dielectric Constant $\epsilon_r = 2.22$
Normalized Cutoff Frequency $b/\lambda_c = 0.1882$

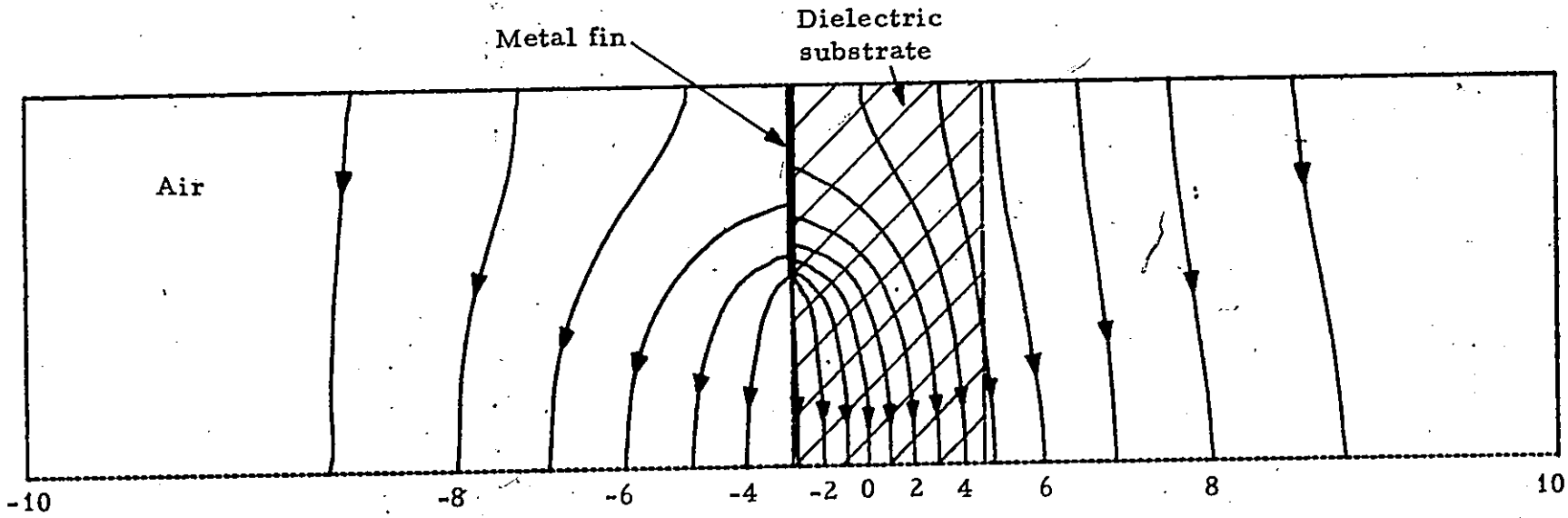

Figure 5.10: The transverse E field lines of the fundamental mode in a unilateral fin line.

Aspect Ratio $b/a = 0.5$
Normalized Gap Width $d/b = 0.5$
Normalized Substrate Thickness $s/b = 0.25$
Dielectric Constant $\varepsilon_r = 2.22$
Normalized Cutoff Frequency $b/\lambda_c = 0.4864$

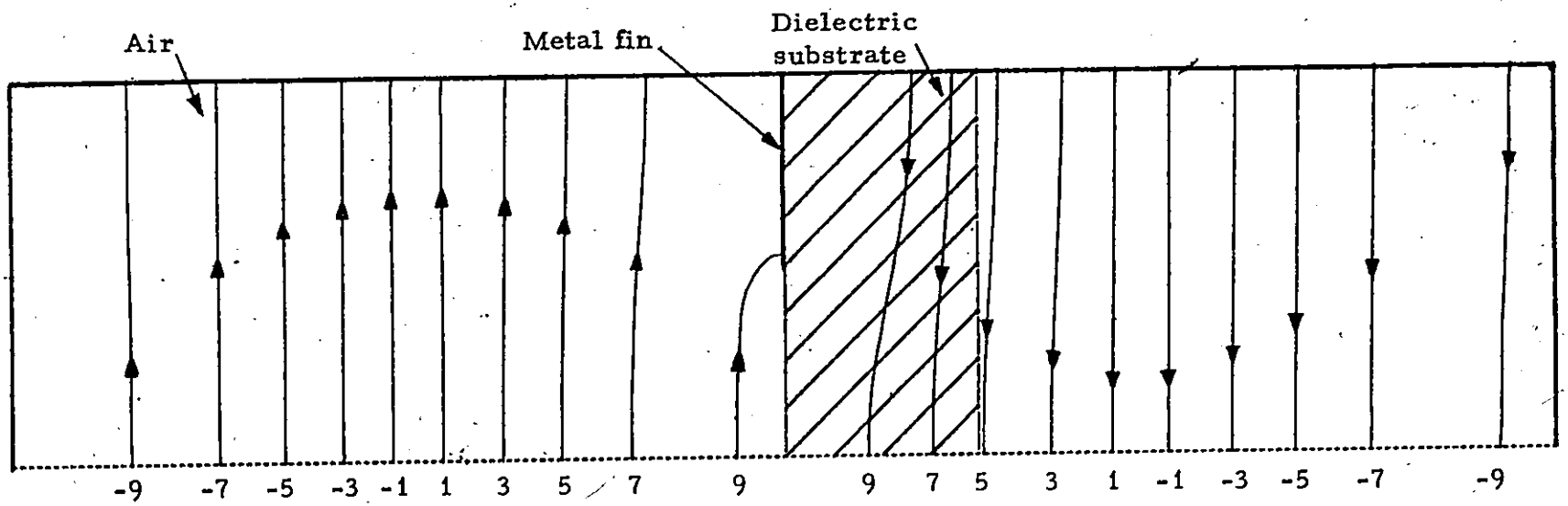

Figure 5.11: The transverse E field lines of the second order mode in a unilateral fin line.

the knowledge of the author, the first showing detailed field plots in fin lines and are certainly useful for the visualization and understanding of the field propagation in this new and attractive transmission medium for millimeter waves.

5.6 DISCUSSION

The two-dimensional TLM method provides an excellent reference for verifying other methods to evaluate the cutoff frequencies of the fundamental and higher order modes in fin lines. By using a sufficient number of iterations in the calculations of the impulse response, the truncation error is kept negligibly small. An accuracy of typically 1 percent is achieved by correcting the velocity and coarseness errors associated with the TLM solutions.

The transverse E field lines of the fundamental and second order modes in fin lines at cutoff are also plotted. These plots are useful for the visualization and understanding of the field propagation in fin lines,

Chapter VI

ANALYSIS OF FIN LINES USING THE THREE-DIMENSIONAL TLM METHOD

6.1 THE TLM SIMULATION

The three-dimensional TLM simulation of fin lines is similar to that of finned waveguide Waveguide walls and fins are assumed to be perfect conductors. They are simulated by short-circuiting the corresponding shunt nodes in the three-dimensional network. The dielectric substrate is simulated by loading series nodes and shunt nodes with shunt-stubs and open-stubs, respectively. Two short-circuited transverse planes separated by a distance ℓ are then introduced to form a cavity. Fig.6.1 shows such a cavity containing a unilateral fin line.

Walls of symmetry (shunt-circuited and/or open-circuited walls) may also be employed to reduce both the simulation storage and the execution time of the program. The TLM program yields the impulse response of the cavity by first exciting the network with an impulse or impulses and then calculating step by step the field propagation in the network. Finally, the desired resonant frequencies are extracted from the impulse response via Fourier transformation.

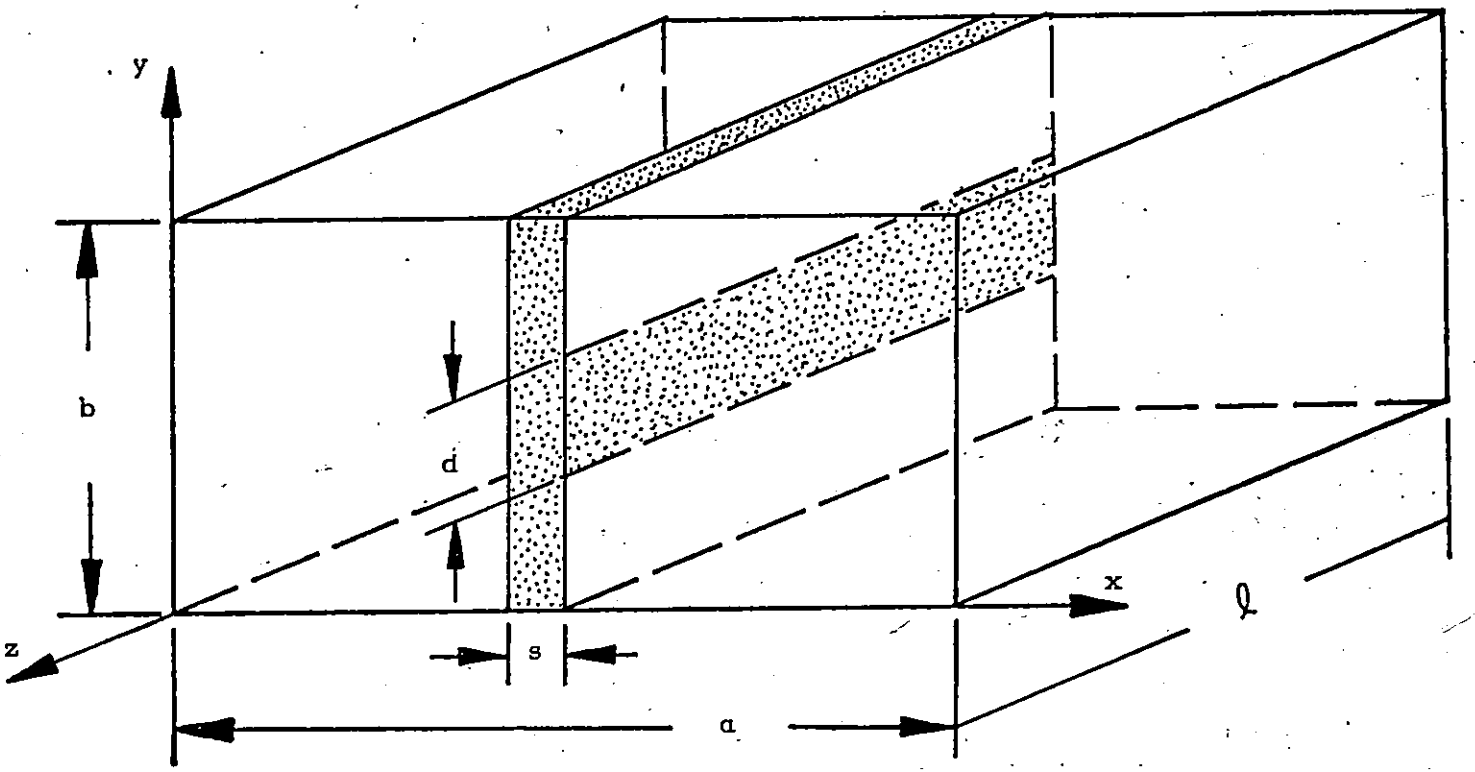

Figure 6.1: Unilateral fin line cavity.

6.2 ERROR ANALYSIS

Basically, the errors associated with the three-dimensional TLM solutions are the truncation error, the velocity error and the coarseness error (both transversal and longitudinal) as discussed in Chapter V. In addition, a significant error occurs due to the problems encountered in the simulation of dielectric boundaries.

In the two-dimensional TLM simulation, all boundaries are located between two nodes. Therefore, there is no problem in matching two different boundaries on the same plane. For example, the electric wall representing the metallic fin should lie in the same plane as the adjacent dielectric boundary in a unilateral fin line. In the three-dimensional TLM simulation, however, the short-circuited boundary and the dielectric boundary may not lie on the same plane in the model[24]. This means that in the TLM model, the dielectric either protrudes or recedes between the fins, as shown in Fig. 6.2. This contributes to another source of error which makes the error analysis of the TLM results more complicated. If the dielectric boundary protrudes, more energy of the field will concentrate in the dielectric region and thus the resonant frequency will be too low. If it recedes, the resonant frequency will be too high. However, the amount of this variation is hard to predict.

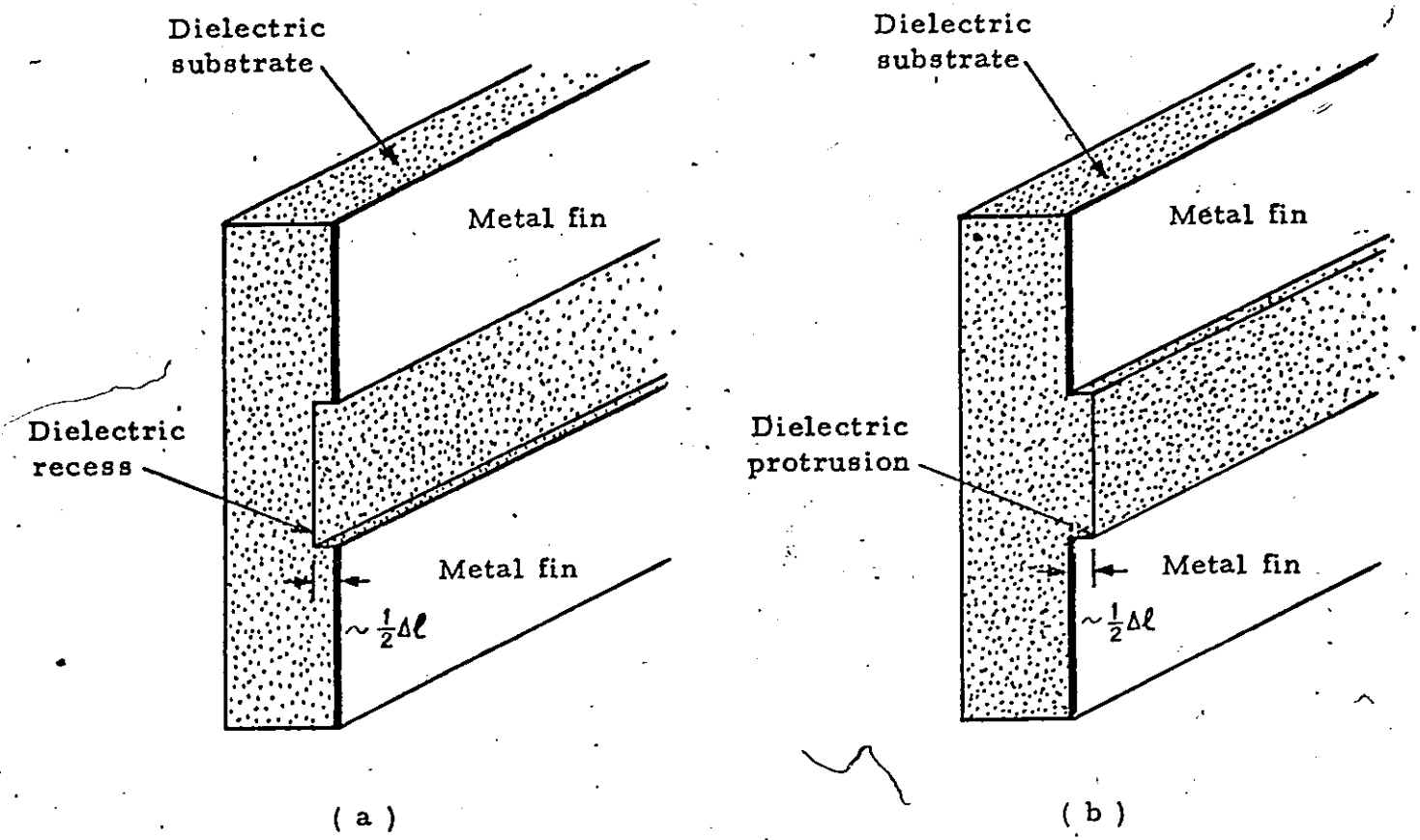

Figure 6.2: (a) Dielectric recess and (b) dielectric protrusion in the three-dimensional TLM simulation.

6.3 UNILATERAL FIN LINE

The two possible situations encountered in the simulation of fin lines give rise to two sets of TLM solutions. Fig.6.3 shows the convergent behavior of these two sets of solutions when the network parameter $\Delta\ell$ decreases. Both solutions merge to the same point as $\Delta\ell$ approaches zero.

The extrapolation technique can be employed again to obtain an accurate value. However, in this case, it is hard to find a set of systematic curves which fit the data. A possible way is to average the two sets of data, presuming that the effects of the dielectric protrusion and recess cancel each other, and using parabolic curve fitting as shown in Fig.6.3. Since this procedure is cumbersome and requires extensive computer time, it is impractical. However, it is observed that when the mesh size is fine ($\Delta\ell/a \leq 1/16$), the results of dielectric protrusion and recess serve as upper and lower bounds respectively for the dispersion characteristic as shown in Fig.6.4. The corresponding transverse resonance solution[4] lies within this range and is therefore considered an acceptable approximation with an accuracy of 2 or 3 percent. In Fig.6.4, the extrapolated value for the normalized propagation constant has been

---

[4]The transverse resonance solutions employed throughout this chapter are the published data by Hoefer[23].

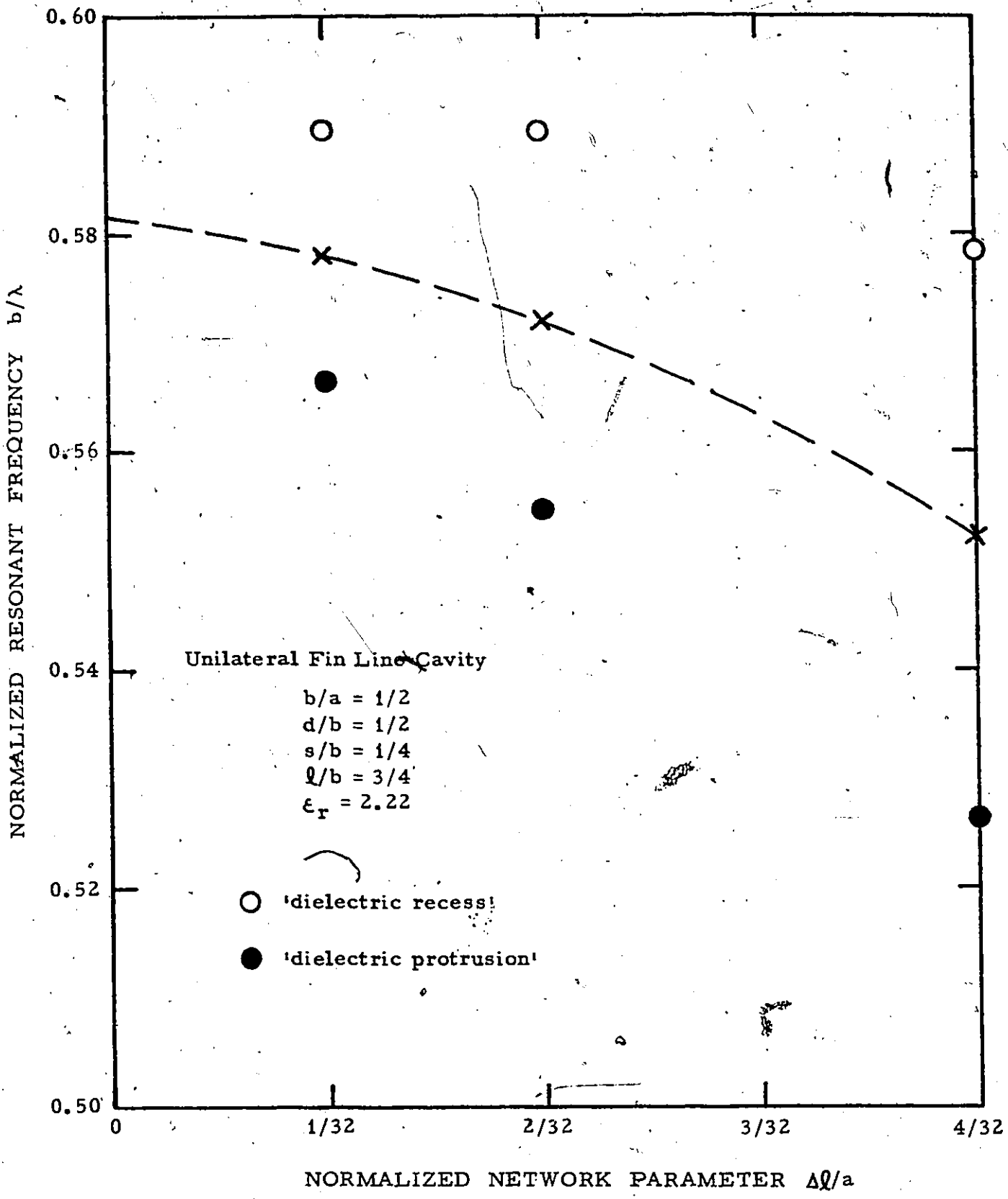

Figure 6.3: Convergence of three-dimensional TLM solutions in unilateral fin lines as $\Delta\ell$ decreases.

obtained graphically and was found to be about 1 percent higher than the transverse resonance solution. Therefore, it is concluded that the dispersion characteristic obtained with the transverse resonance method may be considered as a strict lower bound.

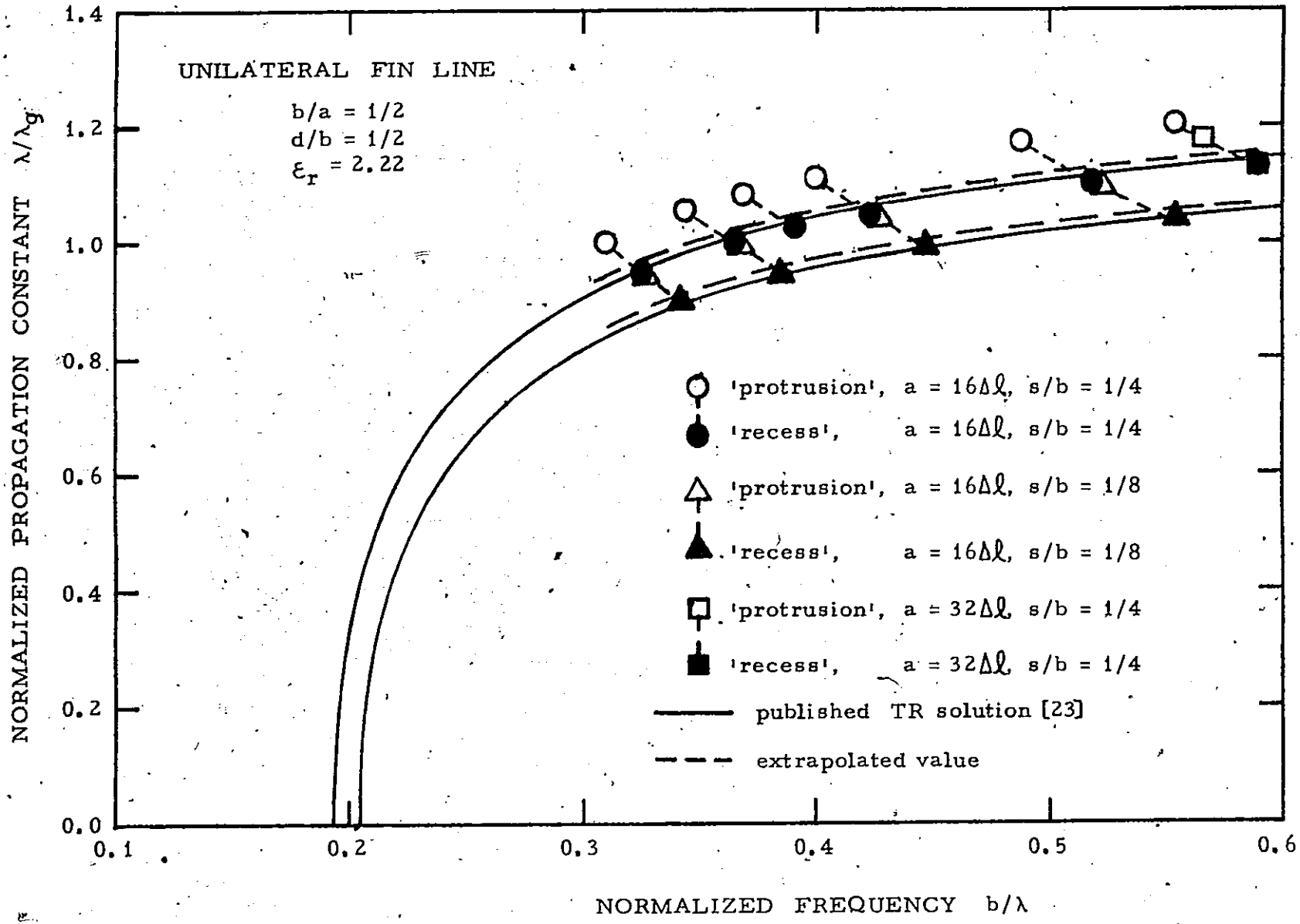

Figure 6.4: Dispersion characteristics of unilateral fin lines obtained with the three-dimensional TLM method.

6.4 BILATERAL FIN LINE

In bilateral fin lines, metallic fins are deposited on both sides of the dielectric substrate and consequently, the problems in the boundary simulation are encountered on both sides in the TLM simulating network. However, if the dielectric protrudes on one side and recedes on the other side, the errors tend to cancel each other, thus reducing this error source considerably. Fig.6.5 shows the TLM solutions for several mesh sizes under such circumstances. As the mesh size $\Delta\ell$ becomes finer, the results move down closer to the transverse resonance solutions. Therefore, the transverse resonance solution is considered as the lower bound and the TLM solution as the upper bound for the dispersion characteristics.

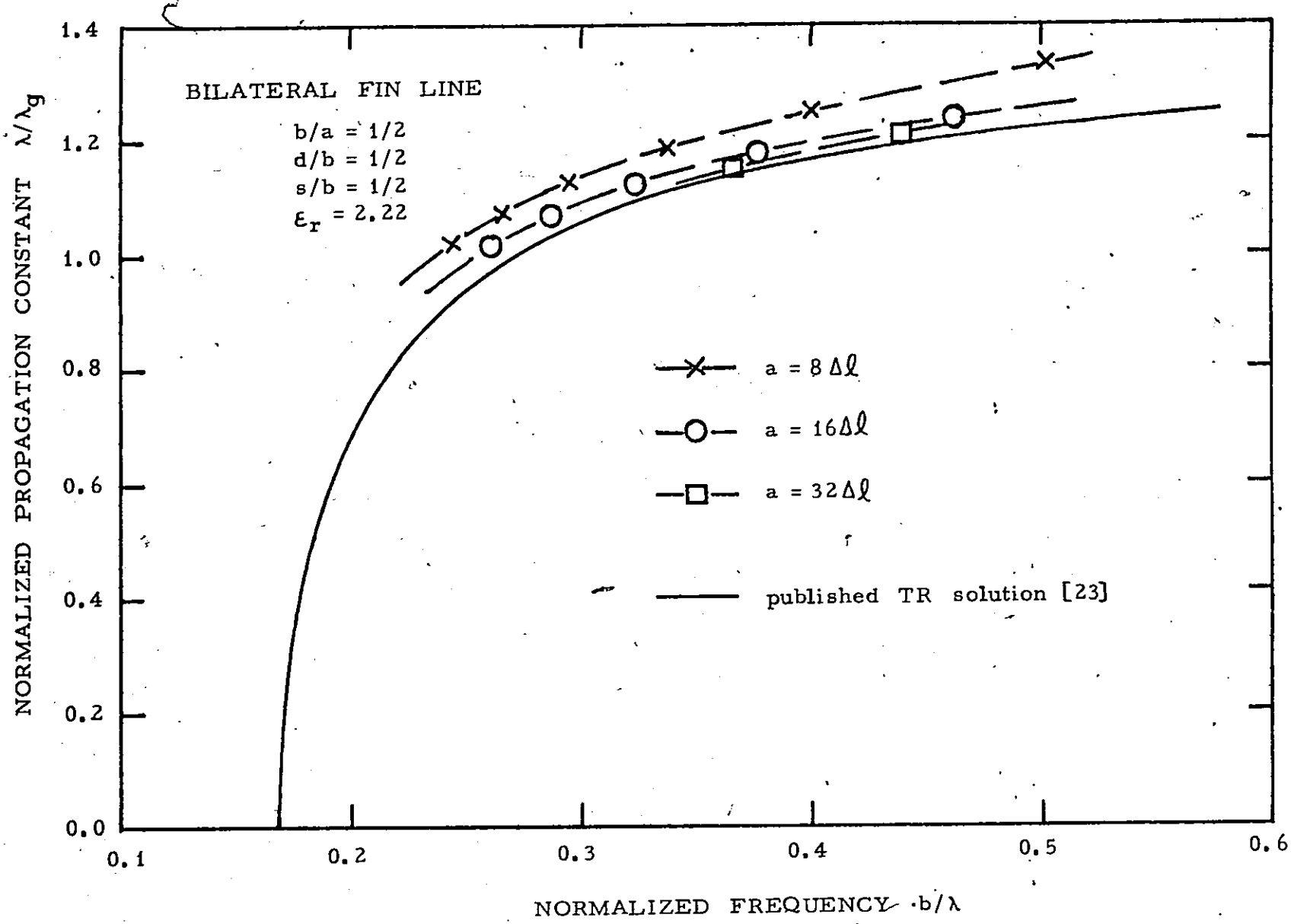

Figure 6.5: Dispersion characteristic of a bilateral fin line obtained with the three-dimensional TLM method.

6.5 INSULATED FIN LINE

The problem of dielectric boundary simulation does not exist in insulated fin lines since there is no overlay of the dielectric boundary and conducting boundary.

Fig.6.6 shows the convergence of the TLM solutions of the normalized propagation constant to accurate values as the mesh size decreases. The extrapolated values obtained graphically are shown to be about 1 to 2 percent larger than the transverse resonance solution. Once again, the transverse resonance solution is considered as the lower bound and the TLM solution as the upper bound of the dispersion characteristics.

Since an insulated fin line is just a superposition of a finned waveguide and a dielectric slab loaded waveguide, another possible approach to obtain accurate results is to combine the coarseness error curves presented in Fig.4.3 and 4.5 to form an error correction curve. The TLM results obtained with a mesh of $\Delta\ell = a/16$ have been corrected in this way, and Fig.6.6 shows that they approach the extrapolated values very closely.

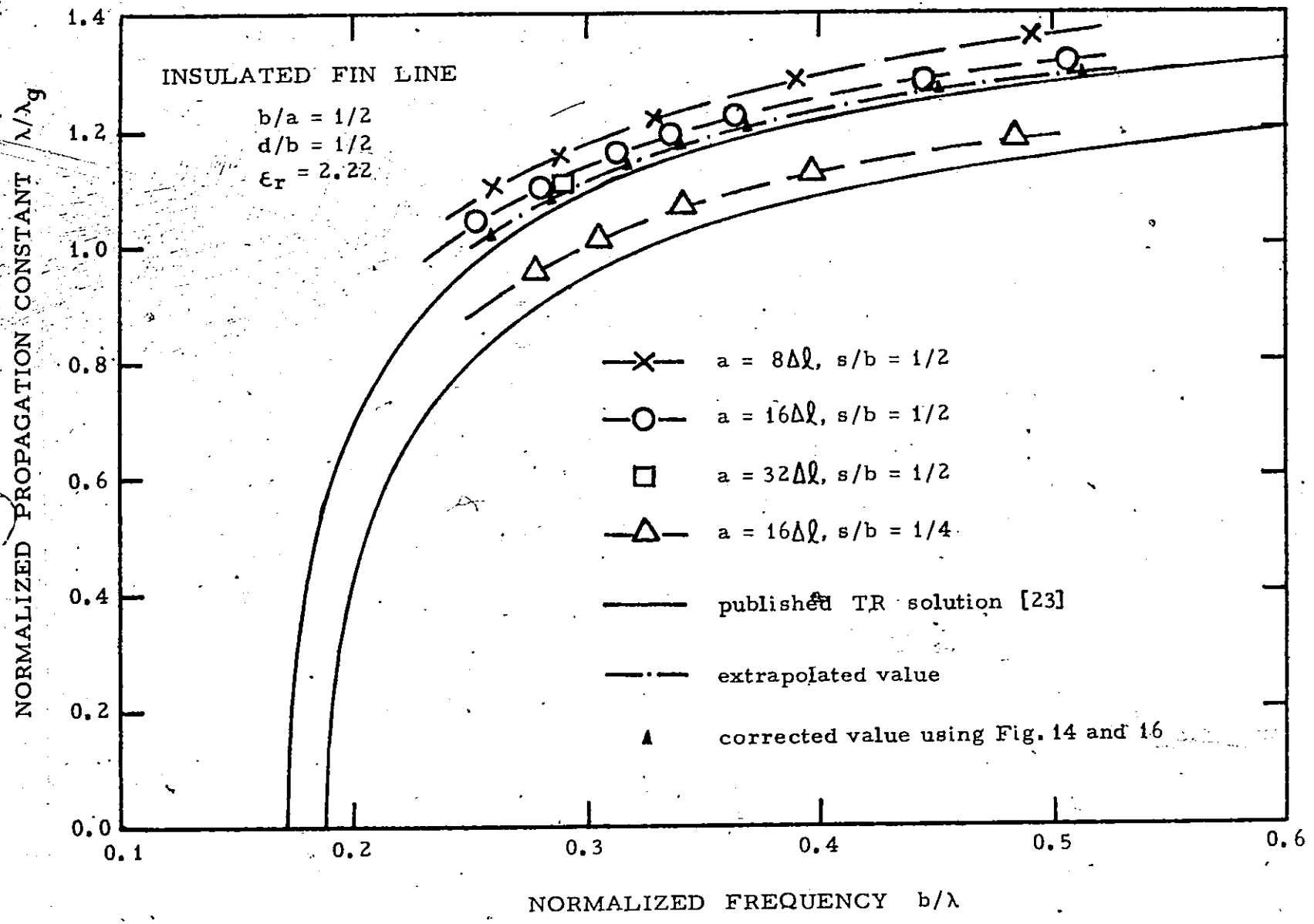

Figure 6.6: Dispersion characteristics of insulated fin lines obtained with the three-dimensional TLM method.

Chapter VII

ANALYSIS OF FIN LINES USING THE TRANSVERSE RESONANCE METHOD

7.1 TRANSVERSE RESONANCE CONDITION IN FIN LINES

The transverse resonance condition in fin lines is similiar to that in finned waveguides. The presence of the dielectric sheet at the transverse discontinuity modifies the susceptance of the fin. Fig.7.1 shows the cross sections of three typical fin line configurations together with their transverse equivalent networks.

When a dielectric sheet of permittivity ε_r is added at one side (or both sides) of the fin, the capacitance of the covered side(s) of the discontinuity is increased by a factor somewhere between 1 and ε_r, depending on the thickness of the sheet. Hoefer[23] has proposed a correction factor F for the susceptance modification in unilateral and insulated fin lines, and a correction factor G for the bilateral fin line. They are defined as

$$F = \frac{\text{Slot susceptance for finite sheet thickness}}{\text{Slot susceptance for infinite sheet thickness}} \qquad (7.1)$$

$$G = \frac{\text{Slot susceptance for finite sheet bounded by a magnetic wall}}{\text{Slot susceptance for infinite sheet}} \qquad (7.2)$$

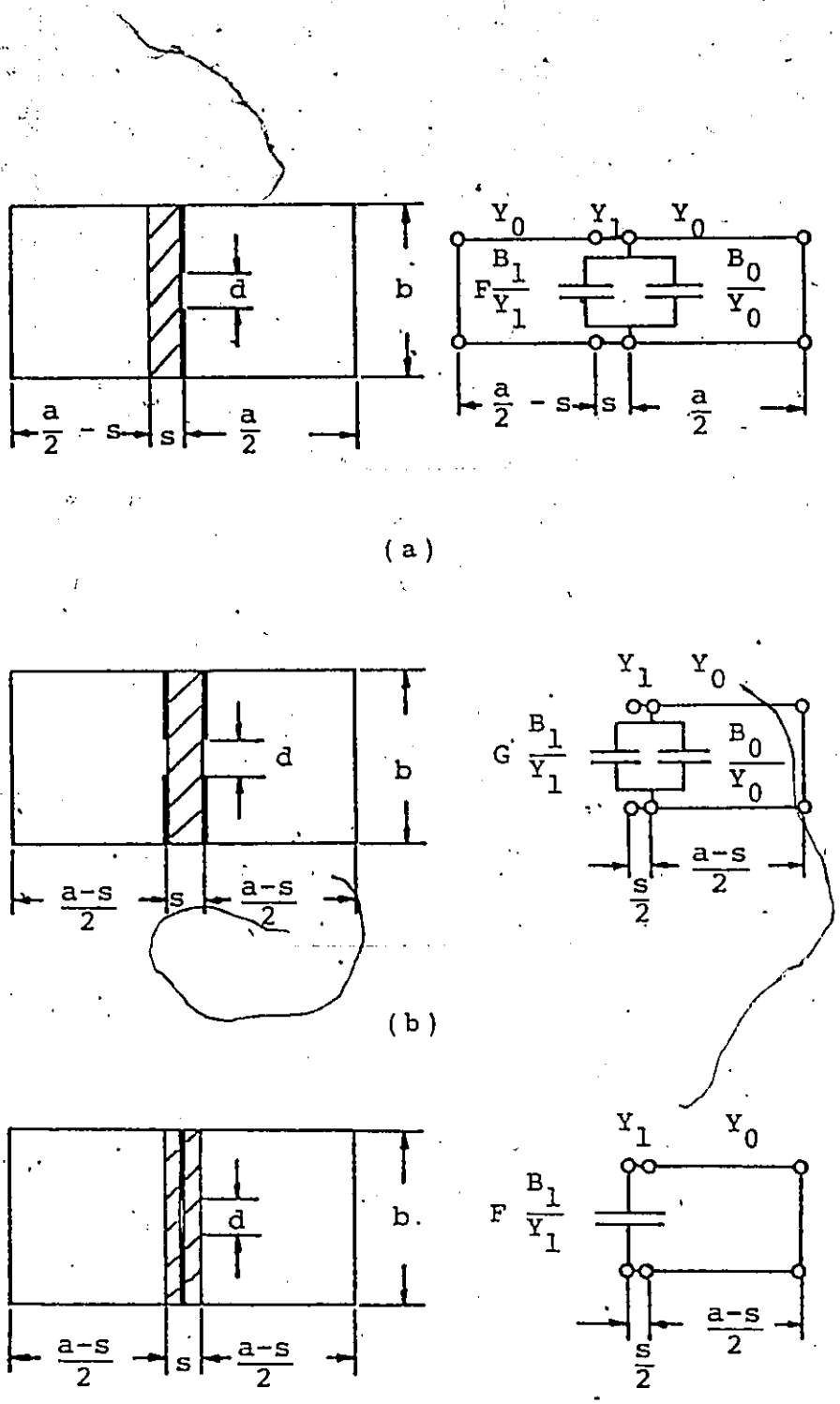

Figure 7.1: Cross sections and transverse equivalent networks of (a) unilateral (b) bilateral (c) insulated fin lines.

and are normalized to be independent of ε_r. By modifying the expression for slot line susceptance given by Cohn[13], the correction factors are obtained[23].

With the introduction of these correction factors, the transverse resonance conditions for fin lines are given by the following transcendental equations. In what follows, the following abbreviations are used:

$$d/b = t \; ; \quad s/b = w \; ; \quad b/a = z \; ; \quad \lambda/\lambda_g = p$$

$$b/\lambda = x \; ; \quad [\varepsilon_r - p^2]^{1/2} = u \; ; \quad [1 - p^2]^{1/2} = v$$

$$\lambda_{co} = x/v \; ; \quad \lambda_{cl} = x/u \; ; \quad b/\lambda_{co} = vx$$

$$b/\lambda_{cl} = ux$$

where λ = free-space wavelength

λ_g = guided wavelength in the fin line

λ_{co} = transverse guided wavelength in air section

λ_{cl} = transverse guided wavelength in dielectric filled section of the fin line.

The transverse resonance condition for unilateral fin lines is

$$-(u/v)\cot\{2\pi wux + \tan^{-1}[(u/v)\tan 2\pi vx(\frac{1}{2z} - w)]\}$$

$$+ F\left[\frac{B_1}{Y_1}\frac{1}{ux}\right](\frac{u}{v})^2 vx + \left[\frac{B_o}{Y_o}\frac{1}{vx}\right]vx - \cot\frac{\pi vx}{z} = 0 \qquad (7.3a)$$

if $p < 1$, and

$$-(u/v)\cot\{2\pi wux + \tan^{-1}[(u/v)\tanh 2\pi vx\,(\tfrac{1}{2z} - w)]\}$$
$$+ F\left[\frac{B_1}{Y_1}\frac{1}{ux}\right](\tfrac{u}{v})^2 vx - \left[\frac{B_o}{Y_o}\frac{1}{vx}\right] vx - \coth\frac{\pi vx}{z} = 0 \qquad (7.3b)$$

if $p > 1$.

The resonance condition for bilateral fin line is

for $p < 1$

$$(u/v)\tan \pi wux + G\left[\frac{B_1}{Y_1}\frac{1}{ux}\right](\tfrac{u}{v})^2 vx + \left[\frac{B_o}{Y_o}\frac{1}{vx}\right] vx - \cot \pi vx(\tfrac{1}{z} - w) = 0 \qquad (7.4a)$$

for $p > 1$

$$(u/v)\tan \pi wux + G\left[\frac{B_1}{Y_1}\frac{1}{ux}\right](\tfrac{u}{v})^2 vx - \left[\frac{B_o}{Y_o}\frac{1}{vx}\right] vx - \coth \pi vx\,(\tfrac{1}{z} - w) = 0 \qquad (7.4b)$$

The resonance condition for insulated fin line is then

for $p < 1$

$$-(u/v)\cot\{\pi wux + \tan^{-1}[(u/v)\tan \pi vx\,(\tfrac{1}{z} - w)]\} + F\left[\frac{B_1}{Y_1}\frac{1}{ux}\right](\tfrac{u}{v})^2 vx = 0 \qquad (7.5a)$$

for $p > 1$

$$-(u/v)\cot\{\pi wux + \tan^{-1}[(u/v)\tanh \pi vx\,(\tfrac{1}{z} - w)]\} + F\left[\frac{B_1}{Y_1}\frac{1}{ux}\right](\tfrac{u}{v})^2 vx = 0 \qquad (7.5b)$$

In the above formulae, the values of B_o/Y_o and B_1/Y_1 are one half the values of B/Y_o given by eqn. (2.2) provided that b/λ_c therein is replaced by b/λ_{co} and b/λ_{c1}, respectively.

7.2 CORRECTION FACTOR OBTAINED FROM TWO-DIMENSIONAL TLM SOLUTIONS

In chapter V, the cutoff frequencies in fin lines have been obtained accurately using the two-dimensional TLM method. By using these results, highly accurate correction factors F and G can be determined from the above-mentioned transcendental equations. Fig.7.2 and 7.3 show the calculated correction factors for a substrate permittivity $\varepsilon_r = 2.22$.

Further study for the cases of larger ε_r ($\varepsilon_r = 3.0$ and $\varepsilon_r = 9.0$)[5] show that as the value of ε_r increases, the values of the correction factors decrease. However, the variation of the factors is very small for low dielectric constant ($\varepsilon_r < 3.0$). Since fin lines usually contain substrates of low permittivity, the values of F and G are accurate for all practical applications.

---

[5]See appendix B.

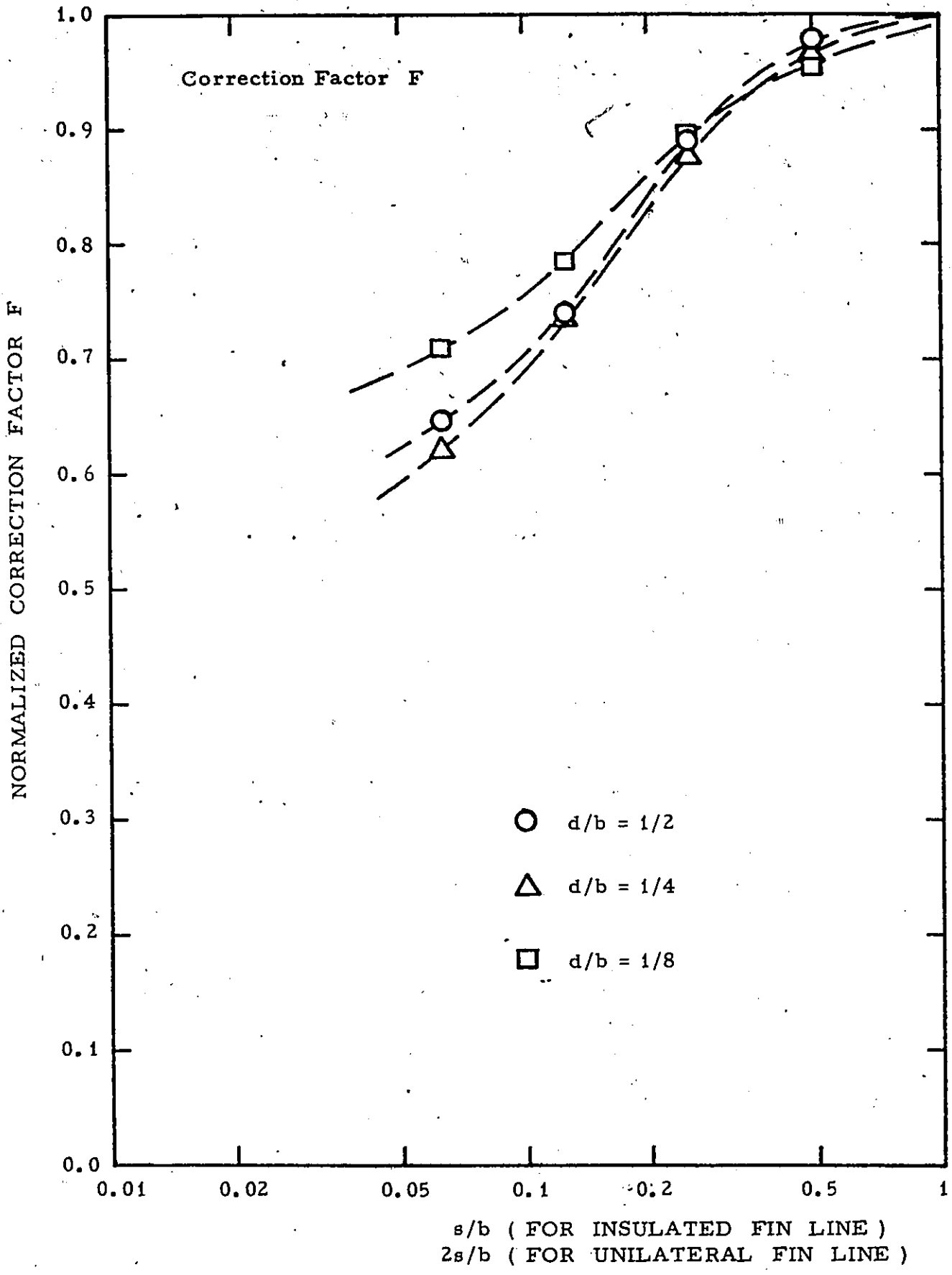

Figure 7.2: Correction factor F for unilateral and insulated fin lines.

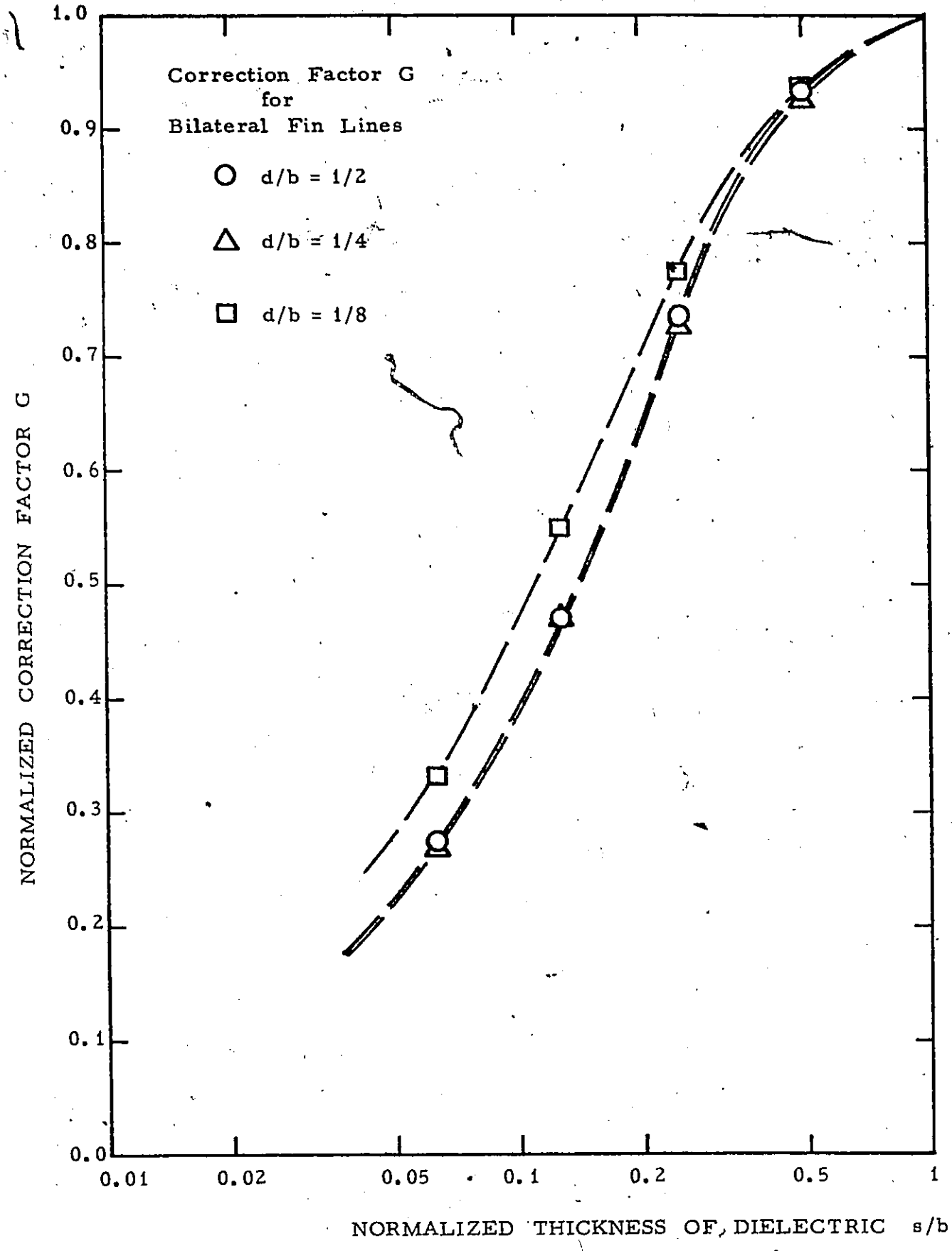

Figure 7.3: Correction factor G for bilateral fin lines.

7.3 RESULTS AND DISCUSSIONS

The transverse resonance method is an elegant method for fin line analysis. The transcendental equations (7.3), (7.4) and (7.5) can be solved easily using a computer or a programmable calculator[27]. A listing of the FORTRAN IV program for solving these equations is given in Appendix A.

The dashed curve in Fig.7.4 represents the normalized propagation constant in a unilateral fin line calculated using the correction factor given in Fig.7.2. Results obtained by other authors are also shown for comparison. It is found that the dashed curve fits Meier's measurements[1] and agrees with Hofmann's numerical solutions[2] within 0.5 percent.

Further comparison of the results with the extrapolated values obtained by the three-dimensional TLM analysis shows again an excellent agreement (better than 0.5 pecent). This suggests that the transverse resonance formulae, combined with the new correction factors F and G, provide the fin line designer with a tool which combines mathematical simplicity and easy applicability with excellent accuracy.

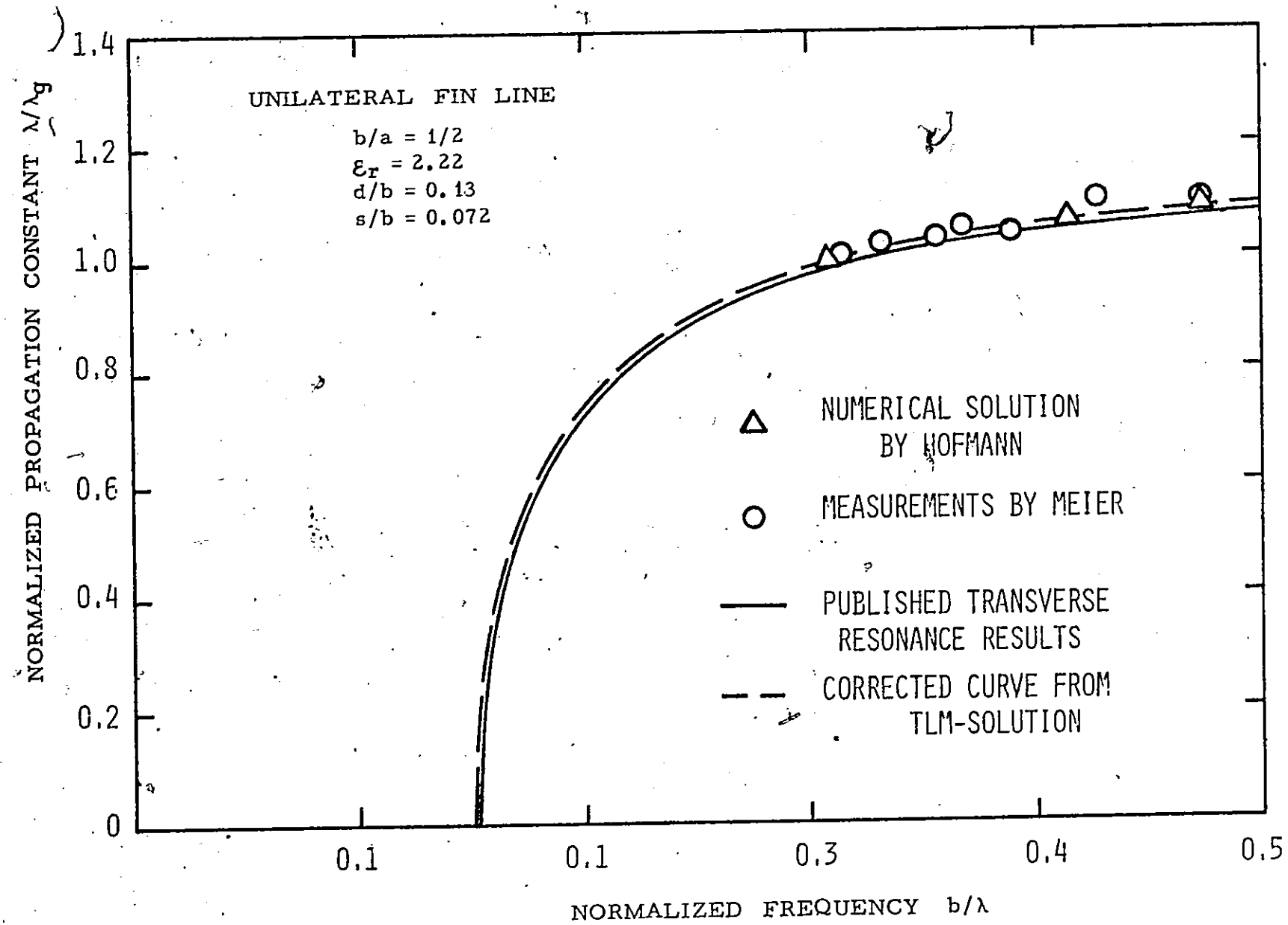

Figure 7.4: Normalized propagation constant of a unilateral fin line obtained from the two-dimensional TLM solutions.

Chapter VIII

FUTURE RESEARCH AND CONCLUSION

8.1 FUTURE RESEARCH

Although several papers dealing with theoretical investigations of the fin line have recently been published, only the straight section of fin lines has been analyzed in detail. The design of discontinuities is still carried out by trial and error in most cases. Saad and Schuenemann[10] have analyzed a discontinuity of a transition from fin line to a below cutoff waveguide by matching the TE_{mo} modes between two sets of equivalent rectangular waveguides. Only recently, Hoefer and Ros[11] have applied the TLM method to evaluate the equivalent susceptance of a discontinuity in a finned waveguide cavity. In order to achieve high accuracy results, however, extensive investigation on the analysis and correction of the errors is required for the TLM analysis. Thus, the field of analysis and design of fin line discontinuities is still wide open for future research.

8.2 CONCLUSION

In this thesis, the cutoff frequencies in unilateral, bilateral and insulated fin lines were obtained with an

accuracy of one percent. The normalized propagation constant (or alternatively the dispersion characteristic) was also evaluated accurately. Simple but nevertheless accurate expressions were obtained by combining the transcendental equations of the transverse resonance conditions in fin lines with the correction factors obtained with the two-dimensional TLM solutions.

An extensive analysis of the errors affecting the two-dimensional and the three-dimensional TLM solutions of fin lines were carried out. The errors were classified as the truncation error, the velocity error and the coarseness error. While the first two types of errors could be readily defined and predicted[20], the coarseness error was more difficult to analyze. A method of the error correction by extrapolation has been developed to obtain a high overall accuracy of the TLM results.

In the two-dimensional TLM analysis of fin lines, the normalized fundamental cutoff frequencies b/λ_c are obtained by Fourier transforming the impulse response of the simulating network. The coarseness error affecting the TLM solutions was found to be practically linearly proportional to the mesh size of the simulating TLM network. Therefore, linear extrapolation minimizes the errors. For the second order mode cutoffs, logarithmic curve fitting was found to

be appropriate for error elimination. In all cases, the two-dimensional TLM method yields, after the error correction, the cutoff frequencies in fin lines with an accuracy better than one percent.

In the three-dimensional TLM analysis of fin lines, the normalized resonant frequencies (b/λ) of fin line cavities are extracted from the impulse response of the simulating network via Fourier transformation. Two components of the coarseness error, the transverse and longitudinal coarseness errors, have been discussed. In addition, the error due to the simulating problem of the dielectric boundary was also discussed. Two sets of error characteristics were proposed for the error corrections of the three-dimensional TLM solutions of the finned waveguides and the slab-loaded waveguides. They are also considered as a guidance to the error evaluation for the three-dimenaional TLM analysis of fin lines.

Finally, by evaluating the equivalent susceptance of the fin in fin lines from the two-dimensional TLM solutions at cutoff, correction factors F and G were obtained. The transcendental equations which represent the transverse resonance conditions in fin lines, were then developed by modifying the susceptance of the fin with an appropriate correction factor. The dispersion characteristics (or the

normalized propagation constants) in fin lines were obtained, and shown to agree with previously published measurements, numerical solutions and the three-dimensional TLM solutions (better than 1%). It is concluded that the transverse resonance formulae, together with the correction factors, provide the fin line designer with a flexible tool which combines mathematical simplicity and easy applicability with excellent accuracy.

Appendix A

COMPUTER PROGRAM

This appendix contains three actual working programs yielding the results worked out in the text. Descriptions of these programs can be found in the comments of the programs themselves. Also attached to the end of each program is an example of input-output data.

The first program, named TR3, is a root-finding algorithm for obtaining the normalized cutoff frequency and the normalized propagation constant from the transcendental equations which describe the transverse resonance conditions in fin lines. The user inserts such parameters as the waveguide aspect ratio (b/a), the normalized gap width (d/b), the normalized dielectric thickness (s/b), the dielectric constant (ε_r), and the correction factor (F or G).

The other two programs, namely ITLM2 and TLM3D, are the general TLM simulation programs for solving two-dimensional and three-dimensional problems, respectively. The user prepares the information on the boundaries, the dielectric

constants in different regions of the structure under study, and the frequency range of interest, which will be the input data. The programs yield the desired results tabulated against the frequency.

```
C
C  ***************************************************************************
C  *                                                                         *
C  *                                                                         *
C  *     PROGRAM NAME : TR3                                                  *
C  *                                                                         *
C  *     PURPOSE    - TO EVALUATE FIN LINE PARAMETERS WITH TRANSVERSE        *
C  *                  RESONANCE METHOD                                       *
C  *                                                                         *
C  *     INPUT                                                               *
C  *          Z     - ASPECT RATIO OF WAVEGUIDE                            *
C  *          T     - GAP WIDTH OF FINS                                    *
C  *          W     - THICKNESS OF DIELECTRIC                              *
C  *          ER    - DIELECTRIC CONSTANT                                  *
C  *          G     - CORRECTION FACTOR                                    *
C  *          NI    - NUMBER OF OUTPUT POINTS                              *
C  *                                                                         *
C  *     OUTPUT     - EFFECTIVE DIELECTRIC CONSTANT AND CHARACTERISTIC      *
C  *                  IMPEDANCE WITH RESPECT TO FREQUENCY                    *
C  *                - PLOT OF EFF. DIEL. CONST. AGAINST FREQUENCY            *
C  *                                                                         *
C  *     VARIABLES                                                           *
C  *          A     - NI BY 100 ARRAY CONTAINING THE POINTS OF GRAPH       *
C  *          P     - SQUARE ROOT OF EFF. DIEL. CONST.                     *
C  *          X     - NORMALIZED FREQUENCY                                 *
C  *          ZF    - CHARACTERISTIC IMPEDANCE                             *
C  *                                                                         *
C  *     LANGUAGE   - FORTRAN                                                *
C  *                                                                         *
C  *     PRECISION  - SINGLE                                                 *
C  *                                                                         *
C  *     COMPUTER   - PDP-11/34                                              *
C  *                                                                         *
C  *     PROGRAMER  - YI-CHI SHIH                                            *
C  *                  DEPARTMENT OF ELECTRICAL ENGINEERING                   *
C  *                  UNIVERSITY OF OTTAWA                                   *
C  *                                                                         *
C  *                                                                         *
C  ***************************************************************************
C
      DIMENSION A(50,100),B(50)
      DIMENSION P(50),X(50),ZF(50)
      INTEGER DOT,HYPHEN,STAR,BLANK,DASH
      INTEGER A,IX,JX
      REAL XP,B,XI,ZO,ZF
      REAL A0,C,E,F,G,P,S,T,U,V,W,X,Z,DI,DO,ER,QI,QO,PI
      REAL A1,A2,A3,A4
      DATA DOT,HYPHEN,DASH/':','-','!'/
      DATA STAR,BLANK/'*',' '/
C **
C **  READ IN INPUT PARAMETERS
C **
      TYPE *,'INPUT DATA,Z,T,W,ER,G,NI'
      ACCEPT *,Z,T,W,ER,G,NI
      NN=NI+1
      TYPE 1
1     FORMAT(' ',' CONFIGURATION ??',/,10X,'0 --UNILATERAL FIN LINE',
     1/,10X,'1 --INSULATED FIN LINE',/,10X,'2 --BILATERAL FIN LINE')
      ACCEPT *,II
```

```
      TYPE *,'WANT PLOT ?   1 --YES;  0 --NO.'
      ACCEPT *,IP
C **
C **    CALCULATE NORMALIZED CUTOFF FREQUENCY OF THE EQUIVALENT RIDGED
C **    WAVEGUIDE AND ITS CHARACTERISTIC IMPEDANCE AT INFINITE FREQUENCY
C **
      PI=3.14159
      S=SIN(T*PI/2.)
      C=COS(T*PI/2.)**4
C ****  SET INITIAL VALUE FOR CUTOFF FREQUENCY
      XI=0.13
C ****  DO LOOP SOLVING TRANSCENDENTAL EQUATION
      DO 5 I=1,30
      QI=1./((1.-XI**2)**0.5)-1.
      DI=2.*XI*(ALOG(1./S)+QI*C/(1.+QI*S**4)+XI**2/16.
     1*(1.-3.*S**2)**2*C)
      IF(II-1)2,2,3
C ****  UNILATERAL, INSULATED FIN LINES
2     E=DI-COS(PI*XI/Z)/SIN(PI*XI/Z)
      GO TO 7
C ****  BILATERAL FIN LINE
3     E=SIN(PI*W*XI)/COS(PI*W*XI)/T+DI-COS(PI*XI*(1./Z-W))/
     1SIN(PI*XI*(1./Z-W))
C ****  CONVERGENCT TO SOLUTION
7     IF(ABS(E).LE.1.E-04)GO TO 10
      IF(E.LE.0.)GO TO 4
      XI=XI-0.13*0.5**I
      GO TO 5
4     XI=XI+0.13*0.5**I
5     CONTINUE
      IR=0
      TYPE 500,IR
C ****  CHARACTERISTIC IMPEDANCE OF RIDGED WAVEGUIDE AT INFINITE
C ****  FREQUENCY IS CALCULATED.
      IF(II-1)10,10,9
C ****  BILATERAL FIN LINE
9     ZO=120.*PI**2*XI/(SIN(PI*W*XI)+DI+SIN(PI*XI/2.*(1./Z-W))
     1*COS(PI*W*XI)/COS(PI*XI/2.*(1./Z-W)))
      GO TO 11
C ****  UNILATERAL, INSULATED FIN LINES
10    ZO=120.*PI**2*XI/(DI+SIN(PI*XI/2./Z)/COS(PI*XI/2./Z))
11    TYPE 12,XI,ZO
12    FORMAT(' ',5X,37HCUTOFF FOR EQUIV. RIDGED WAVEGUIDE IS,F8.4,
     1//,5X,'CHARACTERISTIC IMP. OF RIDGED WAVEGUIDE AT INIFINITE FREQ.'
     2,F10.5,///,5X,' P(WAVELENGTH/GUIDED WAVELENGTH)',5X,
     3' X(B/WAVELENGTH)',5X,'ZF(CHARACT. IMP. OF FIN LINES)',//)
C **
C **    DO LOOP OBTAINING NORMALIZED FREQUENCIES FOR DIFFERENT GUIDED
C **    WAVELENGTH ( OR EFFECTIVE DIELECTRIC CONSTANT ).
C **
      DO 100 I=1,NI
C ****  SET VALUES OF GUIDED WAVELENGTH
      P(I)=0.03*I-0.03
      U=(ABS(ER-P(I)**2))**0.5
      V=(ABS(1.-P(I)**2))**0.5
      S=SIN(T*PI/2.)
      C=COS(T*PI/2)**4
C ****  SET INITIAL VALUES FOR EXPECTED NORMALIZED FREQUENCY
      XIN=0.03*I*I/160.+0.2
      X(I)=XIN
C ****  DO LOOP SOLVING TRANSCENDENTAL EQUATION
      DO 90 J=1,30
      QI=1./((1.-(U*X(I))**2)**0.5)-1.
      DI=2.*U*X(I)*(ALOG(1./S)+QI*C/(1.+QI*S**4)+(U*X(I))**2/16.
     1*(1.-3.*S**2)**2*C)
      IF(P(I).GE.1.)GO TO 20
C ****  P<1; ( P IS THE SQURE ROOT OF EFF. DIEL. CONST.)
      F=(V/U)**2+G*(1.-(V/U)**2)
```

```
      IF(II-1)14,16,18
C ****  UNILATERAL FIN LINE
14    QO=1./((1.-(V*X(I))**2)**0.5)-1.
      DO=2.*V*X(I)*(ALOG(1./S)+QO*C/(1.+QO*S**4)+(V*X(I))**2/16.
     1*(1.-3.*S**2)**2*C)
      A1=2.*PI*X(I)*V*(0.5/Z-W)
      A2=2.*PI*W*X(I)*U+ATAN(U/V*SIN(A1)/COS(A1))
      A3=PI*X(I)*V/Z
      AO=U/V*COS(A2)/SIN(A2)+COS(A3)/SIN(A3)
      E=F*DI*U/V+DO-AO
      GO TO 30
C ****  INSULATED FIN LINE
16    A1=PI*W*X(I)*U+ATAN(U/V*SIN(PI*X(I)*V*(1./Z-W))
      1/COS(PI*X(I)*V*(1./Z-W)))
      AO=U/V*COS(A1)/SIN(A1)
      E=F*DI*U/V-AO
      GO TO 30
C ****  BILATERAL FIN LINE
18    QO=1./((1.-(V*X(I))**2)**0.5)-1.
      DO=2.*V*X(I)*(ALOG(1./S)+QO*C/(1.+QO*S**4)+(V*X(I))**2/16.
      1*(1.-3.*S**2)**2*C)
      AO=COS(PI*X(I)*V*(1./Z-W))/SIN(PI*X(I)*V*(1./Z-W))
      E=U/V*SIN(PI*W*X(I)*U)/COS(PI*W*X(I)*U)+G*DI*U/V+DO-AO
      GO TO 30
C ****  P>1;
20    F=-(V/U)**2+G*(1.+(V/U)**2)
      IF(II-1)24,26,28
C ****  UNILATERAL FIN LINE
24    QO=1./((1.+(V*X(I))**2)**0.5)-1.
      DO=2.*V*X(I)*(ALOG(1./S)+QO*C/(1.+QO*S**4)-(V*X(I))**2/16.
     1*(1.-3.*S**2)**2*C)
      A4=2.*PI*W*X(I)*U+ATAN(U/V*TANH(2.*PI*X(I)*V*(0.5/Z-W)))
      AO=U/V*COS(A4)/SIN(A4)+1./TANH(PI*X(I)*V/Z)
      E=F*DI*U/V-DO-AO
      GO TO 30
C ****  INSULATED FIN LINE
26    A1=PI*X(I)*W*U+ATAN(U/V*TANH(PI*X(I)*V*(1./Z-W)))
      AO=U/V*COS(A1)/SIN(A1)
      E=F*DI*U/V-AO
      GO TO 30
C ****  BILATERAL FIN LINE
28    QO=1./((1.+(V*X(I))**2)**0.5)-1.
      DO=2.*V*X(I)*(ALOG(1./S)+QO*C/(1.+QO*S**4)-(V*X(I))**2/16.
      1*(1.-3.*S**2)**2*C)
      AO=U/V*SIN(PI*W*X(I)*U)/COS(PI*W*X(I)*U)
      E=AO+G*DI*U/V-DO-1./TANH(PI*X(I)*V*(1./Z-W))
C ****  CONVERGING TO SOLUTION
30    IF(ABS(E).LE.1.E-04)GO TO 92
      IF(E.LE.0.)GO TO 80
      X(I)=X(I)-XIN*0.5**J
      GO TO 90
80    X(I)=X(I)+XIN*0.5**J
90    CONTINUE
      IR=1
      TYPE 500,IR
92    IF(P(I).EQ.0.)GO TO 93
C ****  CHARACTERISTIC IMPEDANCE AT FREQUENCIES ABOVE CUTOFF
      ZF(I)=ZO/P(I)
      GO TO 94
C ****  SET CHARACTERISTIC IMPEDANCE AT CUTOFF TO 9999.
93    ZF(I)=9999.
94    TYPE 95,P(I),X(I),ZF(I)
95    FORMAT(' ',16X,F7.3,21X,F7.4,20X,F10.5)
100   CONTINUE
      IF(IP.EQ.0)GO TO 606
C **
C **    THE FOLLOWING PART OF PROGRAM IS USED TO DRAW DIAGRAM
C **
```

```
      TYPE 110
  110 FORMAT('1',1X,38HY-AXIS=P(WAVELENGTH/GUIDED WAVELENGTH),/,
     1 1X,23H X-AXIS=X(B/WAVELENGTH))
      DO 200 I=1,NI
C **** ROUNDING OFF REAL NUMBER TO INTEGER
      XP=X(I)*200
      IX=XP
      IF((XP-IX).GE.0.5)GO TO 150
      JX=IX
      GO TO 160
  150 JX=IX+1
  160 DO 180 J=1,100
C **** SET BLANK WHOLE MATRIX
      A(NN-I,J)=BLANK
      IF(J.EQ.JX)GO TO 170
C **** SET AXIS AND OTHER SYMBOLS
      IF(J.EQ.20.OR.J.EQ.40.OR.J.EQ.60.OR.J.EQ.80.OR.J.EQ.100)
     1 A(NN-I,J)=DOT
      IF(J.EQ.1)A(NN-I,J)=DASH
      IF(I.EQ.1)A(NN-I,J)=HYPHEN
      GO TO 180
C **** SET OUTPUT DATA POINTS
  170 A(NN-I,J)=STAR
  180 CONTINUE
  200 CONTINUE
      DO 300 I=1,NI
      B(I)=(NI-I)*0.03
C **** PLOT WITH LABELS
      TYPE 280,B(I),(A(I,J),J=1,100)
  280 FORMAT(' ',15X,F4.2,1X,100A1)
  300 CONTINUE
      TYPE 350
  350 FORMAT(' ',20X,1H0,17X,3H0.1,17X,3H0.2,17X,3H0.3,17X,3H0.4,
     1 17X,3H0.5,//)
      TYPE 400,Z,T,W,ER,G
  400 FORMAT(' ',15X,35HGUIDED WAVELENGTH IN UNILATERAL FIN,/,
     1 16X,4HB/A=,F4.2,6H; D/B=,F4.2,6H; S/B=,F5.3,5H; ER=,F5.2,
     2 4H; G=,F4.2)
  500 FORMAT(' ',' ITERATIONS USED UP; RETURN CODE ',I2)
  606 STOP
      END
```

```
 RUN TR3
INPUT DATA,Z,T,W,ER,G,NI
0.5 0.13 0.072      2.22 0.37 40
 CONFIGURATION ??
          0 --UNILATERAL FIN LINE
          1 --INSULATED FIN LINE
          2 --BILATERAL FIN LINE
2
WANT PLOT ?   1 --YES;  0 --NO.
1
     CUTOFF FOR EQUIV. RIDGED WAVEGUIDE IS  0.1525
   CHARACTERISTIC IMP. OF RIDGED WAVEGUIDE AT INIFINITE FREQ. 178.87054
```

P(WAVELENGTH/GUIDED WAVELENGTH)	X(B/WAVELENGTH)	ZF(CHARACT. IMP. OF FIN LINES)
0.000	0.1394	9999.00000
0.030	0.1395	5962.35156
0.060	0.1396	2981.17578
0.090	0.1399	1987.45056
0.120	0.1402	1490.58801
0.150	0.1407	1192.47034
0.180	0.1413	993.72528
0.210	0.1419	851.76453
0.240	0.1427	745.29401
0.270	0.1437	662.48352
0.300	0.1447	596.23517
0.330	0.1459	542.03198
0.360	0.1472	496.86264
0.390	0.1487	458.64243
0.420	0.1504	425.88226
0.450	0.1522	397.49011
0.480	0.1543	372.64697
0.510	0.1566	350.72656
0.540	0.1591	331.24173
0.570	0.1619	313.80798
0.600	0.1651	298.11755
0.630	0.1686	283.92151
0.660	0.1725	271.01596
0.690	0.1769	259.23267
0.720	0.1819	248.43130
0.750	0.1876	238.49406
0.780	0.1941	229.32120
0.810	0.2016	220.82784
0.840	0.2104	212.94112
0.870	0.2209	205.59833
0.900	0.2335	198.74504
0.930	0.2490	192.33392
0.960	0.2687	186.32349
0.990	0.2946	180.67732
1.020	0.3303	175.36328
1.050	0.3831	170.35291
1.080	0.4671	165.62086
1.110	0.6027	161.14464
1.140	0.7745	156.90399
1.170	0.9218	152.88081

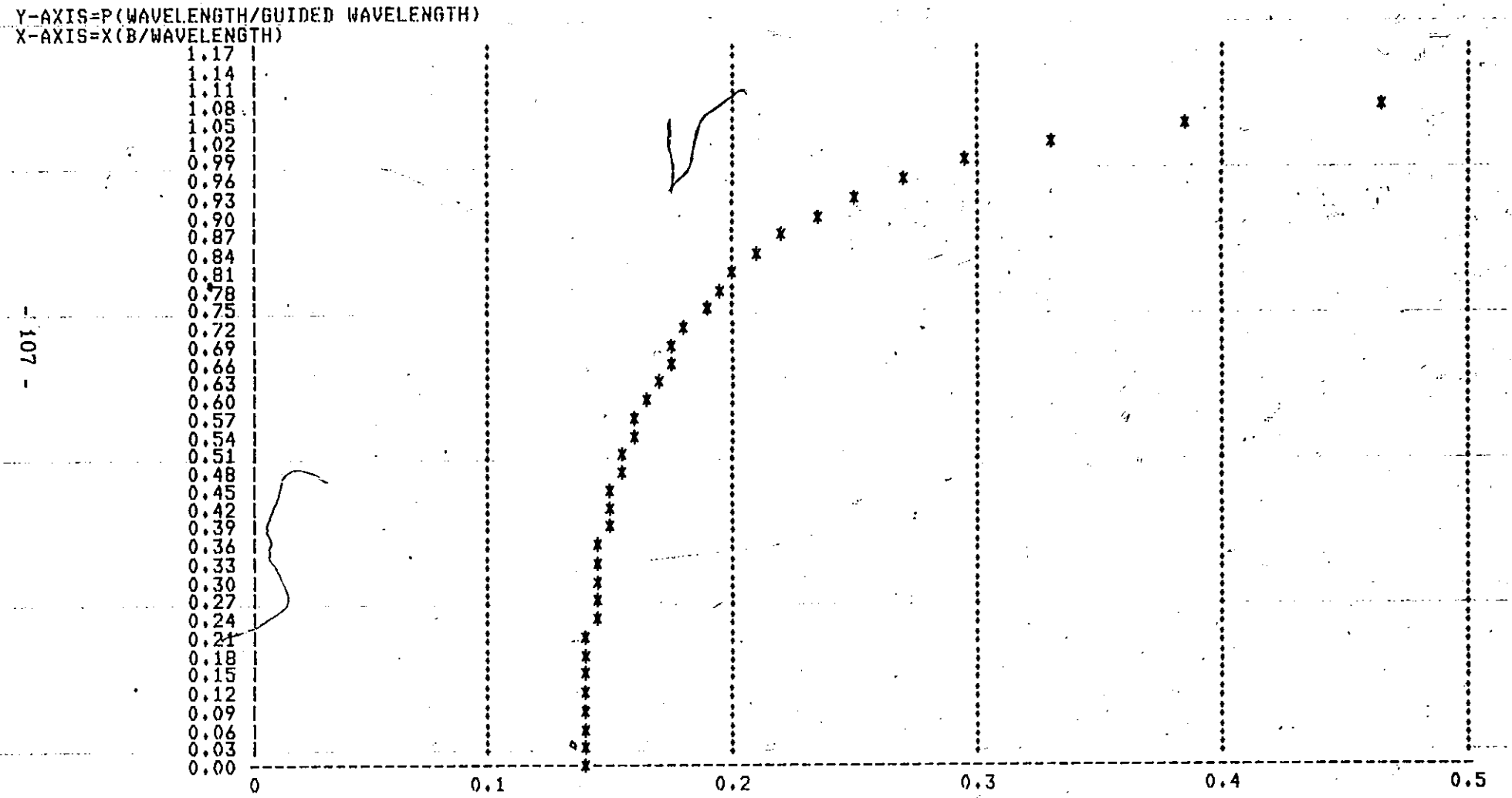

GUIDED WAVELENGTH IN UNILATERAL FIN LINE
B/A=0.50; D/B=0.13; S/B=0.072; ER= 2.22; G=0.37

```
C  ***************************************************************
C  *                                                             *
C  *     PROGRAM NAME - ITLM2                                    *
C  *                                                             *
C  *     PURPOSE  - TWO-DIMENSIONAL TRANSMISSION-LINE MATRIX     *
C  *                SIMULATION OF INHOMOGENEOUS STRUCTURE        *
C  *                                                             *
C  *     INPUTS   - LIMITS OF X AND Y CO-ORDINATES OF SIMULATING *
C  *                MATRIX                                       *
C  *              - BOUNDARIES IN BOTH CO-ORDINATES TOGETHER WITH *
C  *                APPROPRIATE BOUNDARIY CODE, REFLECTION COEF- *
C  *                FICIENTS, AND TERMINATION CODE               *
C  *              - EXCITATION POINTS OR LINES TOGETHER WITH     *
C  *                APPROPRIATE EXCITATION CODE, INITIAL VALUES, *
C  *                AND TERMINATION CODE                         *
C  *              - BOUNDARIES BETWEEN DIELECTRICS AND AIR       *
C  *              - COMPUTING BOXES AND THEIR DIELECTRIC CONSTANTS *
C  *              - FREQUENCY RANGE AND SAMPLING INTERVAL        *
C  *              - OUTPUT POINT AND NUMBER OF ITERATIONS        *
C  *                                                             *
C  *     OUTPUT   - FIELD INTENSITY AGAINST FREQUENCIES          *
C  *                                                             *
C  *     VARIABLES                                               *
C  *        NX    - NUMBER OF NODES (LIMIT) IN X CO-ORDINATE     *
C  *        NY    - NUMBER OF NODES (LIMIT) IN Y CO-ORDINATE     *
C  *        V     - 5 BY NX BY NY MATRIX CONTAINING MAGNITUDES   *
C  *                OF THE FOUR IMPULSES AT EACH NODE            *
C  *        IB    - KB BY 8 MATRIX CONTAINING INFORMATION OF     *
C  *                BOUNDARIES AND BOUNDARY CODE (IB(KB,5-8))    *
C  *                CODE 1310-HORIZONTAL WALL,2401-VERTICAL WALL *
C  *        IE    - KE BY 7 MATRIX CONTAINING EXCITATION POINTS  *
C  *                EXCITATION CODE (IE(KE,5-7))                 *
C  *                CODE 115 IS SUGGESTED                        *
C  *        IBD   - KD BY 8 MATRIX CONTAINING BOUNDARIES BETWEEN *
C  *                DIELECTRIC AND AIR, CODE SAME AS IN (IB)     *
C  *        KB    - NUMBER OF (IB) CARDS INPUT                   *
C  *        KE    - NUMBER OF (IE) CARDS INPUT                   *
C  *        KD    - NUMBER OF (IBD) CARDS INPUT                  *
C  *        R     - RREFLECTION COEFFICIENTS                     *
C  *        VA    - INITIAL EXCITATION VALUES                    *
C  *        RC    - REFLECTION COEFFICIENTS ON DIELECTRIC-AIR BDS *
C  *        IT    - TERMINATION CODE; 1-CONTINUE, 0-END          *
C  *        IA    - KC BY 4 MATRIX CONTAINING WORKING AREA WITH  *
C  *                DIFFERENT PERMITIVITY                        *
C  *        RD    - RELATIVE PERMITIVITY                         *
C  *        D     - ARRAY CONTAINING OUTPUT FREQUENCIES          *
C  *        EHRE  - ARRAY CONTAINING OUTPUT FIELD INTENSITY      *
C  *        D1    - STARTING FREQUENCY                           *
C  *        D2    - ENDING FREQUENCY                             *
C  *        DS    - FREQUENCY OUTPUT INTERVAL                    *
```

```
C  *        IO    - X CO-ORDINATE OF OUTPUT POINT                    *
C  *        JO    - Y CO-ORDINATE OF OUTPUT POINT                    *
C  *        NI    - NUMBER OF ITERATIONS REQUIRED                    *
C  *                                                                 *
C  *    PRECISION    - SINGLE                                        *
C  *                                                                 *
C  *    LANGUAGE     - FORTRAN                                       *
C  *                                                                 *
C  *******************************************************************
C
      DIMENSION V(5,34,18)
      DIMENSION D(300),EHRE(300),EHIM(300)
      DIMENSION IB(10,8),IE(10,7),R(10),VA(10)
      DIMENSION IBD(9,8),RC(9),IA(9,4),RD(9)
C*****
C*****   READ IN DATA CARDS
C*****
C  *****    INPUT LIMITS IN X AND Y CO-ORDINATES (NX,NY)
      READ(5,1)NX,NY
1     FORMAT(2I5)
C  *****    INPUT BOUNDARIES AND REFLECTION COEFFICIENTS (IB,R)
      WRITE(6,1000)
1000  FORMAT('1','BOUNDARIES ARE:',//)
      KB=0
2     KB=KB+1
      READ(5,5)(IB(KB,M),M=1,8),R(KB),IT
5     FORMAT(4I5,I2,3I1,F10.6,I2)
      WRITE(6,1001)(IB(KB,M),M=1,8),R(KB),IT
1001  FORMAT(' ',4I5,I2,3I1,F10.6,I2)
      IF(IT.NE.0)GO TO 2
C  *****    INPUT DIELECTRIC-AIR BOUNDARIES AND REFLECTION
C  *****              COEFFICIENTS (IBD,RC)
      WRITE(6,1100)
1100  FORMAT(' ',//,' BOUNDARIES BETWEEN DIELECTRICS',//)
      KD=0
6     KD=KD+1
      READ(5,5)(IBD(KD,M),M=1,8),RC(KD),IT
      WRITE(6,1001)(IBD(KD,M),M=1,8),RC(KD),IT
      IF(IT.NE.0)GO TO 6
C  *****    INPUT COMPUTING BOXES AND DIELECTRIC CONSTANT (IA,RD)
      WRITE(6,1101)
1101  FORMAT(' ',//,' THE COMPUTING BOXES ARE:',//)
      KC=0
8     KC=KC+1
      READ(5,9)(IA(KC,M),M=1,4),RD(KC),IT
9     FORMAT(4I5,F10.6,I2)
      WRITE(6,7)(IA(KC,M),M=1,4),RD(KC),IT
7     FORMAT(' ',4I5,F10.6,I2)
      IF(IT.NE.0)GO TO 8
```

```
C  *****    INPUT EXCITATION POINTS AND INITIAL VALUES (IE,VA)
      WRITE(6,1003)
1003  FORMAT(' ',//,' EXCITATION POINTS ARE:',//)
      KE=0
10    KE=KE+1
      READ(5,15)(IE(KE,M),M=1,7),VA(KE),IT
15    FORMAT(4I5,I3,2I1,F10.6,I2)
      WRITE(6,1002)(IE(KE,M),M=1,7),VA(KE),IT
1002  FORMAT(' ',4I5,I3,2I1,F10.6,I2)
      IF(IT.NE.0)GO TO 10
C  *****    INPUT INPUT STARTING, ENDING FREQUENCY AND OUTPUT
C  *****          INTERVAL (D1,D2,DS)
      READ(5,20)D1,D2,DS
20    FORMAT(3F10.6)
C  *****    INPUT OUTPUT POINT AND ITERATIONS (IO,JO,NI,YO)
      READ(5,22)IO,JO,NI,YO
22    FORMAT(3I5,F10.6)
C*****
C*****   INITIALIZATION
C*****
C  *****    INITIALIZE WORKING AREA V TO ZERO VALUES
      DO 24 J=1,NY
      DO 24 I=1,NX
      DO 24 M=1,5
24    V(M,I,J)=0.0
C  *****    SET EXCITATION POINTS WITH INITIAL EXCITATION VALUES
      DO 25 NE=1,KE
      IT3=IE(NE,3)
      IT4=IE(NE,4)
      IT1=IE(NE,1)
      IT2=IE(NE,2)
      IT5=IE(NE,5)
      IT6=IE(NE,6)
      IT=IE(NE,7)
      DO 25 J=IT3,IT4
      DO 25 I=IT1,IT2
      DO 25 M=IT5,IT,IT6
25    V(M,I,J)=VA(NE)
C  *****    SET OUTPUT FREQUENCIES AND COUNTER
C  *****    INITIALIZE ARRAR ERE, EHIM TO ZERO VALUES
      JD=1
      D(1)=D1
      EHRE(1)=0.0
      EHIM(1)=0.0
115   JD=JD+1
       D(JD)=D(JD-1)+DS
      EHRE(JD)=0.0
      EHIM(JD)=0.0
       IF(D(JD).LE.D2)GO TO 115
```

```
C*****
C*****   START ITERATION
C*****
117    DO 50 IC=1,NI
C  *****   BOUNDARY CONDITIONS
       DO 30 NB=1,KB
       IT3=IB(NB,3)
       IT4=IB(NB,4)
       IT1=IB(NB,1)
       IT2=IB(NB,2)
       DO 30 J=IT3,IT4
       DO 30 I=IT1,IT2
       VXY=V(IB(NB,6),I,J)
       V(IB(NB,6),I,J)=R(NB)*V(IB(NB,5),I+IB(NB,8),J+IB(NB,7))
30     V(IB(NB,5),I+IB(NB,8),J+IB(NB,7))=R(NB)*VXY
C  *****   IMPEDANCE MODIFICATION AT DIELECTRIC-AIR BOUNDARIES
       DO 33 NB=1,KD
       IT1=IBD(NB,1)
       IT2=IBD(NB,2)
       IT3=IBD(NB,3)
       IT4=IBD(NB,4)
       DO 33 J=IT3,IT4
       DO 33 I=IT1,IT2
       VX=V(IBD(NB,6),I,J)
       VY=V(IBD(NB,5),I+IBD(NB,8),J+IBD(NB,7))
       V(IBD(NB,6),I,J)=-RC(NB)*VY+(1.-RC(NB))*VX
33     V(IBD(NB,5),I+IBD(NB,8),J+IBD(NB,7))=RC(NB)*VX+(1.+RC(NB))*VY
C  *****   BOXES COMPUTATION;BASED ON APPROPRIATE VOLTAGE SCATTERING
C  *****    MATRIX FOR SHUNT-INHOMOGENEOUS-NODE
       DO 43 NB=1,KC
       IT1=IA(NB,1)
       IT2=IA(NB,2)
       IT3=IA(NB,3)
       IT4=IA(NB,4)
       DO 43 J=IT3,IT4
       DO 43 I=IT1,IT2
       A=(V(1,I,J)+V(1,I,J+1)+V(2,I,J)+V(2,I+1,J)+V(5,I,J)*RD(NB))
     1*2./(RD(NB)+4.)
       V(5,I,J)=A-V(5,I,J)
       V(1,I,J)=A-V(1,I,J)
       V(2,I,J)=A-V(2,I,J)
       VY=A-V(1,I,J+1)
       VX=A-V(2,I+1,J)
       V(2,I+1,J)=V(4,I,J)
       V(1,I,J+1)=V(3,I,J)
       V(3,I,J)=VY
43     V(4,I,J)=VX
```

```
C  *****   IMPULSE RESPONSE SAMPLING RATE CONTROL
      I=IC/2
      AI=I
      A=IC/2.
      IF((A-AI).NE.0.)GO TO 50
      EH=(V(1,IO,JO)+V(2,IO,JO)+V(3,IO,JO)+V(4,IO,JO)
     1+V(5,IO,JO)*YO)*2./(YO+4.)
C  *****   FOURIER TRANSFORM
       DO 140 J=1,JD
        CS=6.2831833*D(J)*IC
        EHRE(J)=EHRE(J)+EH*COS(CS)
140    EHIM(J)=EHIM(J)-EH*SIN(CS)
50     CONTINUE
C*****
C*****   OUTPUT THE FREQUENCY RESPONSE VIA FOURIER TRANSFORM
C*****
C  *****    PRINT INFORMATION OF OUTPUT POINT AND ITERATIONS
      WRITE(6,52)IO,JO,NI
52     FORMAT(' ',//,' OUTPUT POINT IS (',I2,',',I2,'),NI=',I4,//)
C  *****    COMPUTE MAGNITUDE OF OUTPUT FIELD AND FIND THE PEAK
      A=0.
      DO 220 I=1,JD
      EHRE(I)=SQRT(EHRE(I)*EHRE(I)+EHIM(I)*EHIM(I))
      IF(EHRE(I).LE.A)GO TO 220
      A=EHRE(I)
      IT=I
220    CONTINUE
C  *****    POLYNORMIAL CURVE FIT TO OBTAIN PEAK POINT VALUE
221    IF((IT.EQ.1).OR.(IT.EQ.JD))GO TO 230
      AI=((EHRE(IT-1)-A)*(D(IT-1)-D(IT+1))-(EHRE(IT-1)-EHRE(IT+1))*(D(IT
     1-1)-D(IT)))/((D(IT-1)-D(IT))*(D(IT)-D(IT+1))*(D(IT-1)-D(IT+1)))
      B=(EHRE(IT-1)-A)/(D(IT-1)-D(IT))-AI*(D(IT-1)+D(IT))
      PEAK=-B/(2.*AI)
C  *****    VELOCITY ERROR CORRECTION
      P=3.14159653*PEAK
      T=SQRT(2.)
      CF=P/ARSIN(T*SIN(P))
      PCF=PEAK/CF
C  *****   PRINT RESULTS
      WRITE(6,225)PEAK,CF,PCF
225    FORMAT(' ',//,3X,'PEAK=',F11.7,//,3X,'CORRECT FACTOR =',F8.5,//,
     13X,'CORRECTED PEAK =',F11.7,///)
      WRITE(6,205)
205    FORMAT('1',3X,'NORMALIZED FREQUENCY',5X,'FIELD INTENSITY',//)
230    WRITE(6,215)((D(I),EHRE(I)),I=1,JD)
215    FORMAT(' ',7X,F10.6,7X,F14.6)
606    STOP
       END
```

```
C ***
C *** INPUT DATA EXAMPLE (ALL DATA MUST BE IN CORRECT FORMAT)
C ***


COL.5     10    15    20    25    30    35
  |     |     |     |     |     |     |
  |     |     |     |     |     |     |
  V     V     |     |     |     |     |
 10     4     V     V     V     V     V
  2     9     1     1  1310  1.000000  1
  9     9     2     3  2401  1.000000  1
  2     9     3     3  1310  1.000000  1
  1     1     2     3  2401  1.000000  1
  5     5     2     2  2401  1.000000  0
  4     4     2     3  2401  0.378882  1
  5     5     3     3  2401 -0.378882  0
  1     4     1     3   0.000000  1
  5     5     1     3   4.880000  1
  6     9     1     3   0.000000  0
  2     3     2     3   115   1.000000  0
0.015000   0.050000   0.000100
  2     3   300   0.000000
```

```
C ***
C *** OUTPUT EXAMPLE
C ***

OUTPUT POINT IS ( 2, 3)  NI =  300


  PEAK             =  0.0307457
  CORRECT FACTOR   =  0.70600
  CORRECTED PEAK   =  0.0435491
  B/WAVELENGTH     =  0.1741962

   NORMALIZED FREQUENCY      FIELD INTENSITY

         0.015000                1.253428
         0.016000                0.724972
         0.017000                0.760593
         0.018000                1.074272
         0.019000                1.020931
         0.020000                0.820458
         0.021000                0.860294
         0.022000                1.339998
         0.023000                1.380057
         0.024000                0.693433
         0.025000                1.783010
         0.026000                2.714580
         0.027000                1.432700
         0.028000                2.853740
         0.029000                8.330346
         0.030000               12.721751
         0.031000               13.707491
         0.032000               10.682185
         0.033000                5.161589
         0.034000                0.496802
         0.035000                3.025558
         0.036000                2.748641
         0.037000                0.708201
         0.038000                1.491686
         0.039000                1.945919
         0.040000                0.915763
         0.041000                0.776778
         0.042000                1.455798
         0.043000                0.989642
         0.044000                0.404112
         0.045000                1.079513
         0.046000                0.976888
         0.047000                0.331850
         0.048000                0.768300
         0.049000                0.902514
         0.050000                0.420556
```

```
C  ***********************************************************************
C  *                                                                     *
C  *     PROGRAM NAME  - TLM3D                                           *
C  *                                                                     *
C  *     PURPOSE - THREE-DIMENSIONAL TRANSMISSION-LINE MATRIX            *
C  *               SIMULATION                                            *
C  *                                                                     *
C  *     INPUTS  - LIMITS IN X, Y AND Z CO-ORDINATES OF                  *
C  *               SIMULATING MATRIX                                     *
C  *             - BOUNDARIES IN ALL THREE CO-ORDINATES TOGETHER         *
C  *               WITH APPROPRIATE BOUNDARY CODE, REFLECTION            *
C  *               COEFFICIENTS, AND TERMINATION CODES                   *
C  *             - EXCITATION POINTS OR AREAS TOGETHER WITH              *
C  *               APPROPRIATE EXCITATION CODES, INITIAL VALUES          *
C  *               AND TERMINATION CODES                                 *
C  *             - COMPUTING BOXES AND CORRESPONDING DIELECTRIC          *
C  *               CONSTANTS                                             *
C  *             - FREQUENCY RANGE AND SAMPLING INTERVAL                 *
C  *             - OUTPUT POINT AND NUMBER OF ITERATIONS                 *
C  *                                                                     *
C  *     OUTPUTS - PEAK VALUE OF RESONANCE                               *
C  *             - PEAK VALUE AFTER VELOCITY CORRECTION                  *
C  *             - LIST OF FIELD INTENSITY AGAINST FREQUENCY             *
C  *                                                                     *
C  *     VARIBLES                                                        *
C  *        NX     - LIMIT IN X CO-ORDINATE (NUMBER OF NODES)            *
C  *        NY     - LIMIT IN Y CO-ORDINATE (NUMBER OF NODES)            *
C  *        NZ     - LIMIT IN Z CO-ORDINATE (NUMBER OF NODES)            *
C  *        IB     - KB BY 6 MATRIX CONTAINING BOUNDARY LOCATIONS        *
C  *        IX     - X-BOUNDARY CODE, CODE 0: BOUNDARY SURFACE IN X      *
C  *                 DIRECTION; CODE 1: NO                               *
C  *        IY     - Y-BOUNDARY CODE; CODE 0: BOUNDARY SURFACE IN Y      *
C  *                 DIRECTION; CODE 1: NO                               *
C  *        IZ     - Z-BOUNDARY CODE; CODE 0: BOUNDARY SURFACE IN Z      *
C  *                 DIRECTION; CODE 1: NO                               *
C  *        LB     - BOUNDARY CODE; CODE 0: SHORT-CIRCUITED;             *
C  *                                CODE 1: OPEN-CIRCUITED               *
C  *        IS     - KS BY 6 MATRIX CONTAINING WORKING AREAS WITH        *
C  *                 DIFFERENT DIELECTRIC CONSTANTS                      *
C  *        ER     - DIELECTRIC CONSTANTS                                *
C  *        L      - TERMINATION CODE; CODE 1; DATA SET INPUT CON-       *
C  *                 TINUING; CODE 0: DATA SET INPUT ENDS                *
C  *        IE     - KE BY 7 MATRIX CONTAINING EXCITATION POINTS         *
C  *                 (IE(KE,1-6)) AND EXCITATION CODE (IE(KE,7))         *
C  *                 CODE 1: X-COMPONENT; CODE 2: Y-COMPONENT            *
C  *                 CODE 3: Z-COMPONENT                                 *
C  *        VA     - EXCITATION VALUES                                   *
C  *        V      - 22 BY NX+1 BY NY+1 BY NZ+1 MATRIX CONTAINING        *
C  *                 IMPULSES INFORMATION REPRESENTING 3D-TLM NODES      *
C  *        D1     - STARTING FREQUENCY (NORMALIZED)                     *
C  *        D2     - ENDING FREQUENCY (NORMALIZED)                       *
```

```
C  *        DS     - FREQUENCY OUTPUT INTERVAL (SAMPLING INTERVAL)    *
C  *        IO     - X CO-ORDINATE OF OUTPUT POINT                    *
C  *        JO     - Y CO-ORDINATE OF OUTPUT POINT                    *
C  *        KO     - Z CO-ORDINATE OF OUTPUT POINT                    *
C  *        NI     - NUMBER OF ITERATIONS                             *
C  *        D      - ARRAY CONTAINING OUTPUT FREQUENCY                *
C  *        EHRE   - ARRAY CONTAINING OUTPUT FIELD INTENSITY          *
C  *                                                                  *
C  *     PRECISION      - SINGLE                                      *
C  *                                                                  *
C  *     LANGUAGE       - FORTRAN                                     *
C  *                                                                  *
C  ********************************************************************
C
      DIMENSION D(200),EHRE(200),EHIM(200)
      DIMENSION V(22,9,33,10)
      DIMENSION IB(10,6),IX(10),IY(10),IZ(10),LB(10),IEC(5,3)
      DIMENSION IS(3,6),ER(3),IE(1,7),VA(1)
      DATA IEC/1,2,3,4,13,5,6,7,8,14,9,10,11,12,15/
C **
C **     READ DATA
C **
C ****     LIMITS OF WORKING AREA
      READ(5,1000)NX,NY,NZ
1000  FORMAT(3I5)
      NXX=NX+1
      NYY=NY+1
      NZZ=NZ+1
      WRITE(6,1003)
1003  FORMAT('0',' BOUNDARIES',/)
C ****     BOUNDARIES AND BOUNDARY CODES
      KB=0
1005  KB=KB+1
      READ(5,1010,ERR=240)(IB(KB,M),M=1,6),IX(KB),IY(KB),IZ(KB),LB(KB),L
1010  FORMAT(6I5,I2,3I1,I2)
      WRITE(6,1010)(IB(KB,M),M=1,6),IX(KB),IY(KB),IZ(KB),LB(KB),L
      IF(L.NE.0)GO TO 1005
      WRITE(6,1080)
1080  FORMAT(' ',//,2X,'COMPUTING BOXES',/)
C ****     COMPUTING BOXES AND DIELECTRIC CONSTANTS
      KS=0
1020  KS=KS+1
      READ(5,1030,ERR=240)(IS(KS,M),M=1,6),ER(KS),L
1030  FORMAT(6I5,F10.6,I2)
      WRITE(6,1030)(IS(KS,M),M=1,6),ER(KS),L
      IF(L.NE.0)GO TO 1020
      WRITE(6,1110)
1110  FORMAT(' ',//,2X,'EXCITATION VALUES',/)
C ****     EXCITATION POINTS AND INITIAL VALUES
      KE=0
1040  KE=KE+1
      READ(5,1050,ERR=240)(IE(KE,M),M=1,7),VA(KE),L
1050  FORMAT(7I5,F10.6,I2)
      WRITE(6,1050)(IE(KE,M),M=1,7),VA(KE),L
```

```
      IF(L.NE.0)GO TO 1040
C ****    OUTPUT FREQUENCY RANGE AND SAMPLING STEP
      READ(5,20)D1,D2,DS
20    FORMAT(3F10.6)
C ****    OUTPUT POINT AND NUMBER OF ITERATIONS
      READ(5,40)IO,JO,KO,NI
40    FORMAT(4I5)
      IF(NI.GT.2000)GO TO 240
C **
C **    INITIALIZATION
C **
C ****    SET WORKING AREA TO ZERO
      DO 70 K=1,NZZ
       DO 70 J=1,NYY
        DO 70 I=1,NXX
         DO 70 M=1,22
70    V(M,I,J,K)=0.0
C ****    SET IMPEDANCE CONSTANT OF THE SERIES-NODE SCATTERING
C ****    FORMULA TO 0.5
      DO 80 K=1,NZ
       DO 80 J=1,NY
        DO 80 I=1,NX
         DO 80 M=20,22
80    V(M,I,J,K)=0.5
C ****    SET-ADMITTANCE CONSTANT OF THE SHUNT-NODE SCATTERING
C ****    FORMULA ACCORDING TO THE DIELECTRIC CONSTANT OF THE
C ****    CORRESPONDING COMPUTING BOX
      DO 90 NS=1,KS
       ER1=4.*(ER(NS)-1.)
       ER2=2./(4.+ER1)
       IT1=IS(NS,1)
       IT2=IS(NS,2)
       IT3=IS(NS,3)
       IT4=IS(NS,4)
       IT5=IS(NS,5)
       IT6=IS(NS,6)
       DO 90 K=IT5,IT6
        DO 90 J=IT3,IT4
         DO 90 I=IT1,IT2
          V(16,I,J,K)=ER1
          DO 90 M=17,19
           V(M,I,J,K)=ER2
90    CONTINUE
C ****    SET UP BOUNDARIES
      DO 100 NS=1,KB
       LX=3*LB(NS)
       IT1=IB(NS,1)
       IT2=IB(NS,2)
       IT3=IB(NS,3)
       IT4=IB(NS,4)
       IT5=IB(NS,5)
       IT6=IB(NS,6)
       DO 100 K=IT5,IT6
```

```
          DO 100 J=IT3,IT4
           DO 100 I=IT1,IT2
            IF(IX(NS).EQ.1)V(17+LX,I,J,K)=0.0
            IF(IY(NS).EQ.1)V(18+LX,I,J,K)=0.0
            IF(IZ(NS).EQ.1)V(19+LX,I,J,K)=0.0
100     CONTINUE
C ****      SET EXCTATION POINTS WITH THE INITIAL VALUES
        DO 110 NS=1,KE
         IT1=IE(NS,1)
         IT2=IE(NS,2)
         IT3=IE(NS,3)
         IT4=IE(NS,4)
         IT5=IE(NS,5)
         IT6=IE(NS,6)
         DO 110 K=IT5,IT6
          DO 110 J=IT3,IT4
           DO 110 I=IT1,IT2
            DO 110 M=1,5
110     V(IEC(M,IE(NS,7)),I,J,K)=VA(NS)
C ****      INITIALIZE OUTPUT-DATA AND TEMPORATORY STORAGE
        JD=1
        D(1)=D1
        EHIM(1)=0.0
        EHRE(1)=0.0
115     JD=JD+1
        D(JD)=D(JD-1)+DS
        EHRE(JD)=0.0
        EHIM(JD)=0.0
        IF(D(JD).LE.D2)GO TO 115
        IF((JD.GT.400).OR.(JD.LE.10))GO TO 240
C **
C **      START ITERATIONS
C **
        DO 200 NS=1,NI
C ****      COMPUTE THE WAVE SCATTERING ON SERIES NODES
         DO 120 K=1,NZ
          DO 120 J=1,NY
           DO 120 I=1,NX
            CALL O(V(8,I,J,K),V(12,I,J,K),V(6,I,J,K+1),V(10,I,J+1,K)
     1       ,V(20,I,J,K))
            CALL O(V(11,I,J,K),V(3,I,J,K),V(9,I+1,J,K),V(1,I,J,K+1)
     1       ,V(21,I,J,K))
            CALL O(V(7,I,J,K),V(4,I,J,K),V(5,I+1,J,K),V(2,I,J+1,K)
     1       ,V(22,I,J,K))
120     CONTINUE
C ****      COMPUTE THE WAVE SCATTERING ON SHUNT NODES
         DO 130 K=1,NZZ
          DO 130 J=1,NYY
           DO 130 I=1,NXX
            CALL S(V(1,I,J,K),V(2,I,J,K),V(3,I,J,K),V(4,I,J,K)
     1       ,V(13,I,J,K),V(16,I,J,K),V(17,I,J,K))
            CALL S(V(5,I,J,K),V(6,I,J,K),V(7,I,J,K),V(8,I,J,K)
     1       ,V(14,I,J,K),V(16,I,J,K),V(18,I,J,K))
            CALL S(V(9,I,J,K),V(10,I,J,K),V(11,I,J,K),V(12,I,J,K)
     1       ,V(15,I,J,K),V(16,I,J,K),V(19,I,J,K))
```

```
130     CONTINUE
C ****      IMPULSE RESPONSE SAMPLING
        I=NS/2
        AI=I
        A=NS/2.
        IF((A-AI).NE.0.0)GO TO 200
        EH=2.*(V(1,IO,JO,KO)+V(2,IO,JO,KO)+V(3,IO,JO,KO)+V(4,IO,JO
       1 ,KO)+V(16,IO,JO,KO)*V(13,IO,JO,KO))/(4.+V(16,IO,JO,KO))
C ****      FOURIER TRANSFORM
        DO 140 J=1,JD
         CS=6.2831833*D(J)*NS
         EHRE(J)=EHRE(J)+EH*COS(CS)
140      EHIM(J)=EHIM(J)-EH*SIN(CS)
200     CONTINUE
C **
C **      OUTPUTS
C **
        WRITE(6,203)IO,JO,KO,NI
203     FORMAT(' ',//,2X,'OUTPUT POINT IS (',I2,',',I2,',',I2,')',
       1'NI=',I5)
C ****      CALCULATE THE AMPLITUDE OF THE FREQUENCY RESPONSE
C ****      AND FIND THE PEAK VALUE
        A=0.
        DO 220 I=1,JD
        EHRE(I)=SQRT(EHRE(I)*EHRE(I)+EHIM(I)*EHIM(I))
        IF(EHRE(I).LE.A)GO TO 220
        A=EHRE(I)
        IT=I
220      CONTINUE
221     IF((IT.EQ.1).OR.(IT.EQ.JD))GO TO 230
        AI=((EHRE(IT-1)-A)*(D(IT-1)-D(IT+1))-(EHRE(IT-1)-EHRE(IT+1))*(D(IT
       1-1)-D(IT)))/((D(IT-1)-D(IT))*(D(IT)-D(IT+1))*(D(IT-1)-D(IT+1)))
        B=(EHRE(IT-1)-A)/(D(IT-1)-D(IT))-AI*(D(IT-1)+D(IT))
        PEAK=-B/(2.*AI)
C ****      VELOCITY CORRECTION
        P=3.141592653*PEAK
        T=SQRT(2.)
        CF=P/ARSIN(T*SIN(P))
        PCF=PEAK/CF*T
C ****      WRITE RESULTS
        WRITE(6,225)PEAK,CF,PCF
225     FORMAT(' ',//,3X,'PEAK=',F10.5,//,3X,'CORRECT FACTOR =',F8.5,//,
       113X,'CORRECTED PEAK =',F10.5)
        WRITE(6,205)
205     FORMAT('1',3X,'NORMALIZED FREQUENCY',5X,'FIELD INTENSITY',//)
230     WRITE(6,215)((D(I),EHRE(I)),I=1,JD)
215     FORMAT(' ',7X,F10.6,7X,F14.6)
        GO TO 606
240     WRITE(6,241)
241     FORMAT(' ','INPUT DATA FORMAT ERROR')
606     STOP
        END
```

```
C
C  ***************************************************************
C  *                                                             *
C  *     SUBROUTINE NAME : O                                     *
C  *                                                             *
C  *     PURPOSE    - TO PERFORM THE WAVE SCATTERING PROPERTY     *
C  *                  ON A SERIES NODE.                          *
C  *                                                             *
C  *     INPUT      - INCIDENT FIELD COMPONENTS AT TIME K        *
C  *                                                             *
C  *     OUTPUT     - REFLECTED FIELD COMPONENTS AT TIME K+1     *
C  *                                                             *
C  ***************************************************************
C
      SUBROUTINE O(V1,V2,V3,V4,Z)
      A=Z*(-V1+V2+V3-V4)
      V1=V1+A
      V2=V2-A
      V3=V3-A
      V4=V4+A
      RETURN
      END
C
C  ***************************************************************
C  *                                                             *
C  *     SUBROUTINE NAME : S                                     *
C  *                                                             *
C  *     PURPOSE      - TO PERFORM THE WAVE SCATTERING PROPERTY   *
C  *                    ON A SHUNT NODE                          *
C  *                                                             *
C  *     INPUT        - INCIDENT FIELD COMPONENTS AT TIME K      *
C  *                                                             *
C  *     OUTPUT       - REFLECTED FIELD COMPONENTS AT TIME K+1   *
C  *                                                             *
C  ***************************************************************
C
      SUBROUTINE S(V1,V2,V3,V4,V5,YO,Y)
      A=Y*(V1+V2+V3+V4+YO*V5)
      V1=A-V1
      V2=A-V2
      V3=A-V3
      V4=A-V4
      V5=A-V5
      RETURN
      END
```

```
C **
C **     INPUT DATA EXAMPLE
C **

COL.5    10    15    20    25    30    35    40    45    50
     |     |     |     |     |     |     |     |     |     |
     |     |     |     |     |     |     |     |     |     |
     |     |     |     |     |     |     |     |     |     |
     V     V     V     |     |     |     |     |     |     |
     4    16     6     V     V     V     V     |     |     |
     1     1     1    17     1     6 0110 1    |     |     |
     5     5     1    17     1     6 0110 1    |     |     |
     1     5     1     1     1     6 1010 1    |     |     |
     1     5    17    17     1     6 1010 1    |     |     |
     1     5     1    17     1     1 1100 1    |     |     |
     1     5     1    17     6     6 1101 1    |     |     |
     2     4     9     9     1     6 1010 0  V  |     |     |
     1     5     1     8     1     6  1.000000 1 |     |     |
     1     5     9    10     1     6  2.220000 1 |     |     |
     1     5    11    17     1     6  1.000000 0  V     V     V
     1     4     1    16     1     6     1  0.100000 0
 0.015000  0.025000  0.000400
     1     9     6  600
```

```
C **
C **     OUTPUT DATA EXAMPLE
C **

 PEAK=    0.01971

 CORRECT FACTOR = 0.70665

 CORRECTED PEAK =    0.03944

 NORMALIZED FREQUENCY      FIELD INTENSITY

        0.015000              5.130810
        0.015400              8.845688
        0.015800              8.342306
        0.016200              3.091698
        0.016600              6.100382
        0.017000             13.554790
        0.017400             15.341691
        0.017800              8.114990
        0.018200              8.770640
        0.018600             31.183731
        0.019000             53.448868
        0.019400             68.774628
        0.019800             72.305283
        0.020200             62.891541
        0.020600             43.526764
        0.021000             20.220169
        0.021400              1.555690
        0.021800             13.076377
        0.022200             15.940392
        0.022600             10.870518
        0.023000              2.421845
        0.023400              6.185817
        0.023800              9.684824
        0.024200              8.099097
        0.024600              3.152251
        0.025000              3.382804
```

Appendix B

ORIGINAL TLM SOLUTIONS

This appendix includes the results obtained with the TLM programs in tabular form. These results are collected as a valuable reference for further investigation on the fin-line analysis using the TLM method.

Unless specified, the truncation error of the results is less than 0.1%.

Normalized Fundamental Cutoff Frequency (b/λ_c) in Finned Waveguide b/a=1/2

b/Δℓ / d/b	8	16	32	64	∞ (extrapolated)
1/2	0.21568	0.22042	0.22271	0.22372	0.22497
1/4	0.17751	0.18548	0.18907	0.19094	0.19294
1/8*	N/A	0.15790	0.16378	0.16670	0.16964
1/16+	N/A	N/A	0.14341	0.14783	0.15225

* Truncation Error $E_T = 0.4\%$
\+ Truncation Error $E_T = 0.2\%$

b/Δℓ / d/b	12	24	48	∞ (extrapolated)
1/3	0.18782	0.19678	0.20107	0.20537
2/3	0.23046	0.23477	0.23703	0.23910

Normalized Fundamental Cutoff Frequency (b/λ_c)
in Slab-Loaded Waveguides
$b/a = 1/2$, $s/a = 1/5$

ε_r \ $a/\Delta\ell$	10	20	30	∞ (TR method)
2	0.21170	0.21145	0.21138	0.21131
4	0.16802	0.16754	0.16746	0.16733
9	0.12054	0.12003	0.11994	0.11979

Normalized Fundamental Cutoff Frequency (b/λ_c) in Unilateral Finline

$b/a=1/2$, $\varepsilon_r = 2.22$

	b/Δℓ / d/b	4	8	16	32	∞ (extrapolated)
s/a = 1/4	1/2	0.16481	0.17321	0.17740	--	0.18156
	1/4	--	0.14226	0.14827	--	0.15428
	1/8	--	--	0.12559	0.13033	0.13507
s/a = 1/8	1/2	0.17447	0.18328	0.18768	0.19007	0.19209
	1/4	--	0.14689	0.15391	0.15764	0.16093
	1/8	--	--	0.12904	0.13436	0.13969

	b/Δℓ / d/b	8	16	32	48	∞ (extrapolated)
s/a = 1/16	1/2	0.19314	0.19784	0.20018	--	0.20253
	1/4	0.15376	0.16115	0.16522	--	0.16854
	1/8	--	0.13365	0.13921	0.14116	0.14477
s/a = 1/32	1/2	--	0.20618	0.20867	0.20981	0.21116
	1/4	--	0.16870	0.17259	0.17378	0.17647
	1/8	--	0.13953	0.14519	0.14699	0.15084

Normalized Second Order Cutoff Frequency (b/λ_c)* in Unilateral Finline

$b/a = 1/2$, $\varepsilon_r = 2.22$

	b/Δℓ / d/b	4	8	16	32	∞ (extrapolated)
s/a = 1/4	1/2	0.42672	0.43635	0.43968	--	0.44160
	1/4	--	0.42079	0.42491	--	0.42741
	1/8	--	--	0.41460	0.41711	0.41890
s/a = 1/8	1/2	0.47902	0.48561	0.48637	0.48746	0.48850
	1/4	--	0.48307	0.48477	0.48533	0.48600
	1/8	--	--	0.48370	0.48437	0.48470

	b/Δℓ / d/b	8	16	32	48	∞ (extrapolated)
s/a = 1/16	1/2	0.49712	0.49761	0.49815	--	0.49840
	1/4	0.49719	0.49679	0.49726	--	0.49720
	1/8	--	0.49679	0.49744	0.49680	0.49721
s/a = 1/32	1/2	--	0.49929	0.49899	0.49904	0.49889
	1/4	--	0.49957	0.49953	0.49860	0.49853
	1/8	--	0.49870	0.49958	0.49933	0.49990

* Truncation Error $E_T = 0.2\%$

Normalized Fundamental Cutoff Frequency (b/λ_c) in Bilateral Finline $b/a=1/2$, $\varepsilon_r = 2.22$

	b/Δℓ / d/b	4	8	16	32	∞ (extrapolated)
s/a=1/4	1/2	0.15118	0.15929	0.16373	0.16604	0.16830
	1/4	--	0.12483	0.13127	0.13462	0.13780
	1/8	--	--	0.10844	0.11305	0.11767
s/a=1/8	1/2	--	0.17083	0.17543	0.17798	0.18020
	1/4	--	0.13034	0.13701	0.14062	0.14400
	1/8	--	--	0.10976	0.11491	0.12005

	b/Δℓ / d/b	16	32	48	64	∞ (extrapolated)
s/a=1/16	1/2	0.18981	0.19214	0.19328	--	0.19447
	1/4	0.14920	0.15273	--	--	0.15625
	1/8	0.11799	0.12335	--	--	0.12870
s/a=1/32	1/2	--	0.20396	--	0.20511	0.20627
	1/4	--	0.16524	--	0.16716	0.16907
	1/8	--	0.13482	--	0.13770	0.14057

Normalized Second Order Cutoff Frequency (b/λ_c)
in Bilateral Finline
$b/a = 1/2$, $\varepsilon_r = 2.22$

	b/λ / d/b	4	8	16	32	∞ (extrapolated)
s/a = 1/4	1/2	0.15383	0.17231	0.18067	0.18464	0.18860
	1/4	--	0.12848	0.13731	0.14129	0.14525
	1/8	--	--	0.11162	0.11691	0.12200
s/a = 1/8	1/2	--	0.19854	0.20913	0.21362	0.21600
	1/4	--	0.15057	0.16138	0.16606	0.16900
	1/8	--	--	0.13508	0.14114	0.14410
s/a = 1/16	1/2	--	--	0.22841	0.23253	0.23450
	1/4	--	--	0.17887	0.18439	0.18680
	1/8	--	--	0.15375	0.16039	0.16370

Normalized Fundamental Cutoff Frequency $(b/\lambda_c)^*$ in Insulated Finline

$b/a = 1/2$, $\varepsilon_r = 2.22$

	b/Δℓ / d/b	8	16	24	32	∞ (extrapolated)
s/a = 1/4	1/2	0.16187	0.16588	0.16766	0.16859	0.17011
	1/4	0.12816	0.13464	--	--	0.14115
	1/8	--	0.11187	--	0.11646	0.12105
s/a = 1/8	1/2	0.17634	0.18101	0.18224	--	0.18533
	1/4	0.13751	0.14434	--	--	0.15117
	1/8	--	0.11770	--	0.12314	0.12858

	b/Δℓ / d/b	16	32	64	∞ (extrapolated)
s/a = 1/16	1/2	0.19436	0.19665	--	0.19894
	1/4	0.15573	0.15938	--	0.16303
	1/8	0.12617	0.13172	--	0.13726
s/a = 1/32	1/2	--	0.20706	0.20792	0.20877
	1/4	--	0.16947	0.17192	0.17438
	1/8	--	0.14213	0.14372	0.14531

* Truncation Error $E_T = 0.2\%$.

Normalized Second Order Cutoff Frequency (b/λ_c)
in Insulated Finline
$b/a=1/2$, $\varepsilon_r = 2.22$

s/a \ b/Δℓ	8	16	32	64	∞ (extrapolated)
1/4	0.23401	0.23502	0.23526	--	0.23538
1/8	0.24702	0.24778	0.24793	--	0.24790
1/16	--	0.24966	0.24975	0.24978	0.24978

Normalized Fundamental Resonant Frequency(b/λ)
in Cavities Containing Unilateral Finline
$a = 16\Delta\ell$, $b/a = 1/2$, $\varepsilon_r = 2.22$

	c/b / d/b	7/8	9/8	11/8	13/8	15/8
s/a = 1/16	1/2*	0.55068	0.44832	0.38528	0.34272	
	1/2+	0.52304	0.42752	0.36776	0.32752	0.29968
	1/4*	0.53288	0.42912	0.36416	0.32032	
	1/4+	0.48704	0.39288	0.33440	0.29440	0.26608
s/a = 1/8	1/2*	0.51888	0.42440	0.36536	0.32552	
	1/2+	0.48840	0.40032	0.34464	0.30776	0.28160
	1/4*	0.50936	0.41112	0.34960	0.30768	
	1/4+	0.45928	0.37152	0.31552	0.27824	0.25168

* 'Dielectric recess'

\+ 'Dielectric protrusion'

Normalized Fundamental Resonant Frequency (b/λ) in Cavities Containing Unilateral Finline

$b/a = 1/2$, $\varepsilon_r = 2.22$

$a/b/c = 8/4/3$, $s/a = 1/8$

d/b \ a/Δℓ	8.	16	32		
1/2*	0.57836	0.58960	0.58960		
1/2+	0.52632	0.55472	0.56654		
1/4*	0.38088	0.39160			
1/4+	0.35444	0.38952			

$a = 32\Delta\ell$, $d/b = 1/8$

s/a \ c/b	17/16	21/16	25/16		
1/16*	0.43552		0.31224		
1/16+	0.39888				
1/32*	0.45312	0.37680			
1/32+	0.42112				

* 'Dielectric recess'

\+ 'Dielectric protrusion'

Normalized Fundamental Resonant Frequency (b/λ) in Cavities Containing Bilateral Finline

$b/a = 1/2$, $\varepsilon_r = 2.22$

$a = 16\Delta\ell$

	d/b \ c/b	7/8	9/8	11/8	13/8	15/8
s/a=1/4	1/2	0.46280	0.37744	0.32368	0.28760	0.26208
	1/4	0.44760	0.36144	0.30680	0.26904	0.24208
s/a=1/8	1/2	0.49624	0.40504	0.34784	0.30896	0.28160
	1/4	0.46840	0.37952	0.32264	0.28272	0.25464

$a = 8\Delta\ell$, $s/a = 1/4$

d/b \ c/b	3/4	4/4	5/4	6/4	7/4
1/2	0.50136	0.40004	0.33720	0.29556	0.26620

$a = 32\Delta\ell$

d/b	s/a	c/b	b/λ	
1/2	1/4	15/16	0.44032	
1/2	1/4	19/16	0.36640	
1/8	1/8	21/16	0.32560	
1/8	1/8	25/16	0.28112	
1/8	1/16	17/16	0.40864	

Normalized Fundamental Resonant Frequency (b/λ) in Cavities Containing Insulated Finline

$b/a = 1/2$, $\varepsilon_r = 2.22$

$a = 16\Delta\ell$

	d/b \ c/b	7/8	9/8	11/8	13/8	15/8
s/a=1/4	1/2	0.44496	0.36376	0.31336	0.27984	0.25592
	1/4	0.42152	0.34000	0.28880	0.25472	0.23016
s/a=1/8	1/2	0.48360	0.39632	0.34112	0.30480	0.27888
	1/4	0.45160	0.36488	0.31016	0.27312	0.24536

$a = 32\Delta\ell$, $d/b = 1/8$

s/a \ c/b	17/16	21/16	25/16		
1/8		0.30512	0.26496		
1/16	0.39232	0.32752	0.28384		

$a = 8\Delta\ell$, $s/ = 1/4$

d/b \ c/b	3/4	4/4	5/4	6/4	7/4
1/2	0.49044	0.39004	0.32864	0.28836	0.26036

$a = 32\Delta\ell$, $d/b = 1/2$, $s/a = 1/4$, $b/\lambda = 0.28896$

$a = 32\Delta\ell$, $d/b = 1/4$, $s/a = 1/8$, $b/\lambda = 0.43008$

Correction Factor F for Unilateral Fin Lines

	d/b / s/b	0.5	0.25	0.125
$\varepsilon_r = 2.22$	0.25	0.9786	0.9654	0.9535
	0.125	0.8900	0.8761	0.8937
	0.0625	0.7404	0.7375	0.7832
$\varepsilon_r = 3.0$	0.25	0.9656	0.9483	0.9568
	0.125	0.8425	0.8340	0.8620
	0.0625	0.6852	0.6753	0.7276
$\varepsilon_r = 9.0$	0.25	0.9591	0.9353	0.9334
	0.125	0.7576	0.7611	0.8102
	0.0625	0.5027	0.5261	0.6098

Correction Factor F for Insulated Fin Lines

	s/b \ d/b	0.5	0.25	0.125
$\varepsilon_r = 2.22$	0.5	0.9994	0.9638	0.9716
	0.25	0.8970	0.8850	0.8944
	0.125	0.7559	0.7486	0.7866
	0.0625	0.6462	0.6192	0.6900
$\varepsilon_r = 3.0$	0.5	0.9663	0.9600	0.9674
	0.25	0.8467	0.8481	0.8710
	0.125	0.6939	0.6872	--
$\varepsilon_r = 9.0$	0.5	0.9541	0.9452	0.9535
	0.25	0.7706	0.7721	0.8138
	0.125	0.5190	0.5376	--

Correction Factor G
for
Bilateral Fin Lines

	s/b \ d/b	0.5	0.25	0.125
$\varepsilon_r = 2.22$	0.5	0.9332	0.9243	0.9364
	0.25	0.7364	0.7274	0.7768
	0.125	0.4720	0.4714	0.5513
	0.0625	0.2759	0.2695	0.3335
$\varepsilon_r = 3.0$	0.5	0.9376	0.9288	--
	0.25	0.7265	0.7281	--
	0.125	0.4582	0.4699	--
$\varepsilon_r = 9.0$	0.5	0.9322	0.9288	--
	0.25	0.7238	0.7265	--
	0.125	0.4439	0.4594	--

REFERENCES

1. Meier, P.J., "Integrated fin-line millimeter components", IEEE Trans. Microwave Theory and Techniques, vol.MTT-22, pp.1209-1216, 1974.

2. Hofmann, H., "Calculation of quasi-planar lines for mm-wave application", 1977 Int. IEEE-MTT-Symposium, San Diego, California, pp.381-383.

3. Hofmann, H., H. Meinel, and B. Adelseck, "New integrated mm-wave components using fin-lines", 1978 Int. IEEE-MTT-Symposium, Ottawa, Canada, pp.21-23.

4. Cohen, L.D., and P.J. Meier, "Advances in E-plane printed millimeter-wave circuits", 1978 Int. IEEE-MTT-Symposium, Ottawa, Canada, pp.27-29.

5. Begemann, G, "An X-band balanced fin-line mixer", 1978 Int. IEEE-MTT-Symposium, Ottawa, Canada, pp.24-26.

6. Knöchel, R., "Design and performance of microwave oscillators in integrated fin-line technique", Microwave, Optics and Acoustics, vol.3, pp.115-120, May 1979.

7. Saad, A.M.K., G. Begemann, "Electrical performance of finlines of various configurations", I.E.E. J. of Microwaves, Optics and Acoustics, vol.1, Jan. 1977, pp.81-88.

8. Chang, C., and T. Itoh,"Spectral domain analysis of dominant and higher order modes in fin lines", 1979 Int. IEEE-MTT-Symposium, Orlando, Florida, Apr.30-May 2, digest pp.344-346.

9. Shih, Y.C., and W.J.R. Hoefer, "The accuracy of TLM analysis of finned rectangular waveguide", IEEE Trans. Microwave Theory and Techniques, vol.MTT-30, July 1980.

10. Saad, A.M.K., Schuenemann,K., "A simple method for analyzing fin line structure", 1978 IEEE MTT-S-Int. Microwave Symposium, Ottawa, pp.405-407.

11. Hoefer, W.J.R., and A. Ros, "Fin line parameters calculated with the TLM-Method", 1979 Int. IEEE-MTT-Symposium, Orlando, Florida, Apr.30-May 2.

12. Beyer, A., and I. Wolff, "A solution of the earthed fin line with finite metallization thickness", 1980 IEEE MTT-S-Int. Microwave Symposium, Washington D.C., pp.258-261, May 27-31, 1980.

13. Cohn, S.B., "Slot line on a dielectric substrate", IEEE Trans. Microwave Theory and Techniques, vol.MTT-17, pp.768-778, Oct. 1969.

14. Cohn, S. B.,"Properties of ridge wave guide", Proc. IRE, Vol.35, August 1947, pp.783-788.

15. Hopfer, S.,"The design of ridged waveguides", Trans. IRE, vol.3, vol. MTT-3, October 1955, pp.20-29.

16. Chen, T. S.,"Calculation of the parameters of ridge waveguides", Trans. IRE, vol. MTT-4, January 1956, pp.12-17.

17. Marcuvitz, N.,"Waveguide Handbook", MIT Radiation Lab. Series, No.10, Boston Technical Publishers, Inc., 1964.

18. Johns,P.B., and R.L.Beurle,"Numerical solution of 2-dimensional scattering problems using a transmission-line matrix",Proc. IEE, Vol.118, No.9, September 1971, pp.1203-1208.

19. Akhtarzad,S, and P.B.Johns,"Generalized elements for TLM method of numerical analysis",Proc. IEE, Vol.122, NO.12, December 1975, pp.1349-1352.

20. Johns,P.B.,"Application of the transmission-line-matrix method to homogeneous waveguides of arbitrary cross-section",Proc. IEE, Vol.119, NO.8, August 1972, pp.1080-1091.

21. Konishi, Y., and K. Uenakada, "The design of a bandpass filter with inductive strip-planar circuit mounted in waveguide", IEEE Trans. Microwave Theory and Tech., vol.MTT-22, No.10, Oct. 1974, pp.869-873.

22. Konishi, Y., "PLanar circuit mounted in waveguide used as a downconverter", IEEE Trans. Microwave Theory and Tech., Vol.MTT-26, No.10,Oct. 1978, pp.716-719.

23. Hoefer, W. J. R., "Fin line design made easy", 1978 IEEE-MTT-S Int. Microwave Symposium, June 1978, Ottawa, Ont., Canada.

24. Akhtarzad,S., "Analysis of lossy microwave structures and microstrip resonantors by the TLM-method", Ph.D. thesis, University of Nottingham, May 1975.

25. Akhtarzad,S., and P.B.Johns, "Solution of Maxwell's equations in three space dimensions and time by the TLM-method of numerical analysis", Proc. IEE, vol.122, No.12, December 1975, pp.1344-1348.

26. Akhtarzad,S., and P.B.Johns, "Three-dimensional transmission-line matrix computer analysis of microstrip resonators", IEEE Trans. on Microwave Theory and Techniques, vol.MTT-23, No.12, Dec. 1975, pp.990-997.

27. Hoefer,W.J.R., "Quickly now, where does waveguide cutoff occur", Microwaves, Dec. 1979, pp.70-74.

28. Shih, Y.C., W.J.R. Hoefer, and A. Ros, "Cutoff frequencies in fin lines calculated with a two-dimensional TLM-program", 1980 Int. IEEE-MTT-Symposium, Washington D.C., digest pp.261-263.

29. Hoefer, W.J.R., and Y.C. Shih, "Field configuration of fundamental and higher order modes in fin lines obtained with the TLM-method", NARSM and Int. IEEE-AP-S, Quebec, Canada, Jun.2-6 1980.

30. Shih, Y.C., and W.J.R. Hoefer, "Dominant and second order mode cutoff frequencies in fin lines calculated with a two-dimensional TLM program", to appear in the IEEE Trans. Microwave Theory and Techniques.